Drell-Yan Production at Hadron Colliders

Radja Boughezal

Argonne National Laboratory

Lectures at the CTEQ School on QCD and Electroweak Phenomenology

Pittsburgh, July 18-28, 2017

Topics we will cover

- Historical importance of Drell-Yan
- Modern applications of Drell-Yan
  - The W-boson mass using Drell-Yan
  - PDF measurements using Drell-Yan
  - New physics searches using Drell-Yan (W', Z', …)
- Predicting hadronic cross sections: theoretical framework
- Drell-Yan at LO and NLO in QCD: a detailed calculation of the partonic cross section
- Vector boson plus jet production at the LHC
  - What is a jet?
  - Phenomenological applications of Z/W+jet processes
- A future 100 TeV pp collider
- Summary

The Drell-Yan Process

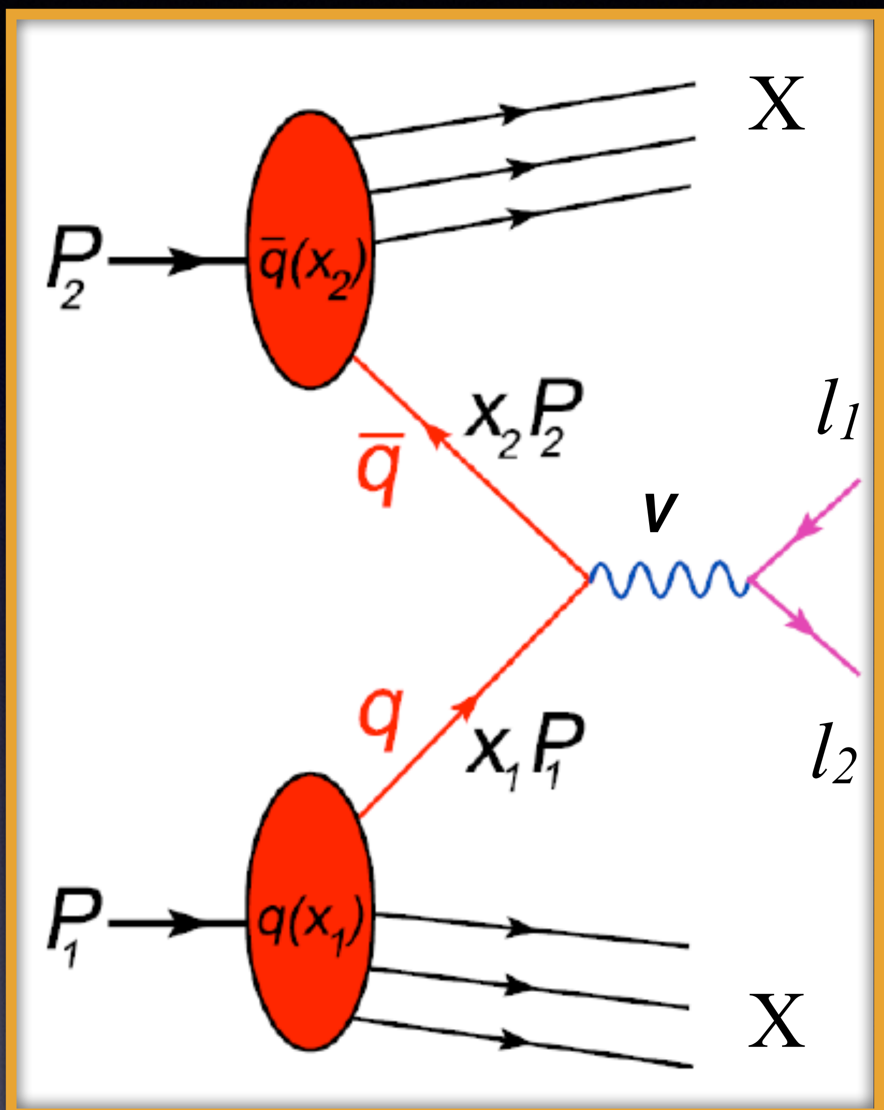

- Drell-Yan is the production of lepton pairs in the s-channel. Drell-Yan like processes include:

$$h(P_1) + h'(P_2) \to (\gamma^*, Z \to l^+ l^-)X \quad \text{with} \quad l = e,\mu$$

$$h(P_1) + h'(P_2) \to (W \to l\nu)X$$

$$h(P_1) + h'(P_2) \to V_{BSM}X; \quad V = Z', \ldots$$

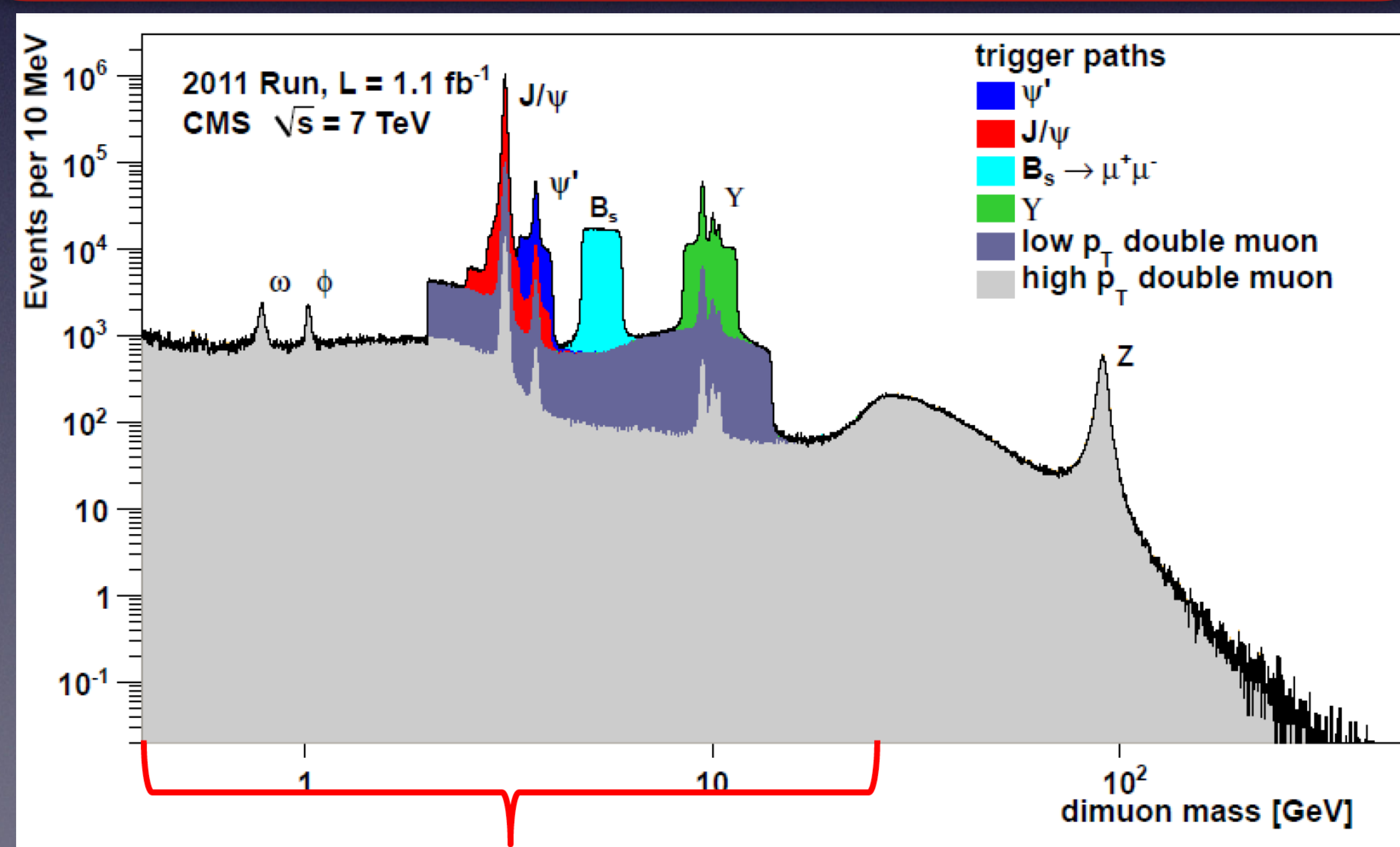

Non perturbative effects in the spectrum...

Facts about Drell-Yan

- Clean signal at hadron colliders, since the lepton pair does not interact strongly
- One of the best theoretically studied processes at a hadron collider with uncertainties at the few percent level
- Factorization is proved to all orders in QCD perturbation theory (Collins-Soper-Stermann)
- Standard Candle for detector calibration (eg. detector response to lepton energy)

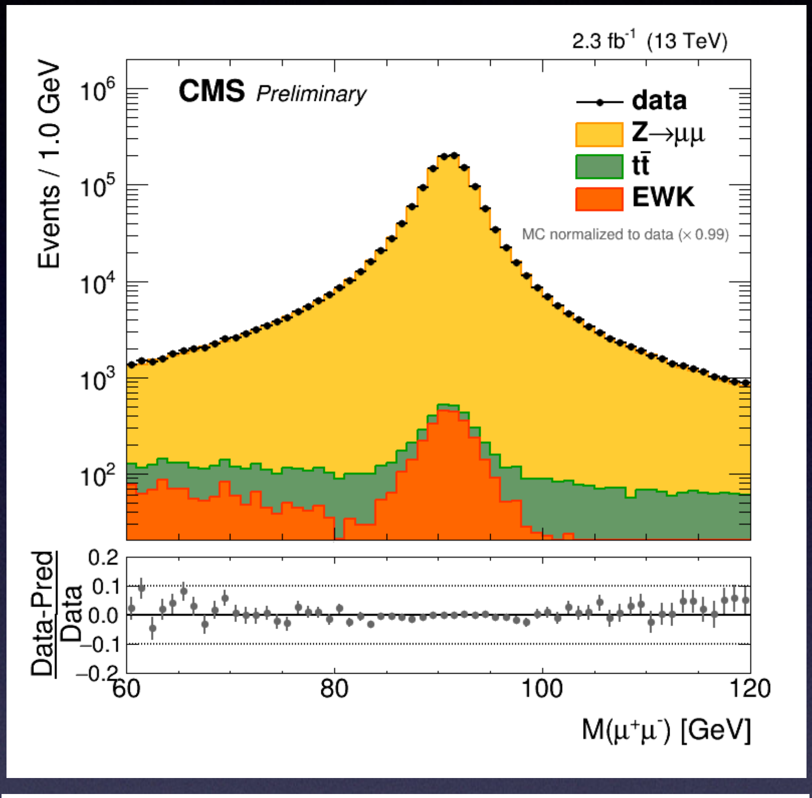

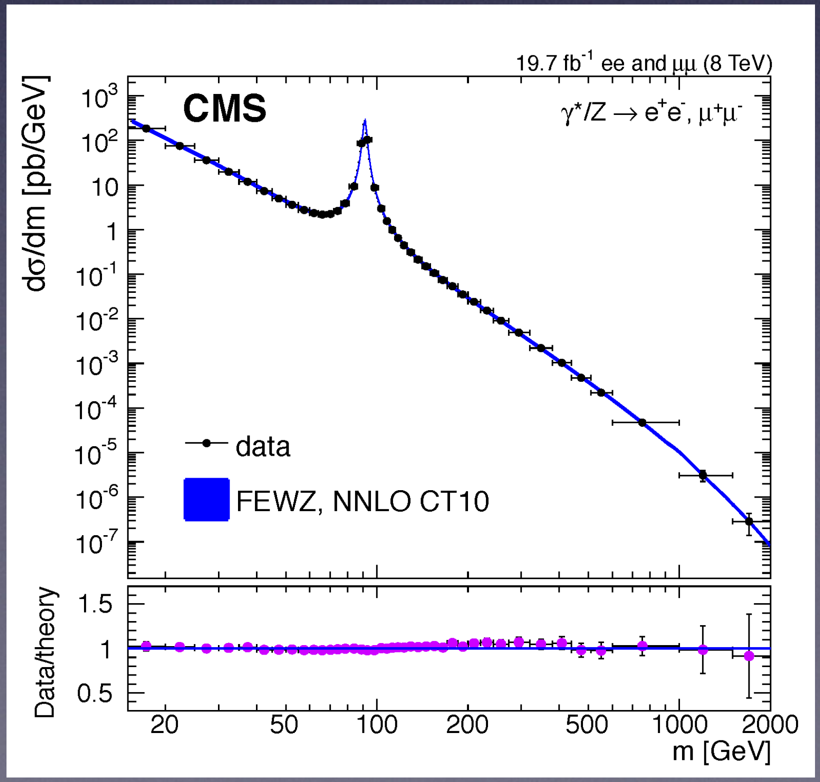

Historical importance

- Study of the Drell-Yan process was critically important in establishing QCD as a quantitative theory

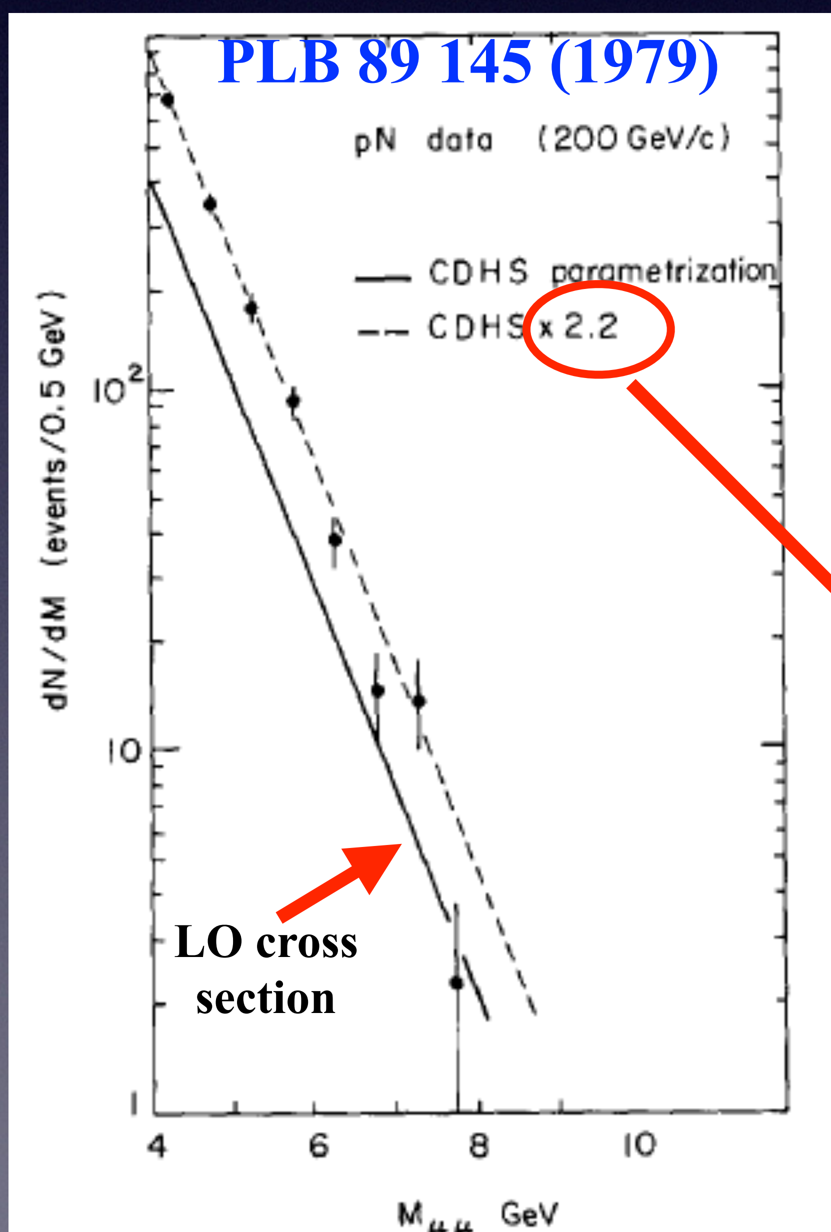

Comparison of dimuon data from the NA3 experiment at CERN in 1979:

In all the channels studied the experimental cross section is significantly larger by a factor of 2.3 ± 0.5 than expected

The first introduction of a "K-factor" to explain discrepancies between theory and data

$K = (d^2\sigma/dx_1 dx_2)_{exp}/(d^2\sigma/dx_1 dx_2)_{DY\ model}$.

Reaction	pN	$\bar{p}$N
K	2.2 ± 0.4	2.4 ± 0.5

Historical importance

- Study of the Drell-Yan process was critically important in establishing QCD as a quantitative theory

TOT= sum of all partonic channels @ NLO

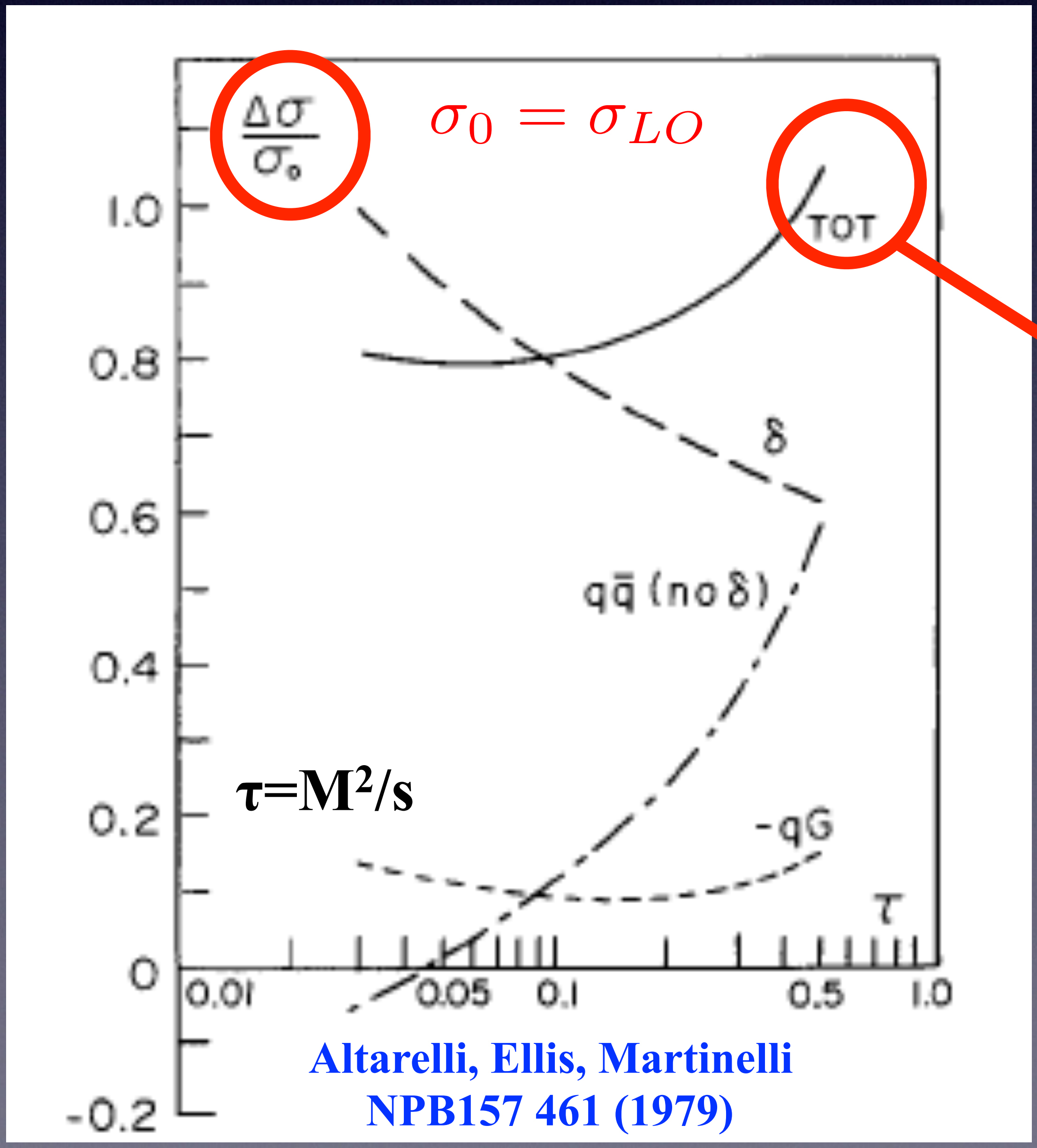

$$\Delta\sigma_{TOT}/\sigma_0 \sim 0.8 - 1.0$$

$\Delta\sigma =$ **pure NLO coefficient**

$$\sigma_{NLO} = \sigma_0 + \Delta\sigma_{TOT}$$

NLO QCD corrections reach nearly a factor of 2, greatly reducing tension between theory and experiment

Discrepancy resolved by next-to-leading order QCD!

Historical importance

- Understanding of vector boson production through the Drell-Yan process has required continued advances in our ability to understand QCD precisely, with data from the Tevatron and the LHC requiring NNLO corrections

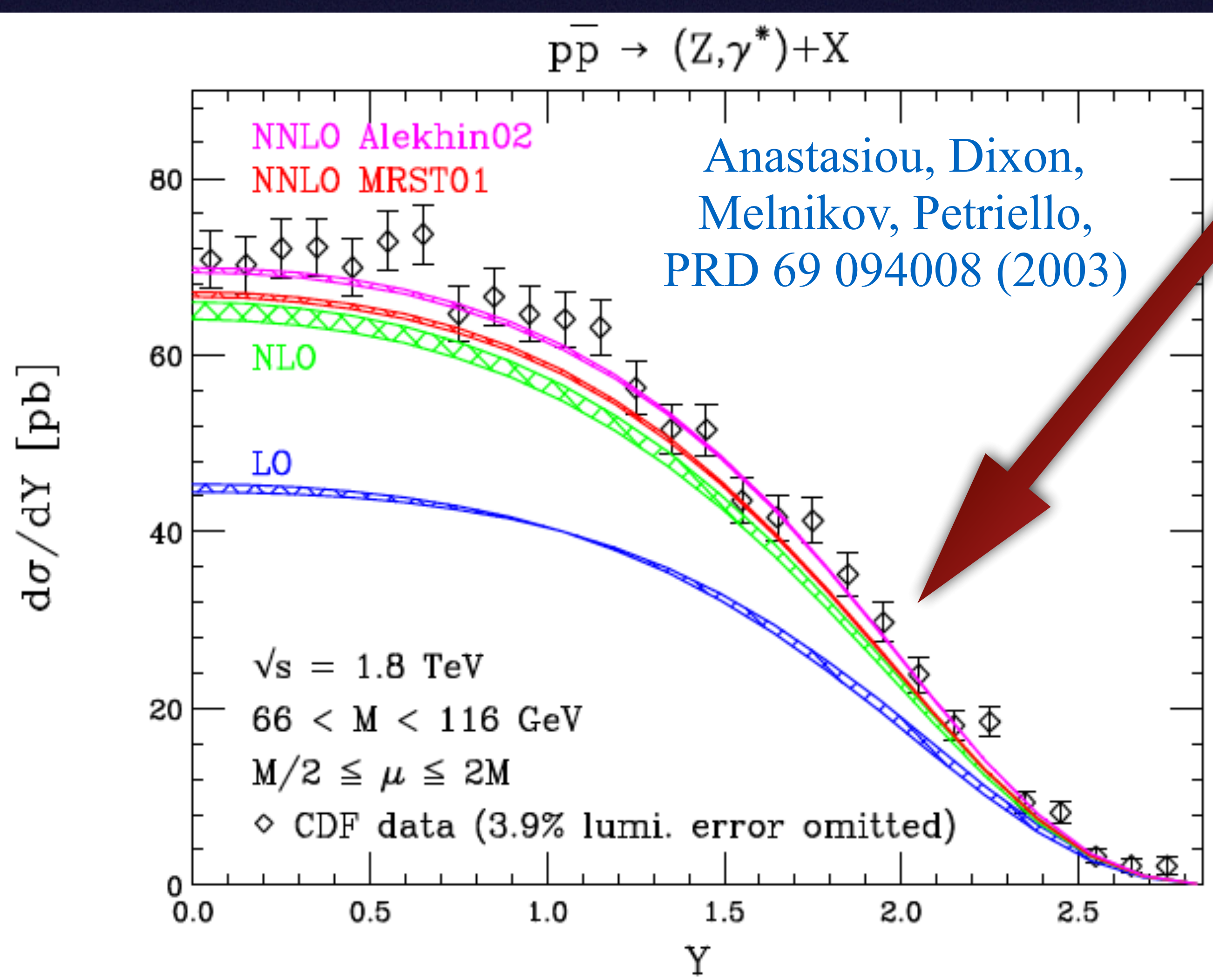

- Drell-Yan data and predictions can be used to to improve our understanding of proton structure

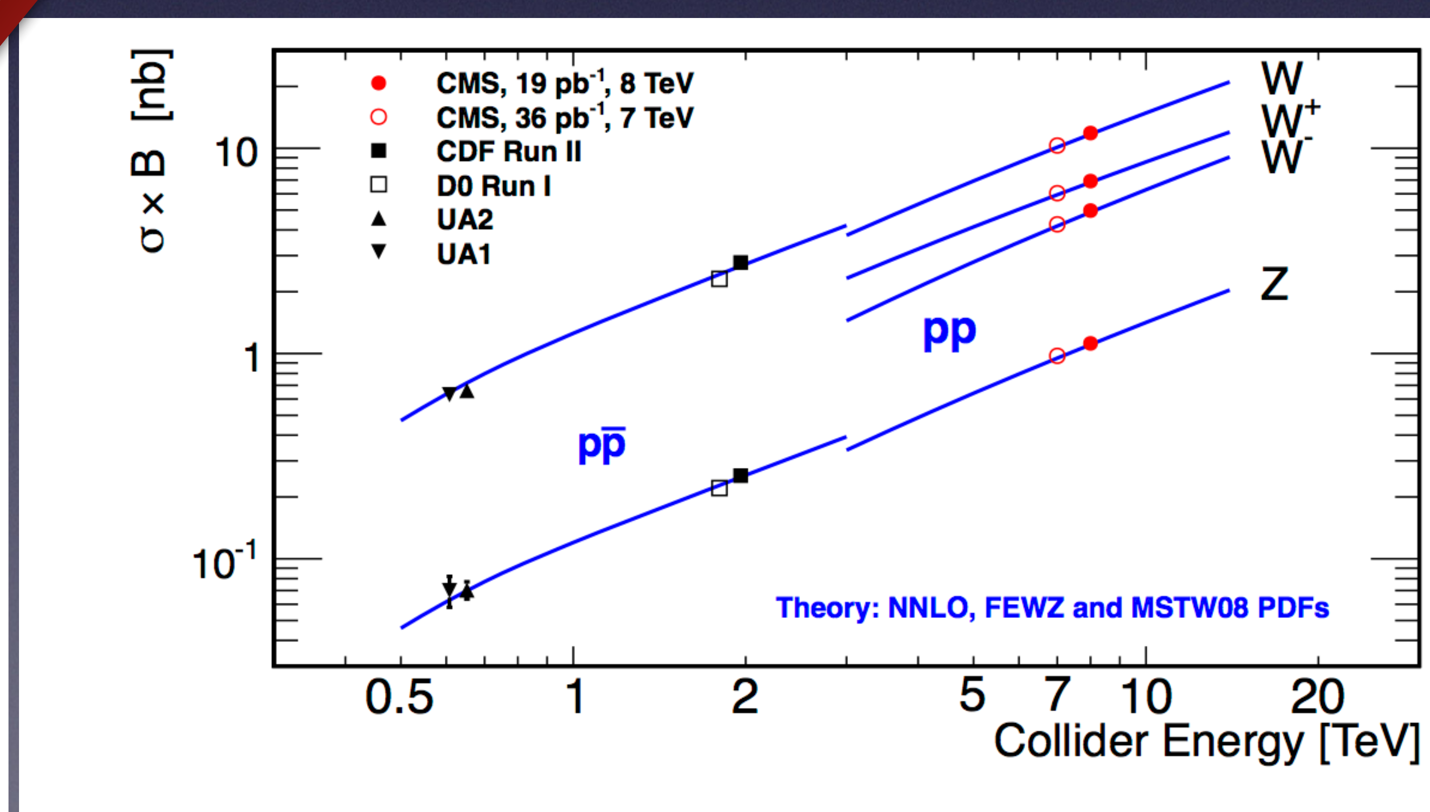

Historical importance

- The Drell-Yan process has been an important discovery mode throughout the modern history of high energy physics

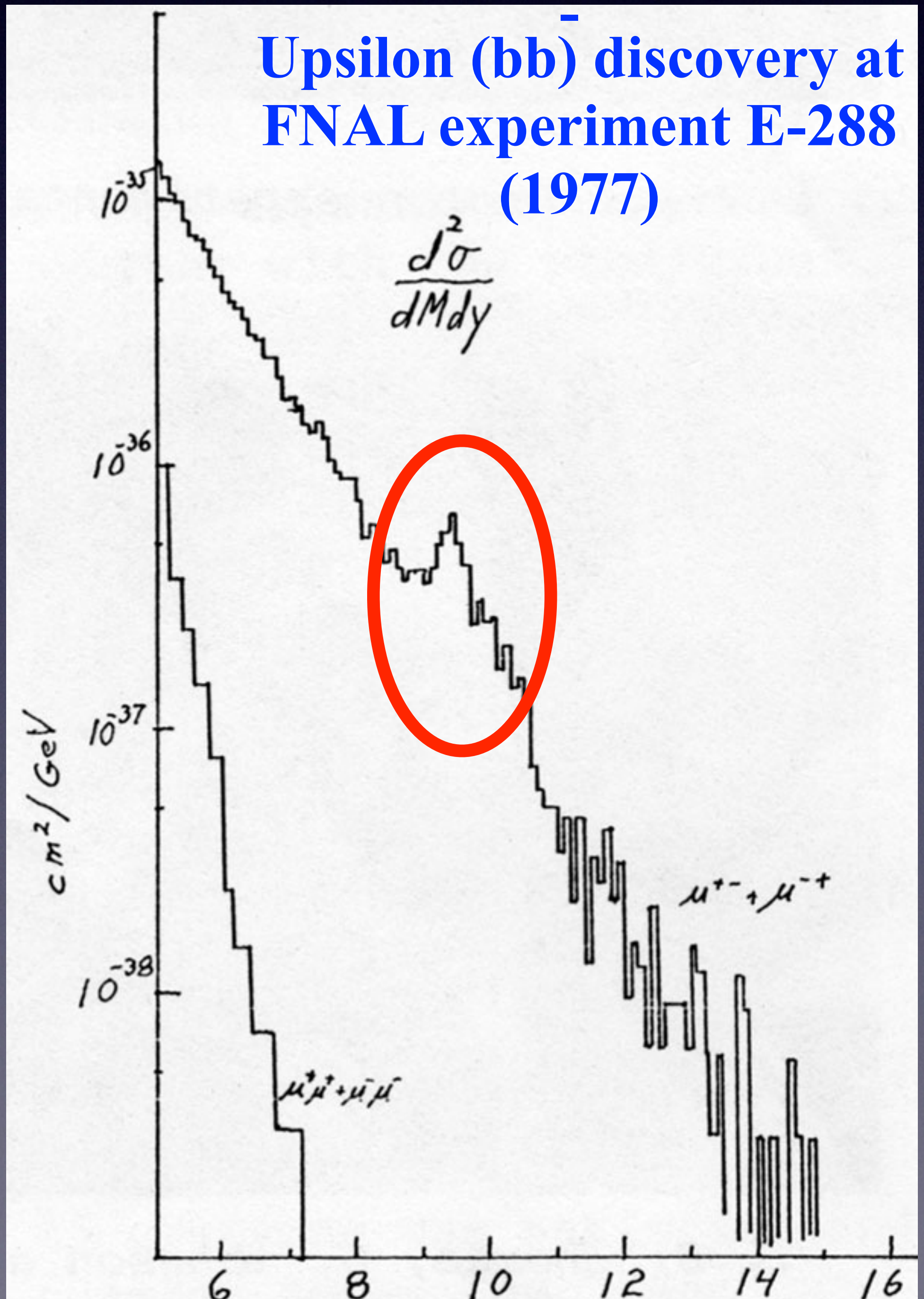

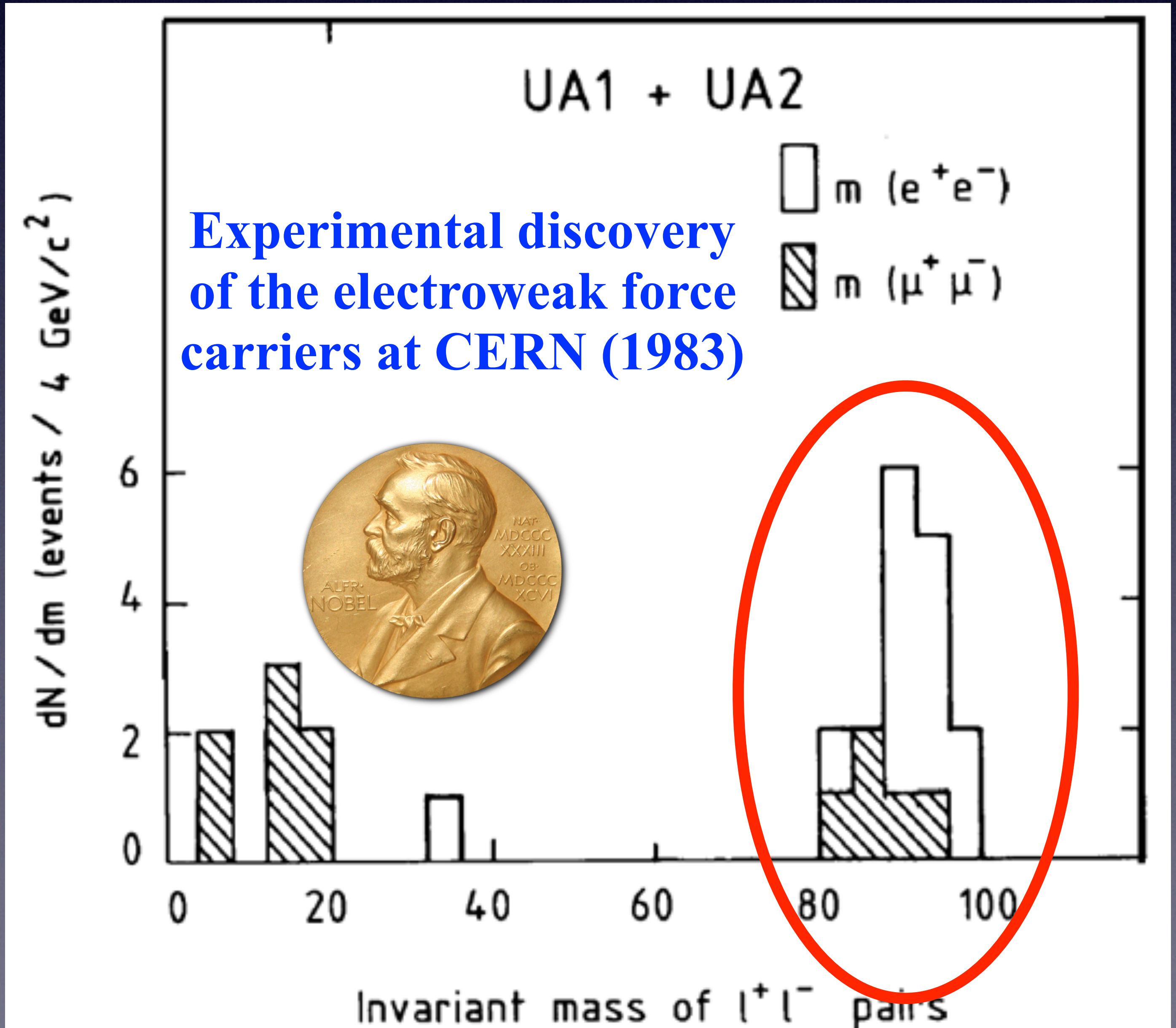

Historical importance

- The Drell-Yan production of vector bosons has also played a prominent role in famous non-discoveries in particle physics…

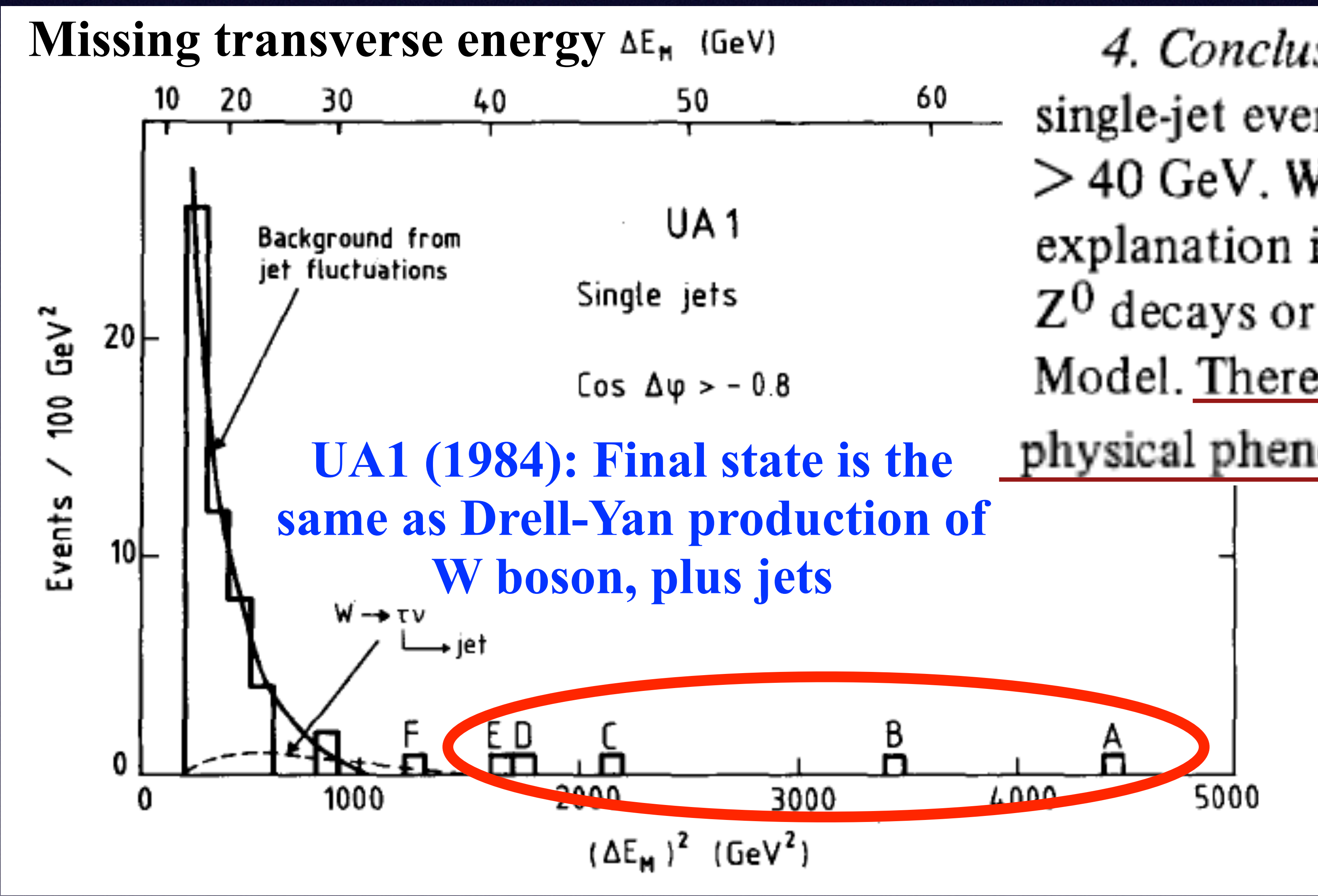

4. Conclusions. We have presented a sample of five single-jet events and two "photon" events with $\Delta E_M > 40$ GeV. We have been unable to find a reasonable explanation in terms of background including W and Z^0 decays or within the expectation of the Standard Model. Therefore we believe they are due to some new physical phenomenon.

Historical importance

- The Drell-Yan production of vector bosons has also played a prominent role in famous non-discoveries in particle physics…

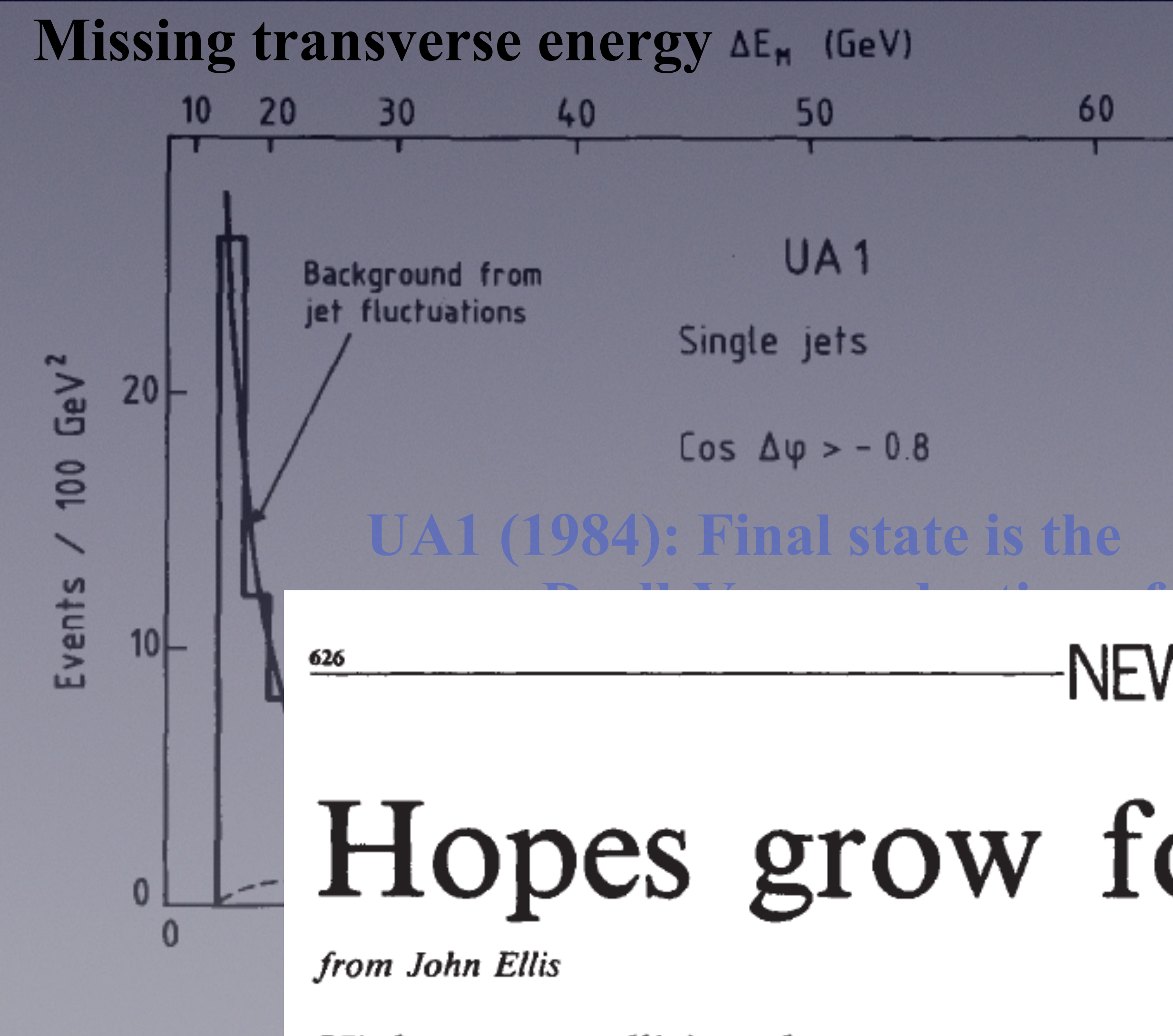

UA1 (1984): Final state is the

4. *Conclusions.* We have presented a sample of five single-jet events and two "photon" events with $\Delta E_M > 40$ GeV. We have been unable to find a reasonable explanation in terms of background including W and Z^0 decays or within the expectation of the Standard Model. Therefore we believe they are due to some new physical phenomenon.

626 NEWS AND VIEWS NATURE VOL. 313 21 FEBRUARY 1985

1985

Hopes grow for supersymmetry

from John Ellis

High-energy collisions between protons and antiprotons produce strange events in which momentum fails to balance. Missing momentum may be carried by photinos, super-partners of the photon.

Historical importance

- The Drell-Yan production of vector bosons has also played a prominent role in famous non-discoveries in particle physics…

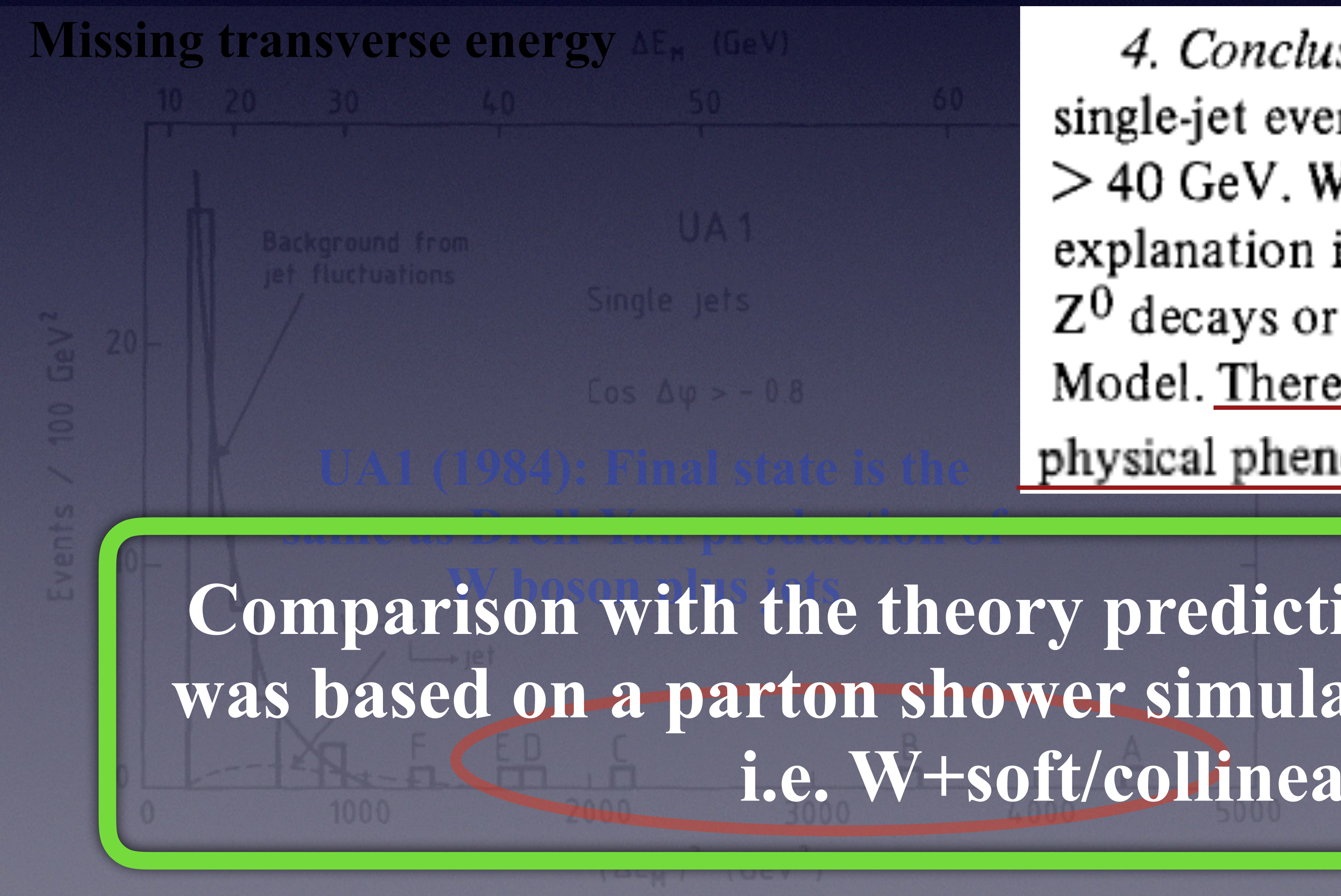

4. *Conclusions.* We have presented a sample of five single-jet events and two "photon" events with $\Delta E_M > 40$ GeV. We have been unable to find a reasonable explanation in terms of background including W and Z^0 decays or within the expectation of the Standard Model. Therefore we believe they are due to some new physical phenomenon.

Comparison with the theory prediction for the background was based on a parton shower simulation for W-production, i.e. W+soft/collinear jets

Historical importance

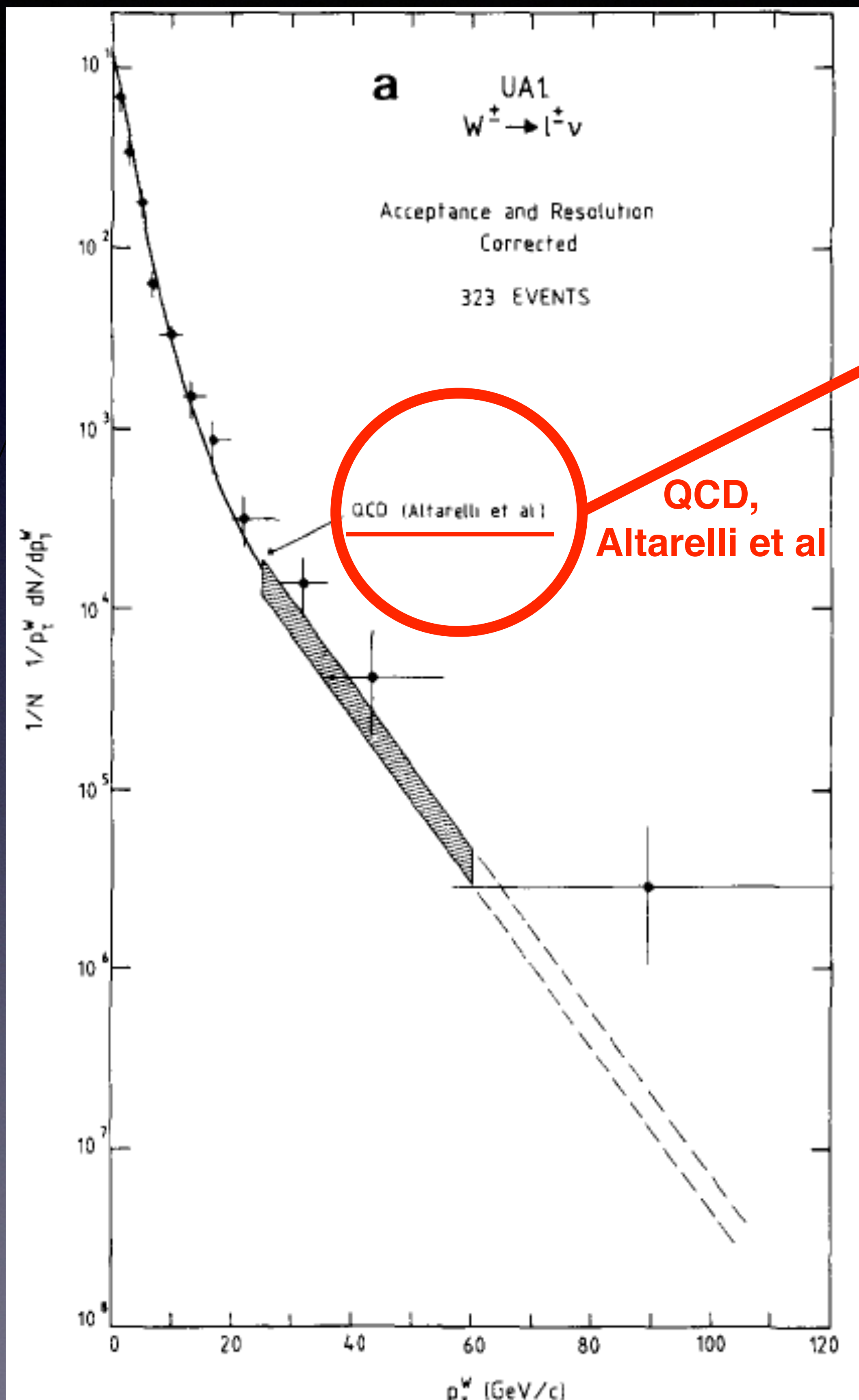

A proper SM prediction for the background requires W+hard jet emissions. This explained the discrepancy, not SUSY!

Parton showers (without matching to exact tree level matrix elements) do not explain hard emissions correctly

UA1 CM energy = 540 GeV $\Longrightarrow$ 40 GeV missing energy is hard, not soft !

From Drell-Yan Yesterday to Drell-Yan Today

Modern applications

- The W-boson mass is an important observable in the global fit to electroweak precision data. The agreement between the direct M_W measurement and the indirect determination from fitting other data is a powerful constraint on Standard Model extensions.

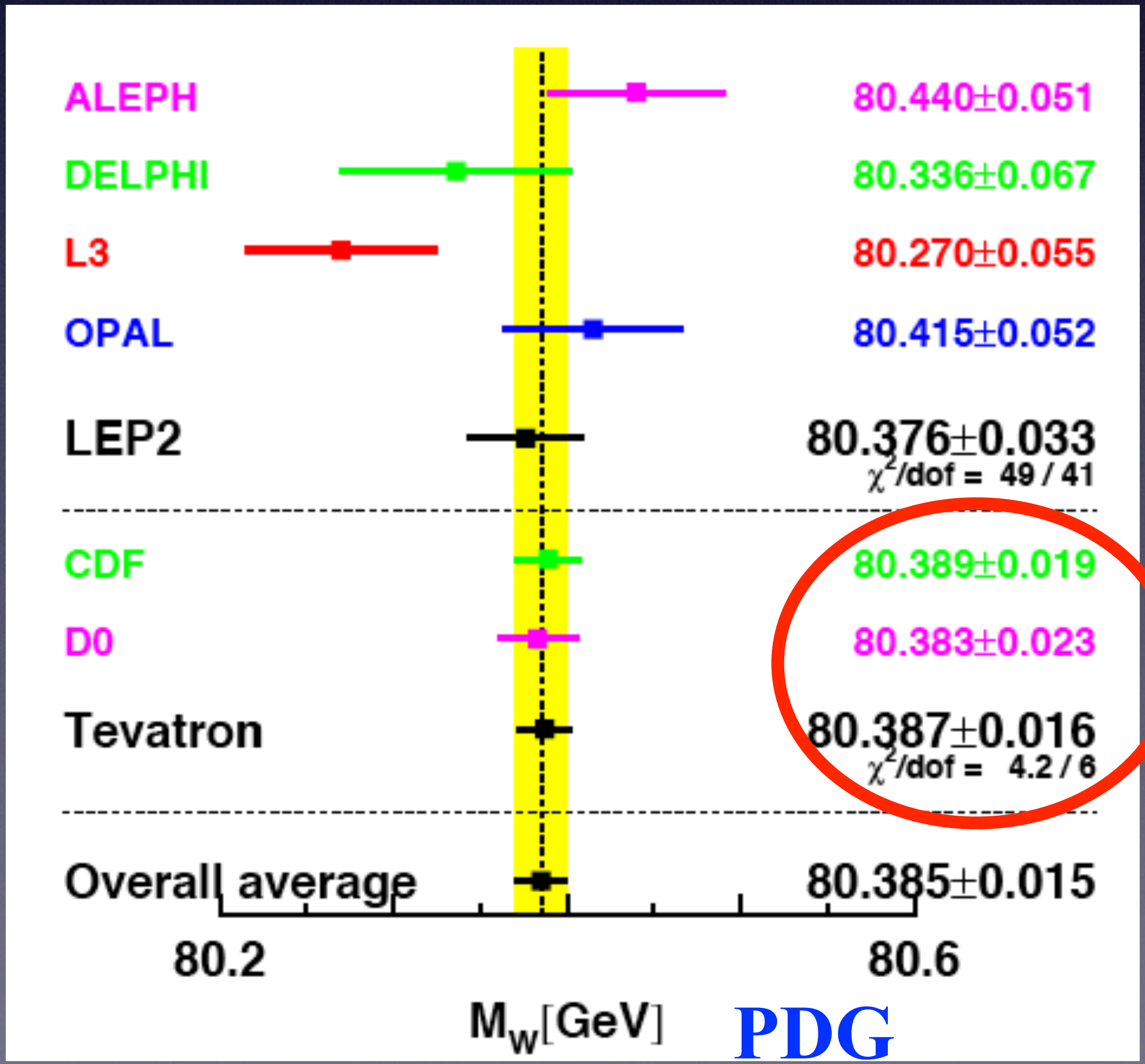

Direct measurement

Most precise determinations of M_W are from Drell-Yan production at the Tevatron

Modern applications

- The W-boson mass is an important observable in the global fit to electroweak precision data. The agreement between the direct M_W measurement and the indirect determination from fitting other data is a powerful constraint on Standard Model extensions.

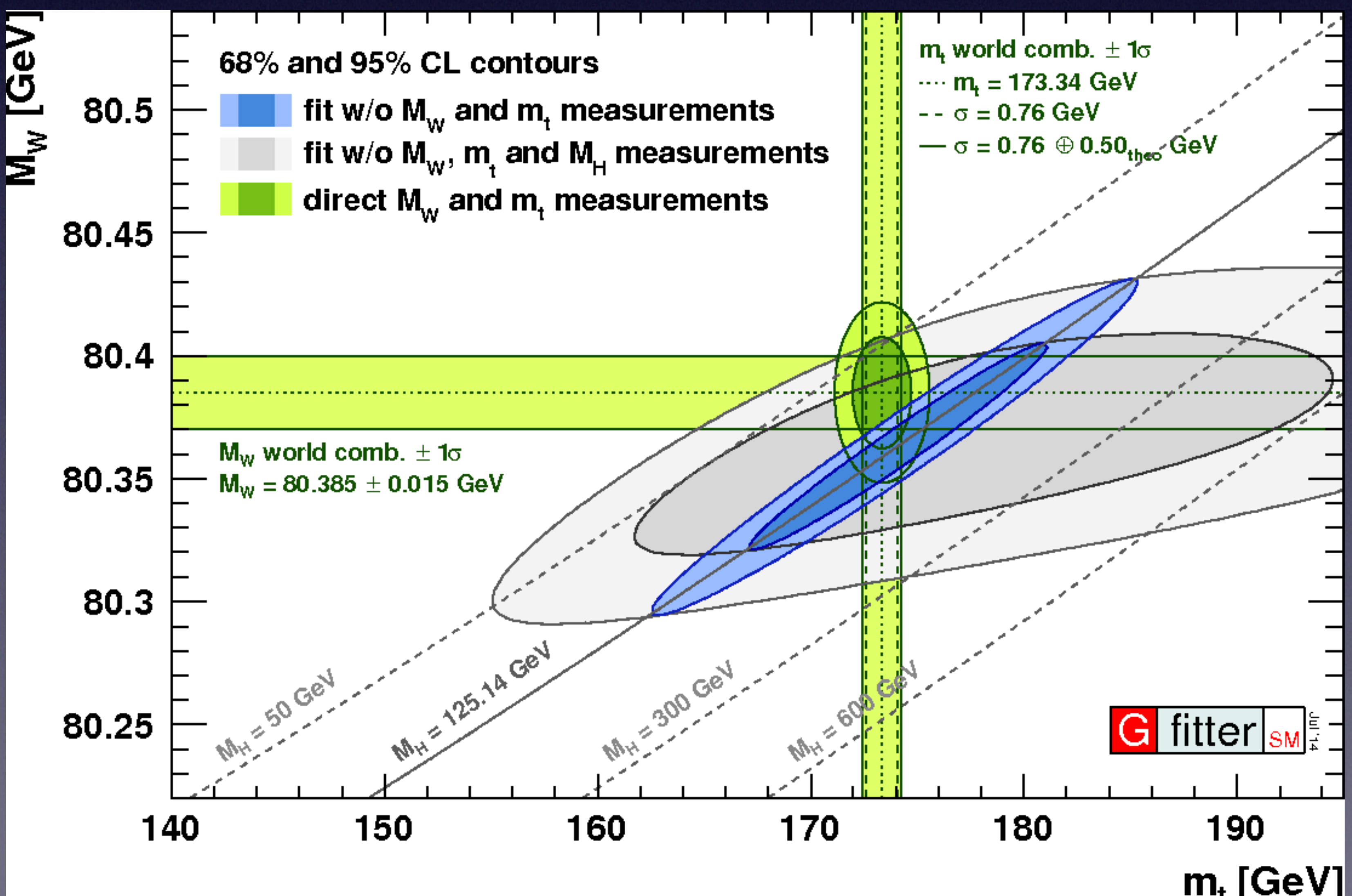

Indirect measurement

✳ All fits: use primarily LEP data (eg. forward-backward asymmetries in lepton pair production, total hadronic cross section, etc)

✳ Blue fit: uses in addition LHC Higgs measurements

✳ Grey fit: does not use LHC Higgs measurements

Good agreement between direct and indirect measurements

Measuring the W mass

- The W→lν contains final-state missing energy; cannot reconstruct the W mass peak

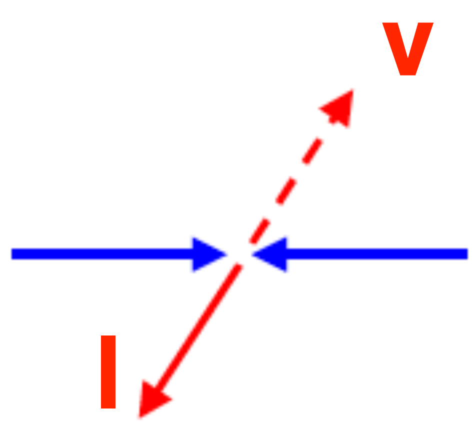

In the W rest frame:

- $\left|\vec{p}_\ell\right| = \left|\vec{p}_\nu\right| = \frac{M_W}{2}$
- $\left|p_\ell^T\right| \le \frac{M_W}{2}$

$$\frac{d\sigma}{dp_T^e} = \underbrace{\left|\frac{d\cos\theta_*}{dp_T^e}\right|}_{\text{Jacobian}} \frac{d\sigma}{d\cos\theta_*} = \frac{1}{\sqrt{1-\left(\frac{2p_T^e}{M_W}\right)^2}} \frac{4p_T^e}{M_W^2} \frac{d\sigma}{d\cos\theta_*}$$

This is a smooth function (can write it in terms of spherical harmonics)

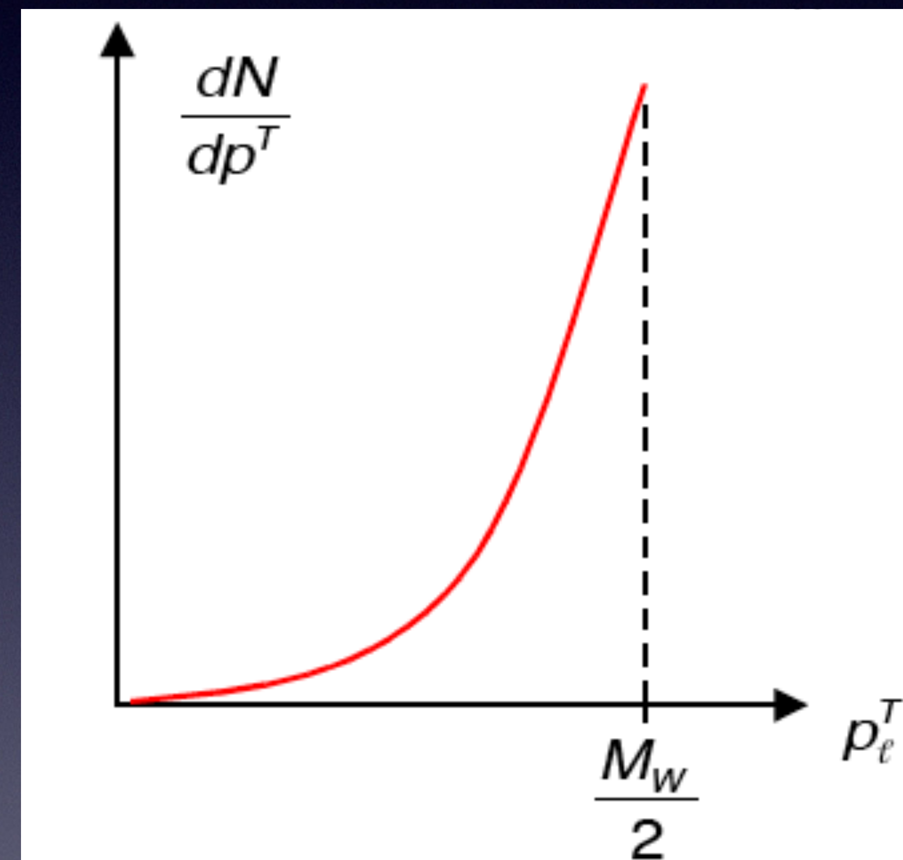

Predict a sharp drop at $M_W/2$; this distribution sensitive to W mass! Called a “Jacobian peak”

Measuring the W mass

- Sensitivity to M_W reduced by several effects: width of the W boson, addition of finite p_{TW} (the previous derivation was valid for $p_{TW}=0$), detector smearing

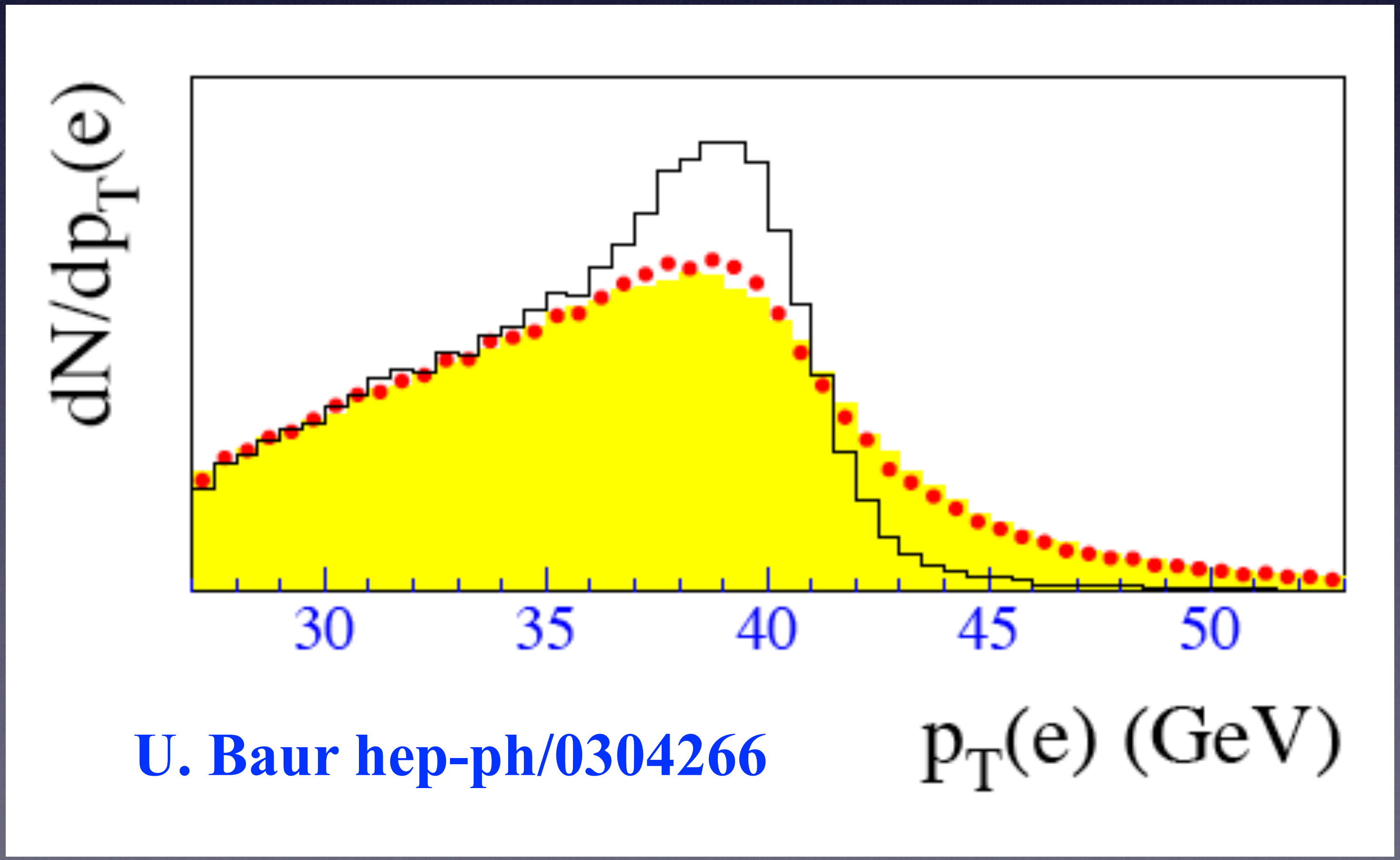

✳ Black histogram: shows the effect of the width Γ_W

✳ Red dots: show the effect of a non-zero p_{TW} due to the hadronic radiation

✳ Yellow histogram: shows the effect of detector smearing

Measuring the W mass

- Can construct the transverse mass, which is less sensitive our theoretical understanding of p_{TW}

$$M_T = \sqrt{2p_T(\ell)p_T(\nu)(1-\cos(\phi_{\ell,\nu}))}$$

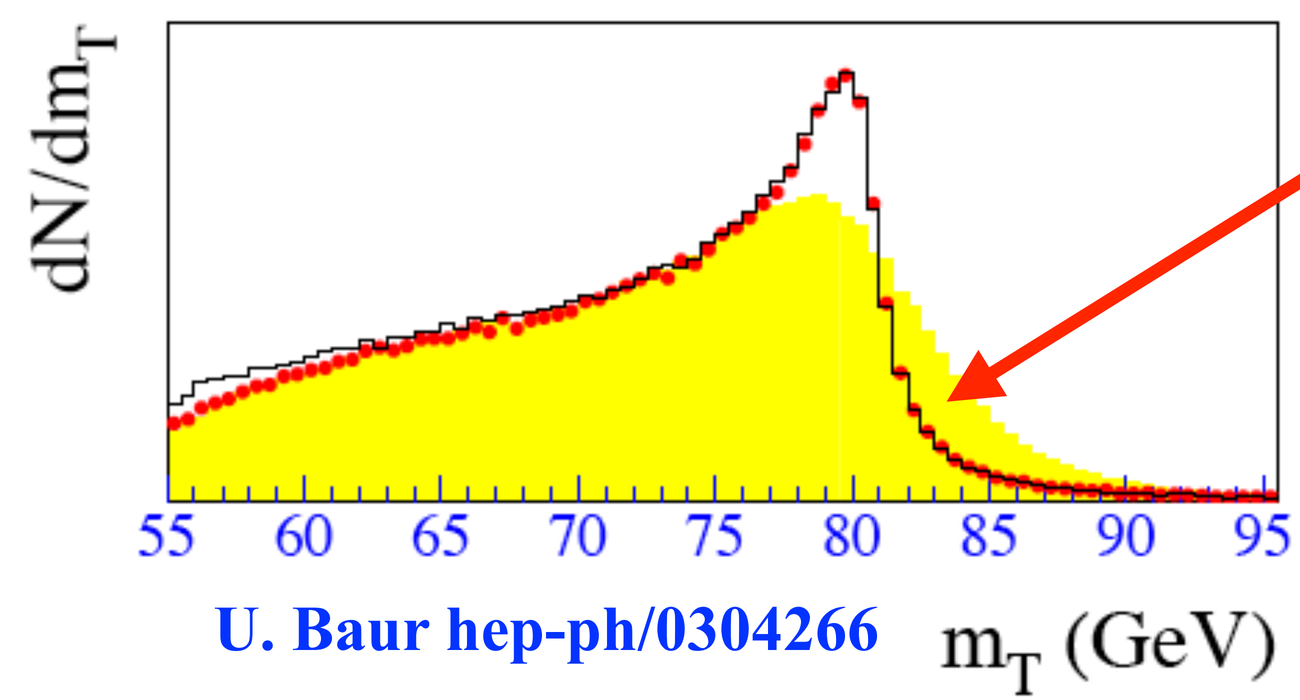

U. Baur hep-ph/0304266

- Finite-p_{TW} corrections to the m_T distribution are suppressed by p_{TW}^2/M_W^2
- However, it is still sensitive to detector smearing
- In practice, m_T and p_T of both the electron and missing energy are used

Distribution	W-boson mass (MeV)	χ^2/dof
$m_T(e,\nu)$	$80\ 408 \pm 19_{\text{stat}} \pm 18_{\text{syst}}$	52/48
$p_T^\ell(e)$	$80\ 393 \pm 21_{\text{stat}} \pm 19_{\text{syst}}$	60/62
$p_T^\nu(e)$	$80\ 431 \pm 25_{\text{stat}} \pm 22_{\text{syst}}$	71/62

CDF, PRL 108 151803 (2012)

Measuring the W mass

- Sensitivity to M_W reduced by several effects: width of the W boson, addition of finite p_{TW} (the previous derivation was valid for p_{TW}=0), detector smearing

All these effects make the precise extraction of M_W a complicated task!

First LHC measurement just appeared!

U. Baur hep-ph/0304266

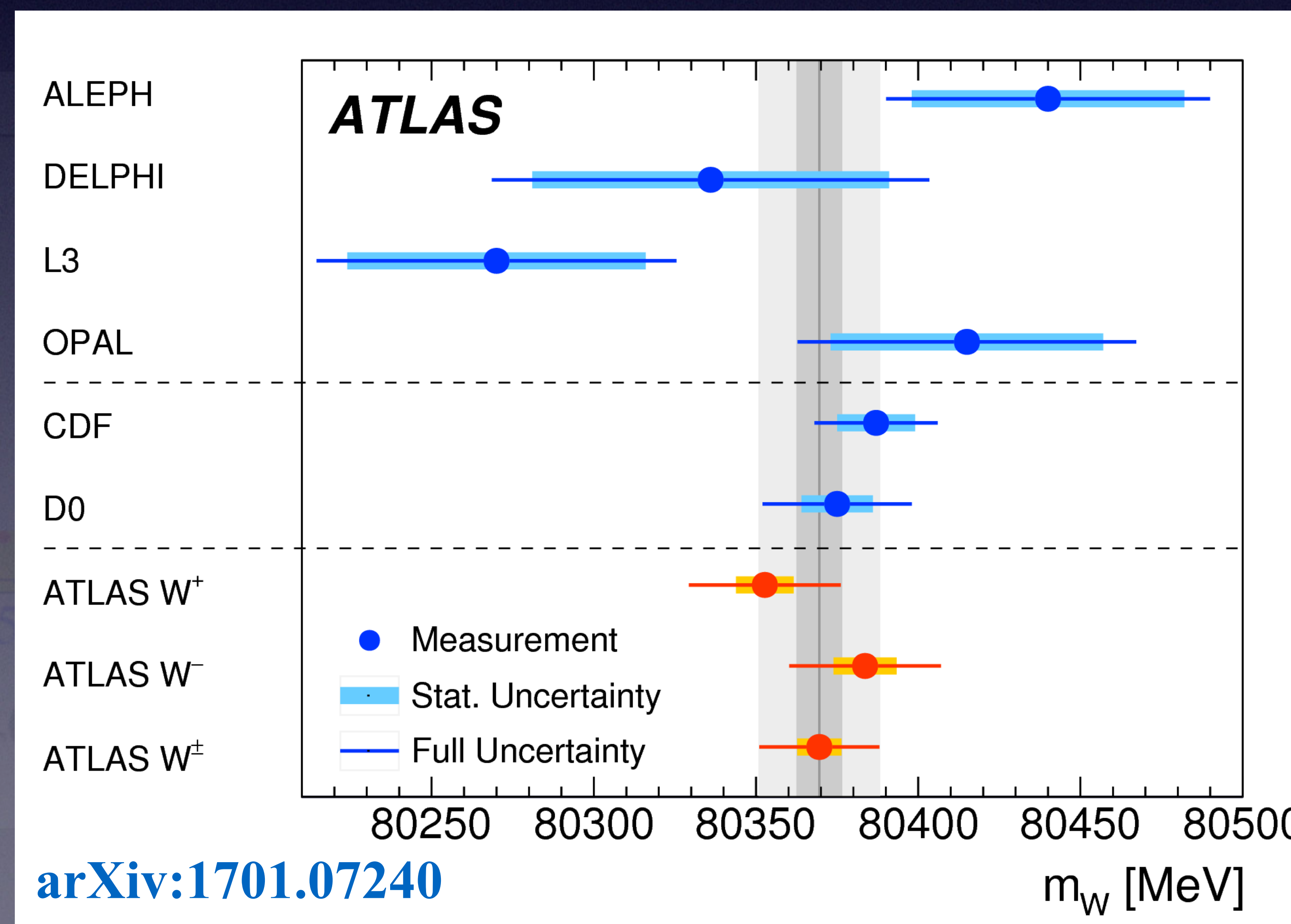

Modern applications

- Drell-Yan is the primary search mode for W' and Z' bosons that would signal an extension of the Standard Model gauge group

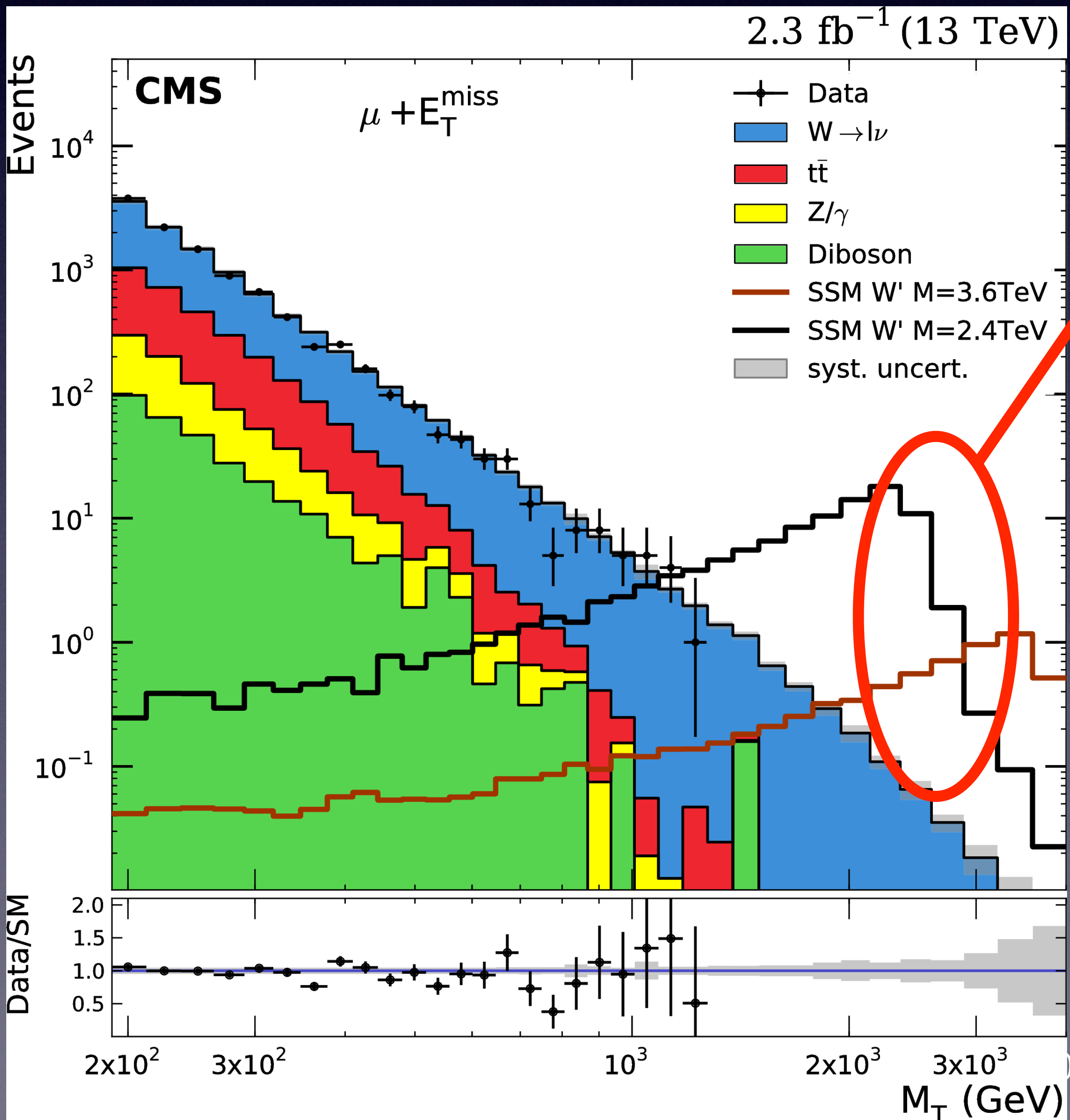

- Hypothetical signature of a W' boson with fermionic couplings identical to the Standard Model W couplings in the muon+missing transverse energy channel in CMS
- Probes extensions of the Standard Model to several TeV
- Note the Jacobian peak that appears for $M_T = M_{W'}$; same structure that appears for the Standard Model W

Modern applications

- Drell-Yan is the primary search mode for W' and Z' bosons that would signal an extension of the Standard Model gauge group

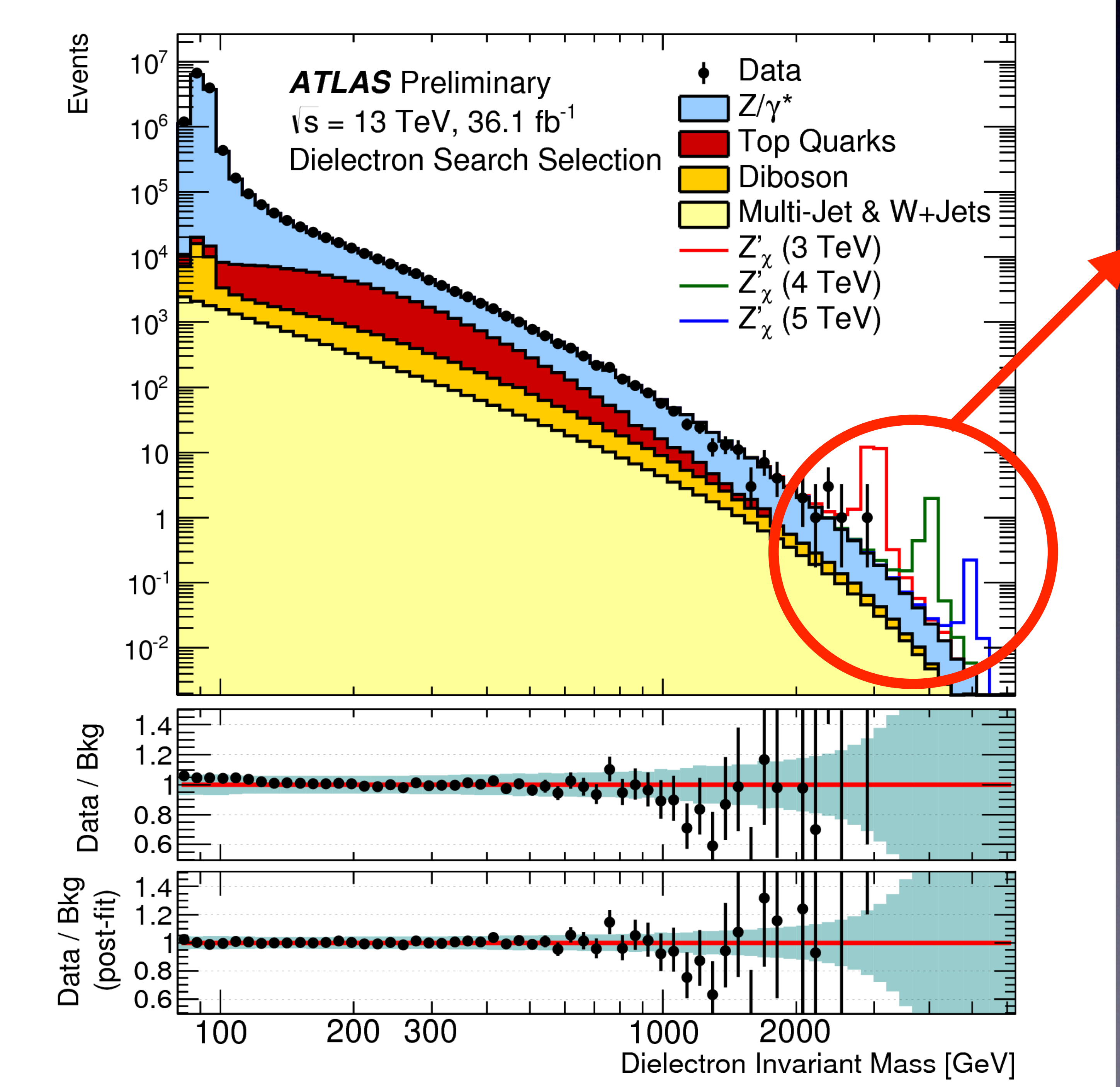

- Hypothetical signatures of an example Z' boson in the dielectron channel in ATLAS
- Probes extensions of the Standard Model to 4 TeV or beyond, depending on the exact model
- In this case the mass peak can be fully reconstructed

Modern applications (PDFs)

- Drell-Yan production, at both collider energies and fixed-target energies, provides invaluable information on PDFs

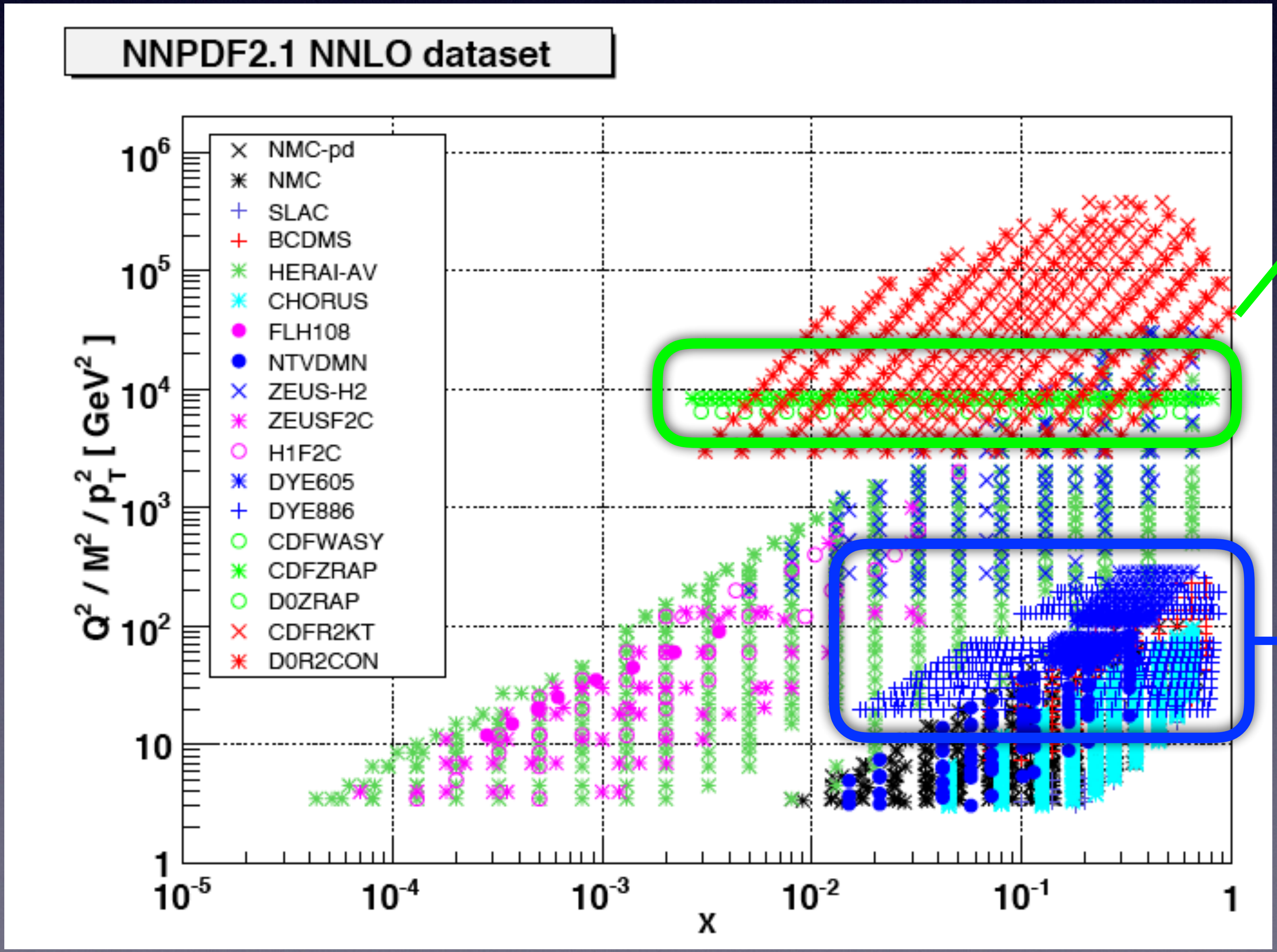

Tevatron W and Z production probe quark PDFs down to $x \sim 10^{-3}$ **(CDFWASY, CDFZRAP, D0ZRAP)**

Important constraints on quark/anti-quark PDFs at higher-x from fixed-target Drell-Yan **(DYE605, DYE866)**

Modern applications (PDFs)

- Drell-Yan production, at both collider and fixed-target energies, provides invaluable information on PDFs

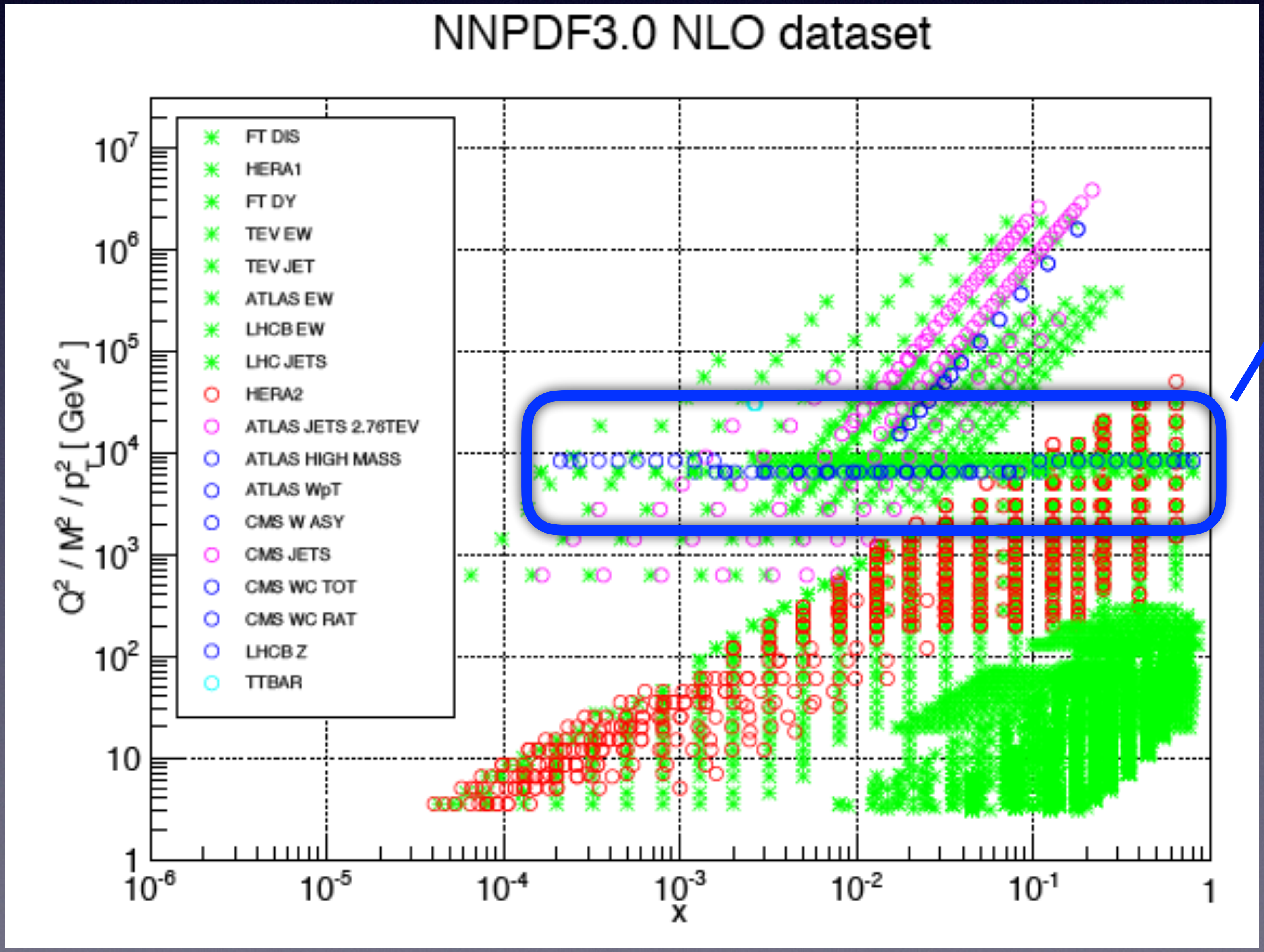

High-precision LHC data on W/Z production increasingly becoming an important element of modern PDF fits (eg. CMS W ASY)

Flavor separation of sea quarks

- Measuring Drell-Yan on a variety of nuclear targets probes differences in sea-quark PDFs

σ_{pd}: proton-deuterium xsection

deuterium has 1 proton and 1 neutron

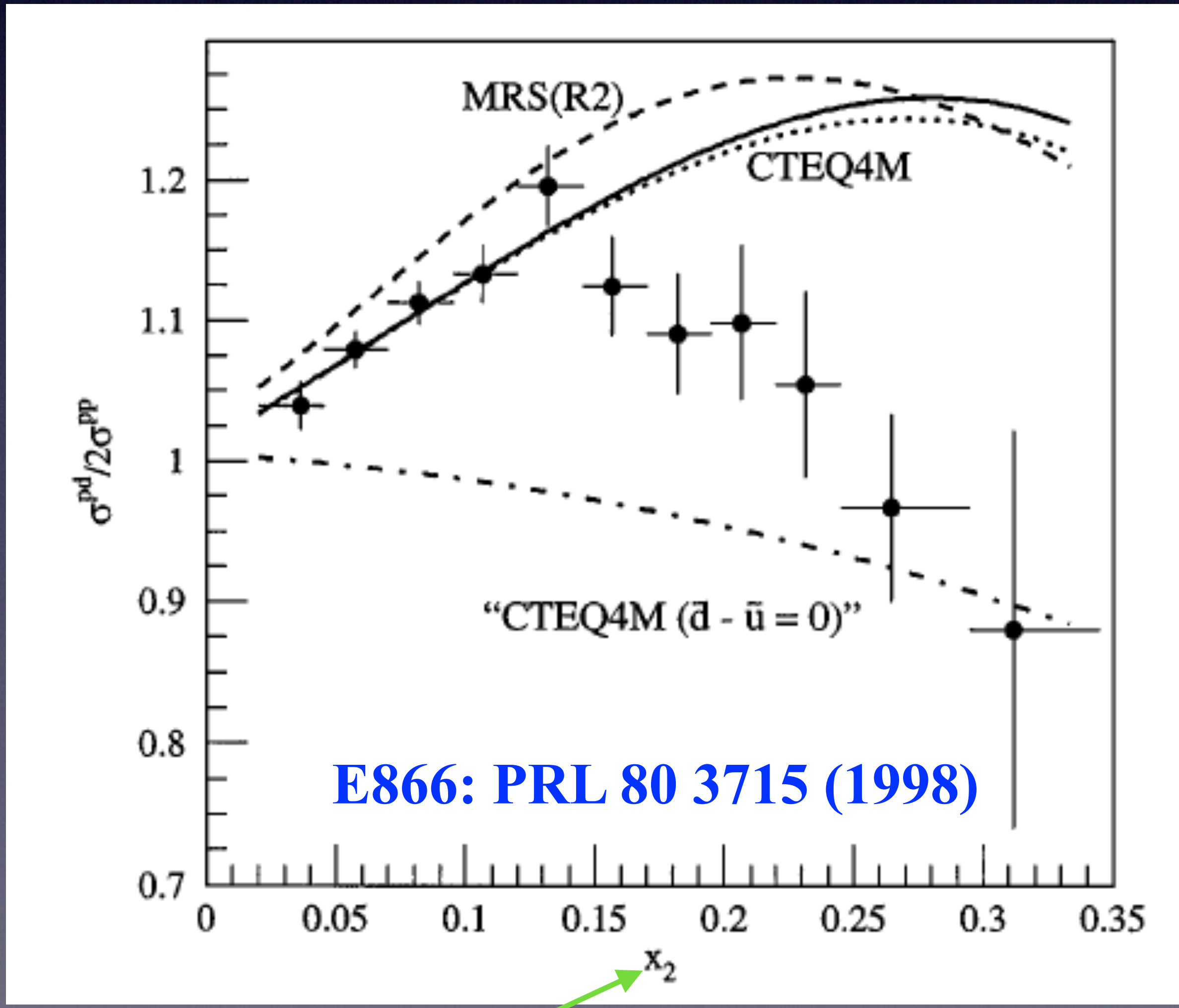

momentum fraction of the target quark

Historically important in ensuring an appropriate parameterization of the sea quarks in the high-x region

Accounting for E866 in CTEQ5:

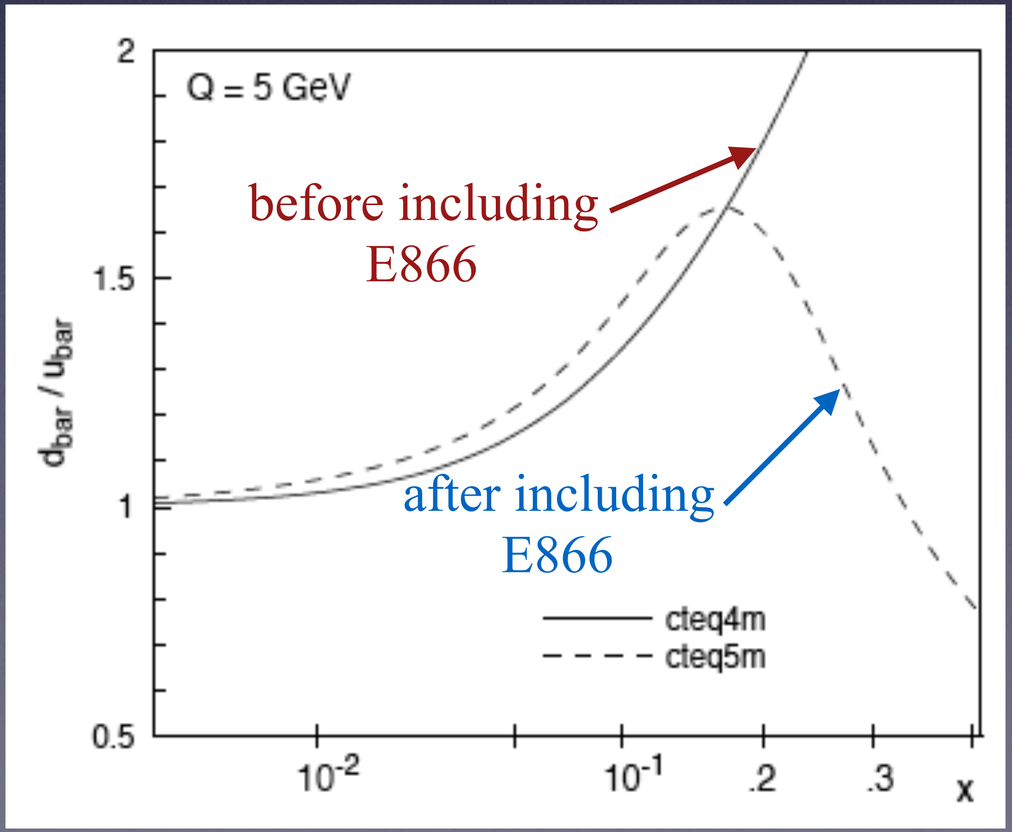

Flavor separation of valence quarks

- Tevatron measurements of the W-boson charge asymmetry probes the flavor separation of the up/down valence quark ratio

$$A_{ch}(y_W) = \frac{\frac{d\sigma^{W^+}}{dy_W} - \frac{d\sigma^{W^-}}{dy_W}}{\frac{d\sigma^{W^+}}{dy_W} + \frac{d\sigma^{W^-}}{dy_W}} \approx \frac{\frac{u(x_A)}{d(x_A)}\frac{\bar{d}(x_B)}{\bar{u}(x_B)} - 1}{\frac{u(x_A)}{d(x_A)}\frac{\bar{d}(x_B)}{\bar{u}(x_B)} + 1}$$

$$x_A = \frac{M_W}{\sqrt{s}} e^{y_W}; \quad x_B = \frac{M_W}{\sqrt{s}} e^{-y_W}$$

Assuming born kinematics and valence quarks domination of the cross section

- As y_W goes to its maximum value (large rapidity), x_B becomes small (while $x_A \rightarrow 1$) and the ratio dbar/ubar $\rightarrow$ 1. This allows us to constrain $u(x_A)/d(x_A)$.

Flavor separation of valence quarks

- Tevatron measurements of the W-boson charge asymmetry probes the flavor separation of the up/down valence quark ratio

electron charge asymmetry predicted using different codes and PDF sets

The intermediate rapidity range ($y_W \sim 1$) shows differences between MSTW and NNPDF when using the same code **(MC@NLO)**

The charge asymmetry dataset is needed to better determine the proton structure

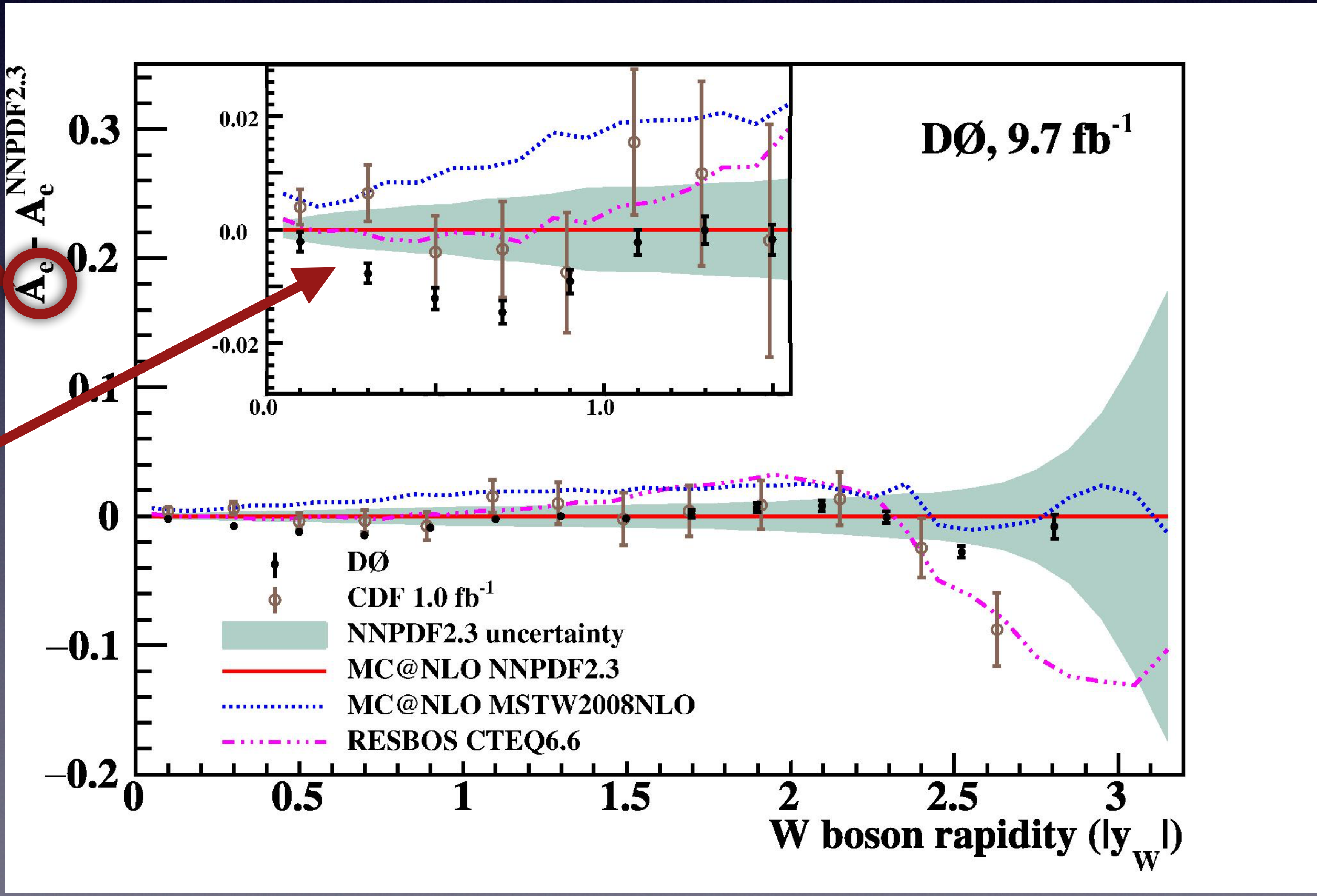

Gluon PDF from Z p_T

- New development: can constrain the intermediate-x gluon relevant for Higgs production using the Z-boson p_T spectrum

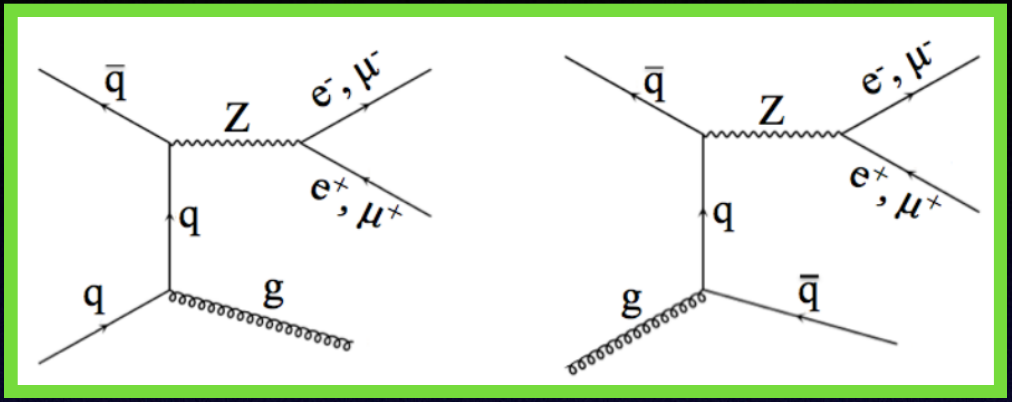

RB, Guffanti, Petriello, Ubiali 1705.00343

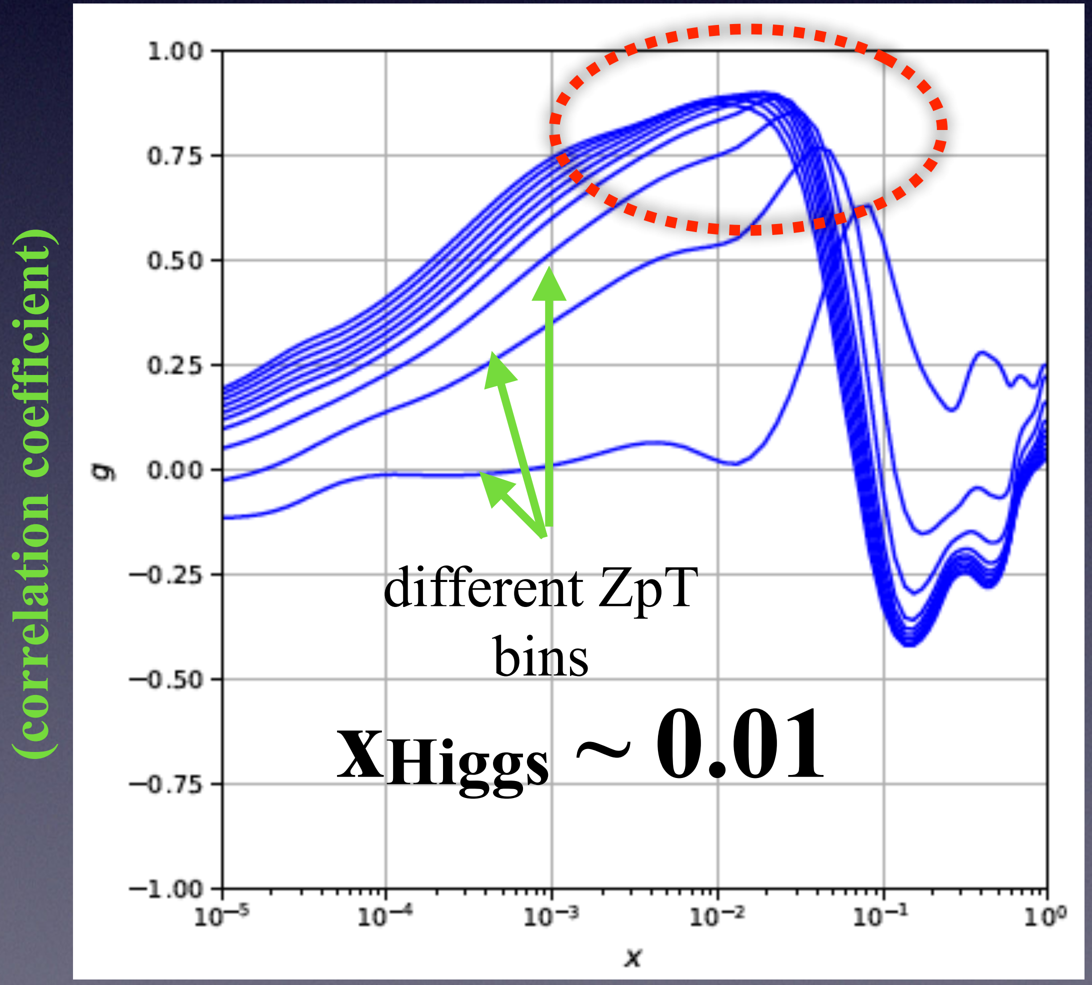

Z p_T is highly-correlated with gluon in x-region for Higgs

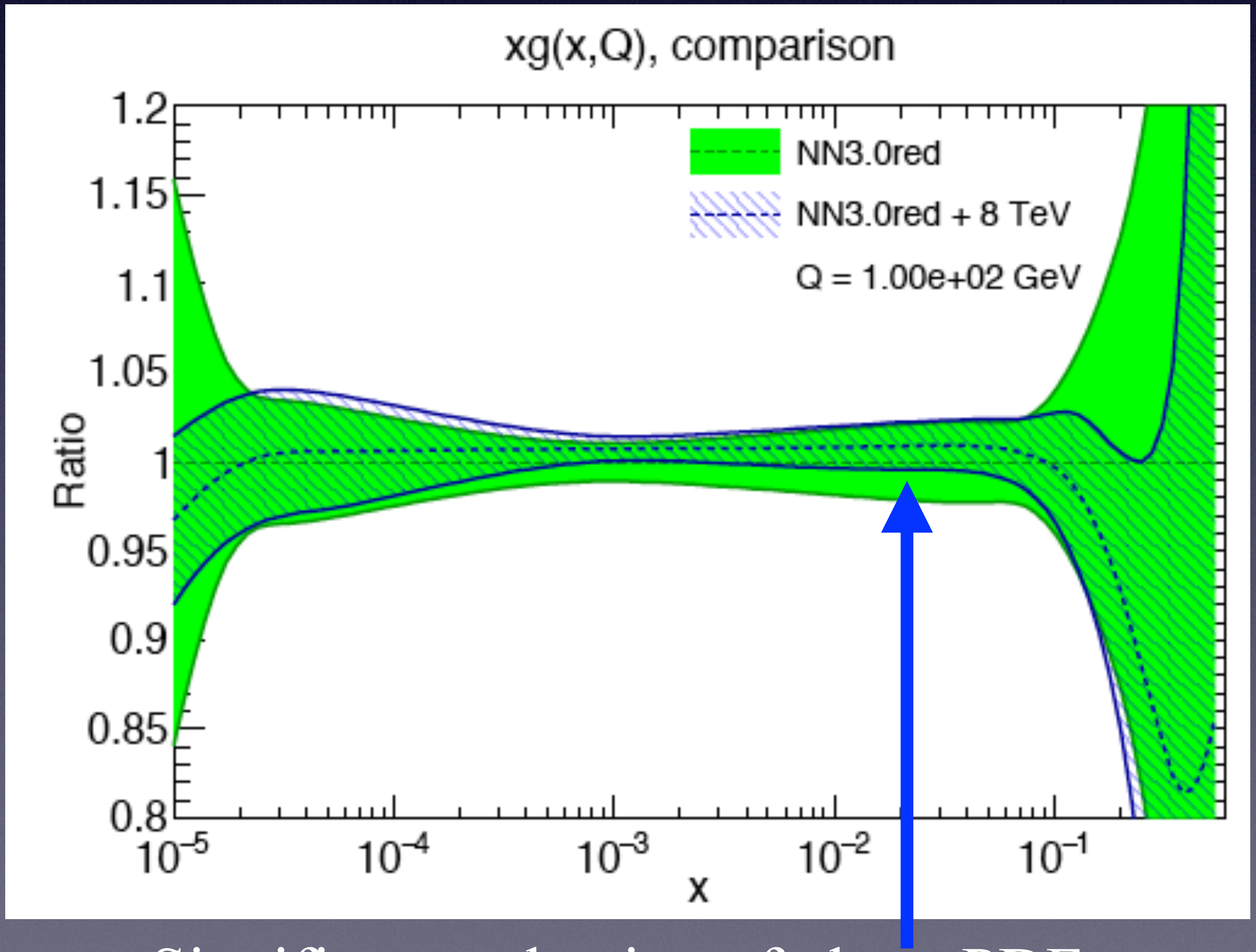

Significant reduction of gluon PDF error after including Z p_T

Predicting Drell-Yan in QCD Perturbation Theory

Predicting Cross Sections

- How does theory allow us to peer into the inner hard-scattering in a typical hadron collider process?

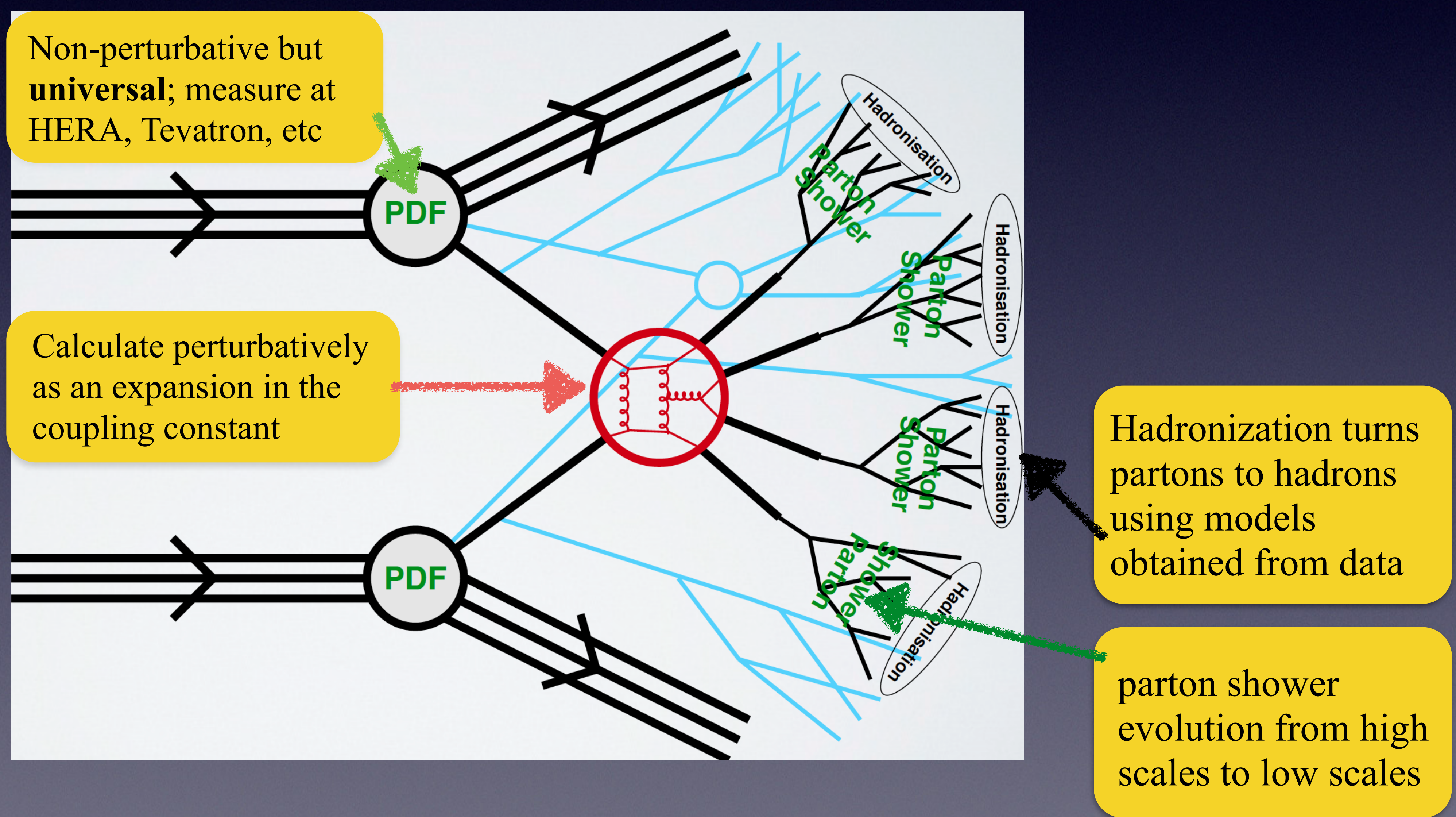

We rely on factorization: divide and conquer!

Predicting Hadronic Cross Sections

- The master equation for predicting hadronic cross sections neglecting power corrections:

renormalization scale

$$d\sigma = \sum_{a,b} \int dx_1 dx_2 \;\; f_a(x_1, \mu_F) f_b(x_2, \mu_F) \, d\hat{\sigma}_{ab \to X}(\hat{s}, \mu_F, \mu_R)$$

Parton density functions

Parton-level (differential) cross section

factorization scale

- Parton-level cross sections are obtained from the matrix elements. They are model and process dependent.

- Parton density functions (PDFs) are universal, i.e. process independent.

Predicting Partonic Cross Sections

$\hat{\sigma}_{ab\to X}(\hat{s}, \mu_F, \mu_R)$ Parton-level cross section

Computed perturbatively as an expansion in the coupling constant, for example the strong coupling:

$$\hat{\sigma} = \sigma^{\mathrm{Born}}\left(1 + \frac{\alpha_s}{2\pi}\sigma^{(1)} + \left(\frac{\alpha_s}{2\pi}\right)^2\sigma^{(2)} + \left(\frac{\alpha_s}{2\pi}\right)^3\sigma^{(3)} + \ldots\right)$$

Predicting Partonic Cross Sections

$\hat{\sigma}_{ab\to X}(\hat{s}, \mu_F, \mu_R)$ Parton-level cross section

Computed perturbatively as an expansion in the coupling constant, for example the strong coupling:

$$\hat{\sigma} = \sigma^{\mathrm{Born}}\left(1 + \frac{\alpha_s}{2\pi}\sigma^{(1)} + \left(\frac{\alpha_s}{2\pi}\right)^2\sigma^{(2)} + \left(\frac{\alpha_s}{2\pi}\right)^3\sigma^{(3)} + \dots\right)$$

known for up to W+5jets

known for most $2 \to 2$ processes (this is recent progress)

known for inclusive Higgs production

Predicting Partonic Cross Sections

Drell-Yan as an exemple:

$$\hat{\sigma} = \sigma^{\mathrm{Born}}\left(1 + \frac{\alpha_s}{2\pi}\sigma^{(1)} + \ldots\right)$$

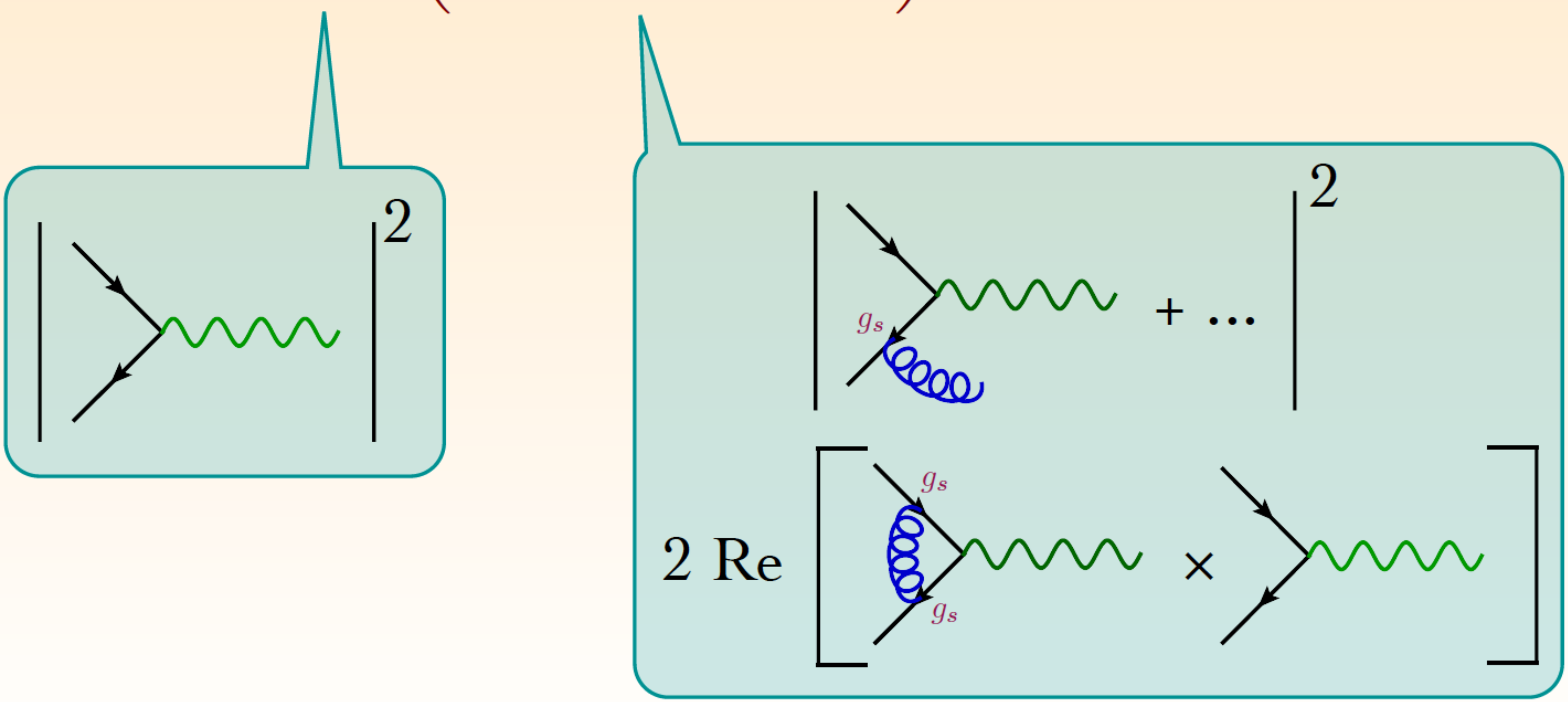

Predicting Partonic Cross Sections

Drell-Yan as an exemple:

$$\hat{\sigma} = \sigma^{\text{Born}}\left(1 + \frac{\alpha_s}{2\pi}\sigma^{(1)} + \dots\right)$$

Both real and virtual corrections are needed to cancel all singularities arising from soft and collinear emissions

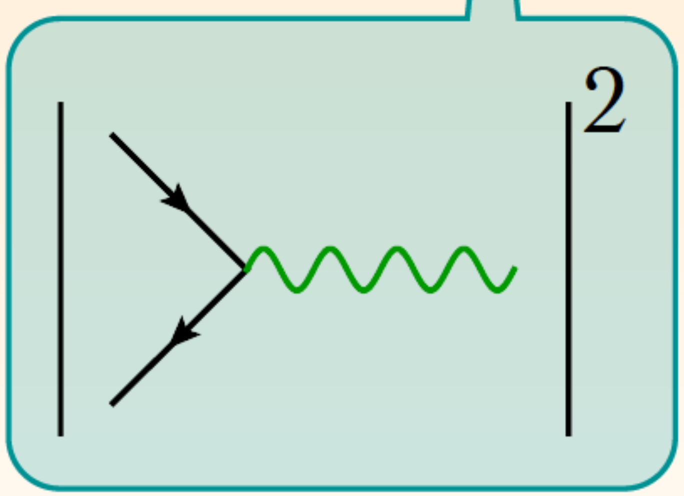

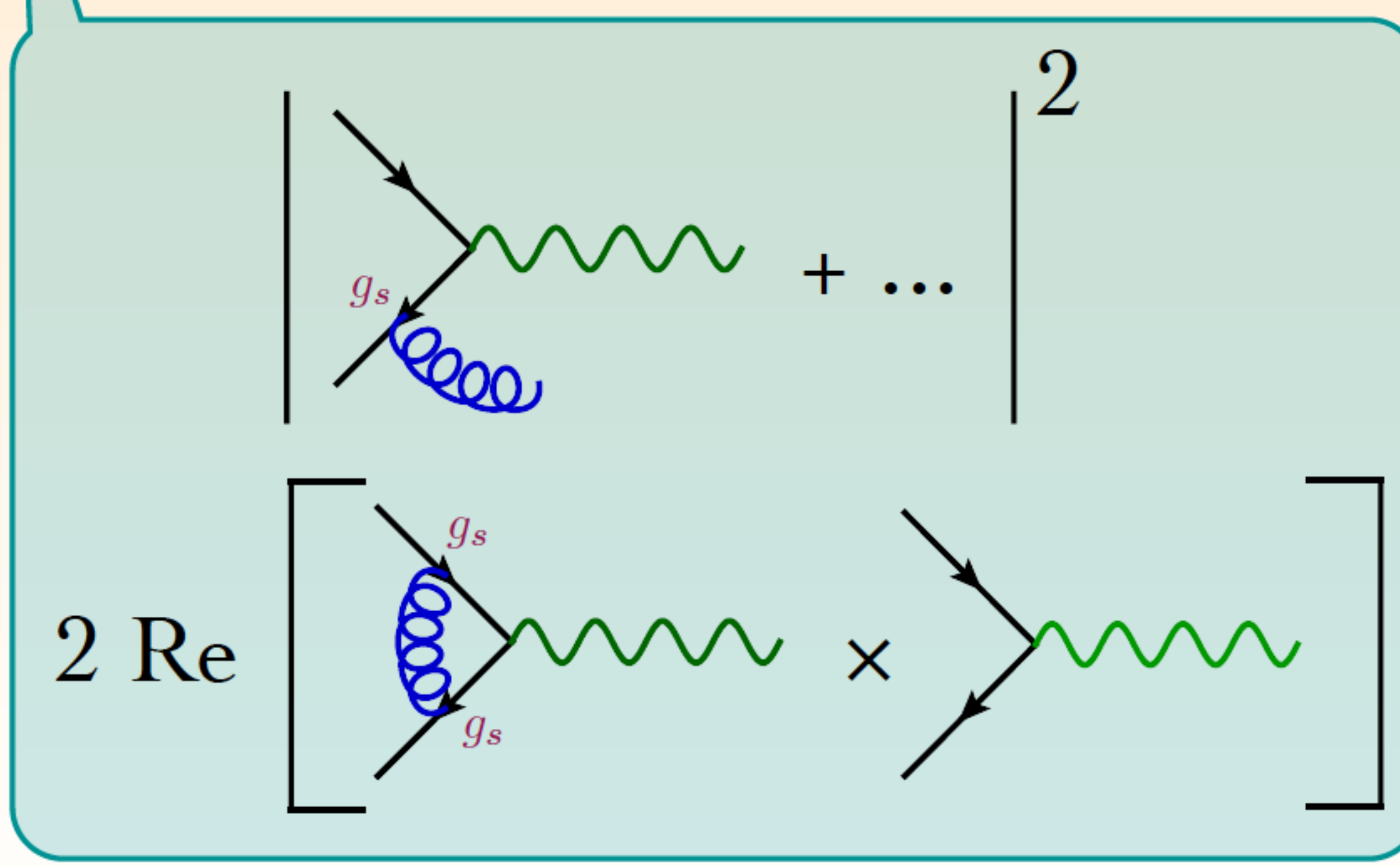

Predicting Partonic Cross Sections

$\hat{\sigma}_{ab\to X}(\hat{s}, \mu_F, \mu_R)$ Parton-level cross section

Computed perturbatively as an expansion in the coupling constant, for example the strong coupling:

$$\hat{\sigma} = \sigma^{\mathrm{Born}}\left(1 + \frac{\alpha_s}{2\pi}\sigma^{(1)} + \left(\frac{\alpha_s}{2\pi}\right)^2\sigma^{(2)} + \left(\frac{\alpha_s}{2\pi}\right)^3\sigma^{(3)} + \dots\right)$$

Including higher orders in the expansion improves the accuracy of our prediction and reduces the dependence on non-physical parameters such as μ_F and μ_R.

Predicting Partonic Cross Sections

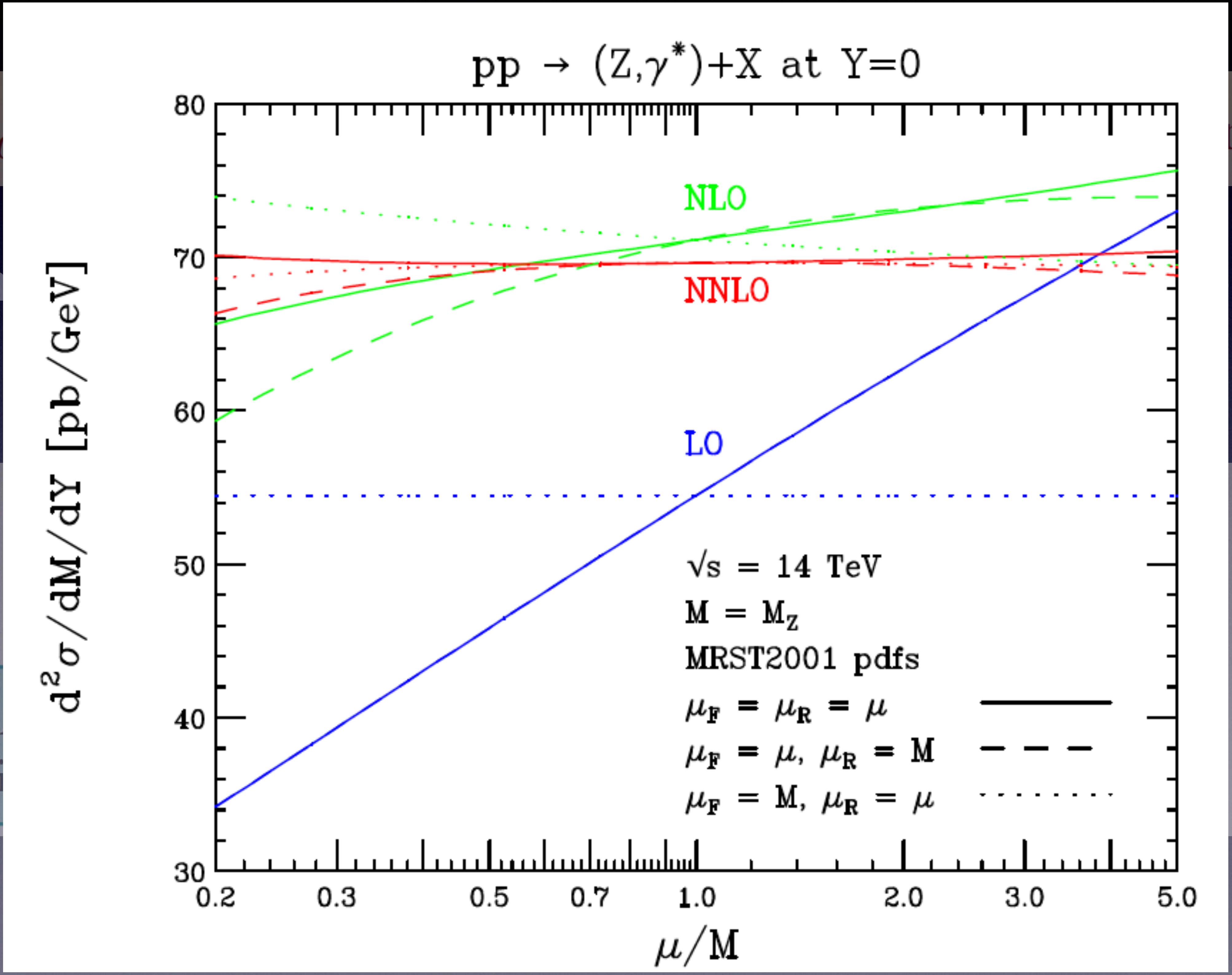

Anastasiou, Dixon, Melnikov, Petriello

Predicting Partonic Cross Sections

- LO tree-level predictions are not sufficient to describe the data. NLO QCD corrections were the first qualitatively reliable prediction.
  - ~50% increase in the cross section was observed for the rapidity distribution when going from LO ➞ NLO

$$Y = \frac{1}{2}\ln\left(\frac{E+p_z}{E-p_z}\right)$$

  - NNLO QCD results available for the inclusive and fully exclusive case, as well as Electroweak and QED corrections.
  - How about exact mixed QCD-EW and QCD-QED corrections? still not known

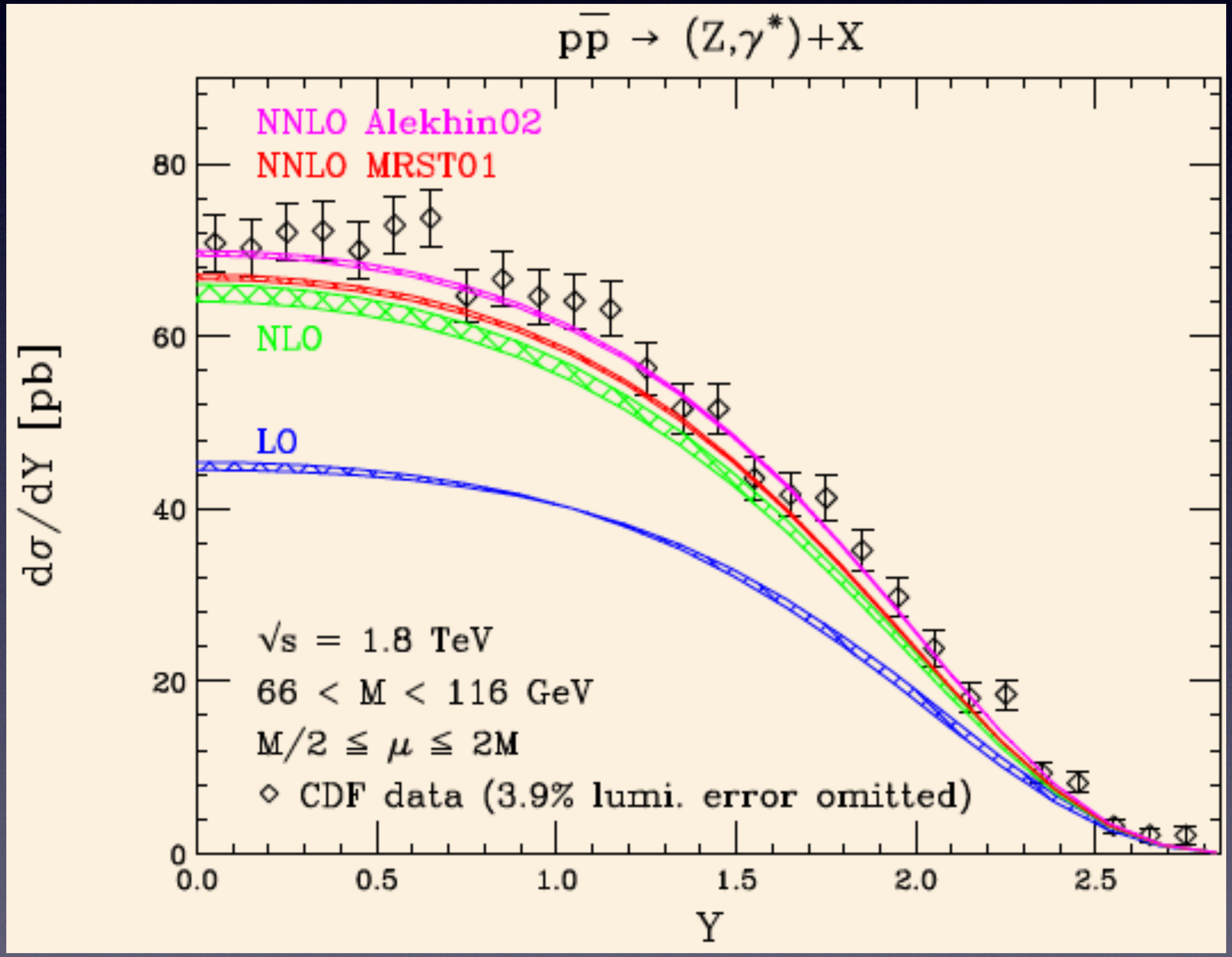

Anastasiou, Dixon, Melnikov, Petriello

Part II

Drell-Yan @ LO

Drell-Yan @ LO

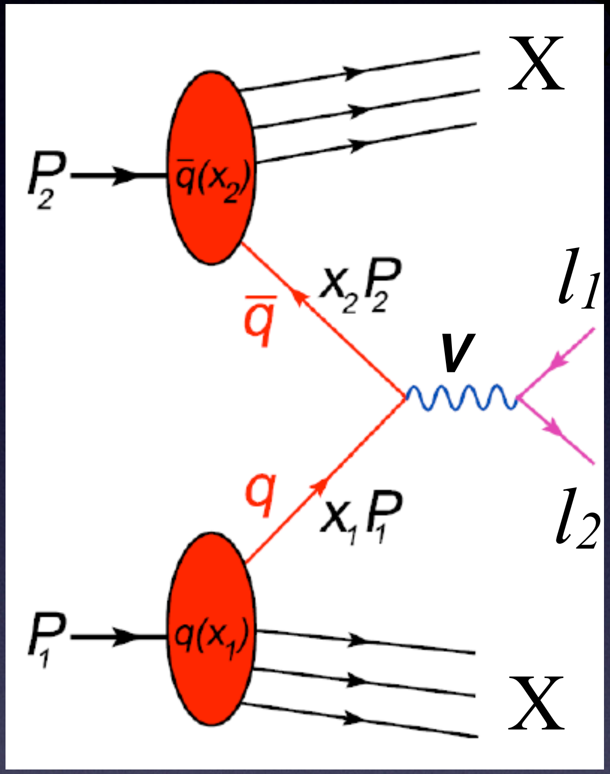

$$h(P_1) + h'(P_2) \to W^+(\to e^+ \nu_e) X$$

$$\hat{s} = S\, x_1\, x_2 = M^2_{l_1 l_2}$$

partonic s

hadronic s = $(P_1+P_2)^2$

Drell-Yan @ LO

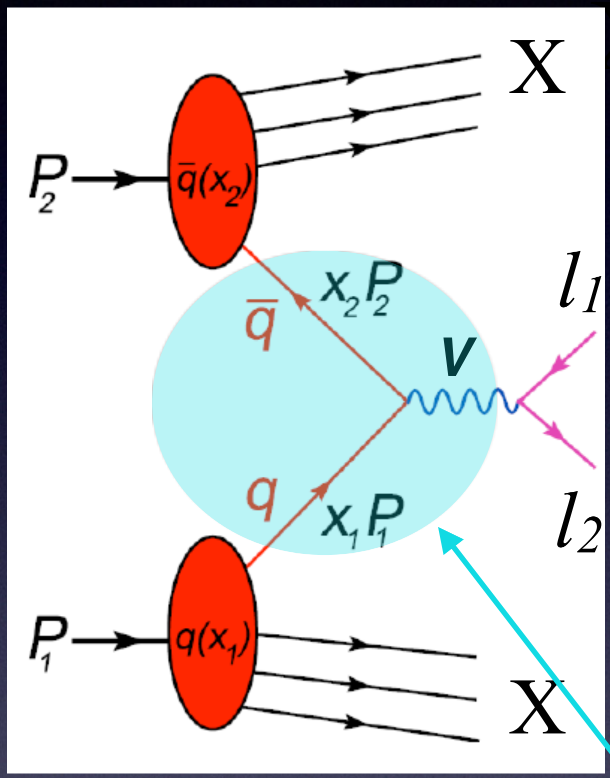

$$h(P_1) + h'(P_2) \to W^+(\to e^+\nu_e)X$$

$$\hat{s} = S\, x_1\, x_2 = M^2_{l_1 l_2}$$

partonic s

hadronic s = $(P_1+P_2)^2$

- LO partonic cross section:

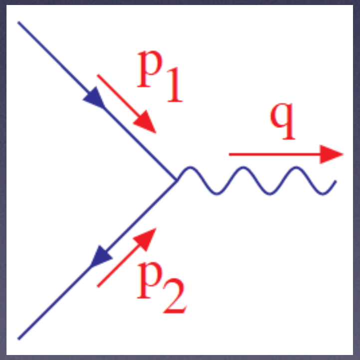

$p_1 = x_1 P_1,\ p_2 = x_2 P_2$

$$\hat{\sigma}_{q\bar{q}'} = \frac{1}{2\hat{s}} \int \frac{d^3q}{(2\pi)^3 2q_0} (2\pi)^4 \delta^4(p_1 + p_2 - q) \cdot \overline{|\mathcal{M}|}^2$$

Drell-Yan @ LO

- LO partonic cross section:

$$\hat{\sigma}_{q\bar{q}'} = \frac{1}{2\hat{s}} \int \frac{d^3q}{(2\pi)^3 2q_0} (2\pi)^4 \delta^4(p_1 + p_2 - q) \cdot \overline{|\mathcal{M}|}^2$$

where

$$\overline{|\mathcal{M}|}^2 = \underbrace{\left(\frac{1}{3}\cdot\frac{1}{3}\right)\left(\frac{1}{2}\cdot\frac{1}{2}\right)}_{\text{average color and spin}} \sum_{spin} \sum_{color} \left| \quad \right|^2$$

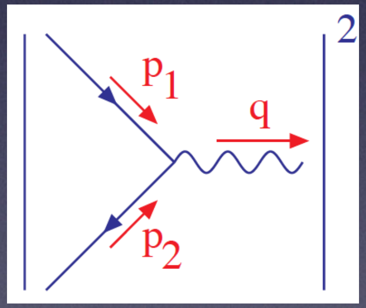

and

$$-i\mathcal{M}_\mu = \bar{v}(p_2) \frac{ig_w}{\sqrt{2}} \gamma_\mu \frac{1}{2}(1-\gamma_5) u(p_1)$$

Drell-Yan @ LO

- LO *partonic* cross section (for on-shell W):

$$\boxed{\hat{\sigma}_{q\bar{q}',LO} = \frac{\pi}{12\,\hat{s}} g_w^2\, \delta(1-z)} \qquad z = \frac{M_{l\nu}^2}{\hat{s}}$$

- LO *hadronic* cross section:

$$\sigma_{q\bar{q}',LO} = \int_0^1 dx_1 dx_2 \underbrace{\sum_q \left(q(x_1)\bar{q}'(x_2) + \bar{q}(x_1)q'(x_2)\right)}_{\text{quark PDFs}}\ \hat{\sigma}(\hat{s}, z)$$

Drell-Yan @ NLO in QCD

Drell-Yan @ NLO in QCD

- Several ingredients contribute to the NLO QCD cross section for Drell-Yan:
  - Virtual corrections for the $q\bar{q}'$ channel:

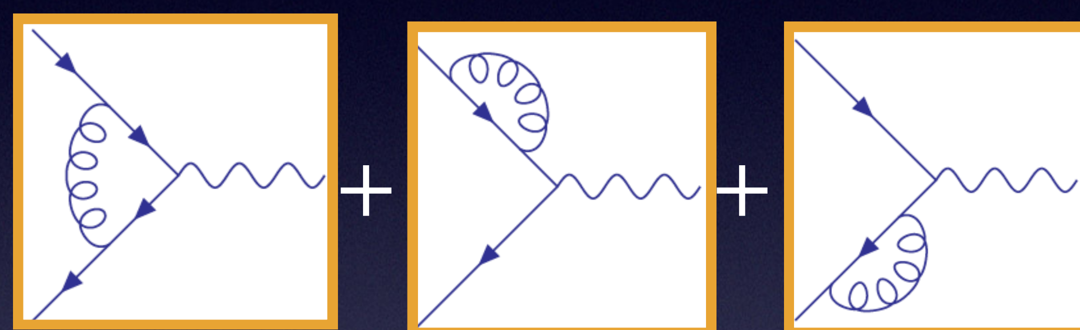

  - Real corrections for the $q\bar{q}'$ channel:

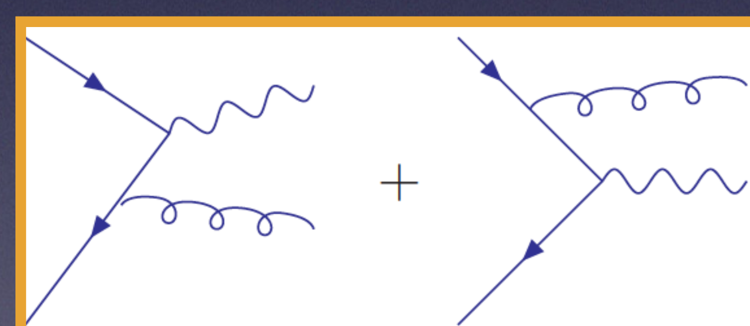

  - Real corrections for the qg and $g\bar{q}'$ channel:

These are new channels that appear for the first time at NLO!

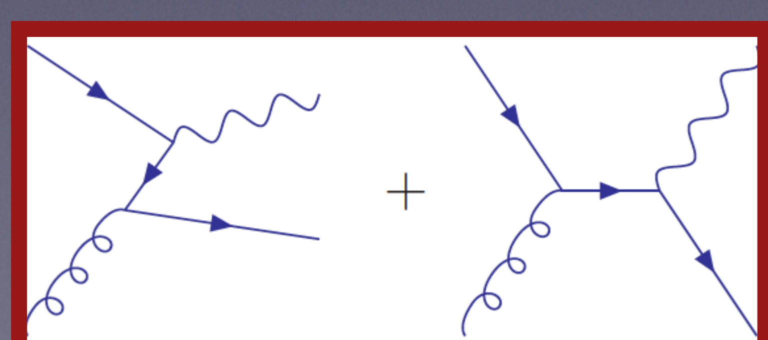

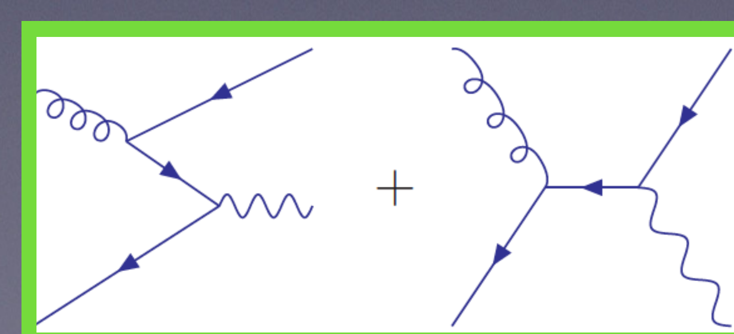

Drell-Yan @ NLO in QCD

- Feynman rules:

Quark-propagator

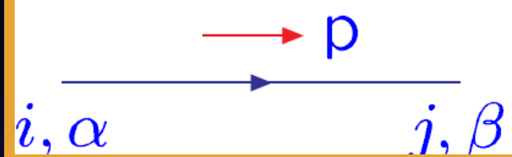

$$\frac{i(\not{p}+m)_{\beta\alpha}}{p^2-m^2+i\epsilon}\delta_{ij}$$

$i,j=1,..3$

Gluon-propagator

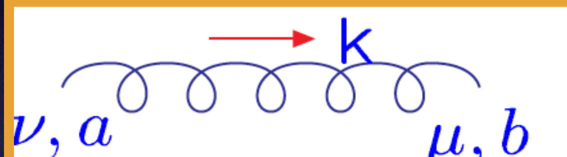

$$\frac{i(-g_{\mu\nu})}{k^2+i\epsilon}\delta_{ab}$$

$a,b=1,..8$

Quark-W vertex

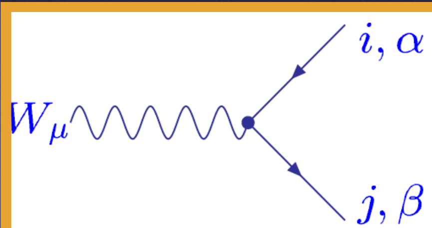

$$i\frac{g_W}{\sqrt{2}}(\gamma_\mu)_{\beta\alpha}\frac{(1-\gamma_5)}{2}\delta_{ij}$$

$g_w = \frac{e}{\sin\theta_w}$, weak coupling

Quark-gluon vertex

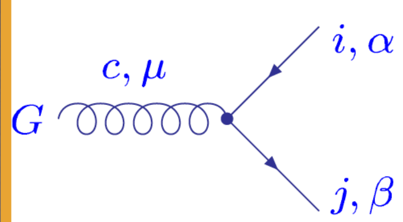

$$-ig\,(t_c)_{ji}\,(\gamma_\mu)_{\beta\alpha}$$

t_c is the $SU(N)_{N\times N}$ generator

Color generators for the quarks

$$[t_a, t_b] = if_{abc}t_c$$

$$\sum_c t_c^2 = C_F\, I_{N\times N}$$

$$C_F = \frac{N^2-1}{2N} = \frac{4}{3}\ , \quad (N=3)$$

$$Tr(\sum_c t_c^2) = N\, C_F$$

Drell-Yan @ NLO in QCD

- The UV and IR problem and the need for dimensional regularization:

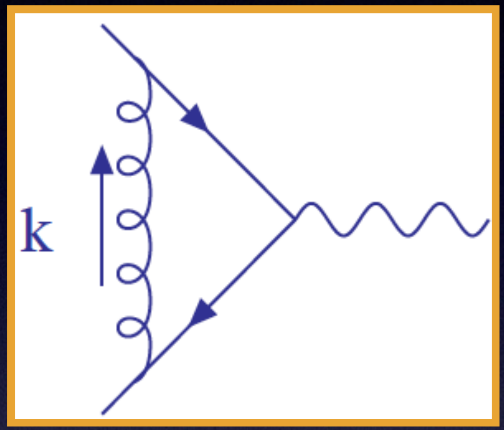

$$\sim \int_0^\infty d^4k \, \frac{\not{k} \; \not{k}}{k^2 \, k^2 \, k^2} \to \infty \text{ for } (k \to \infty)$$

UV logarithmic divergence

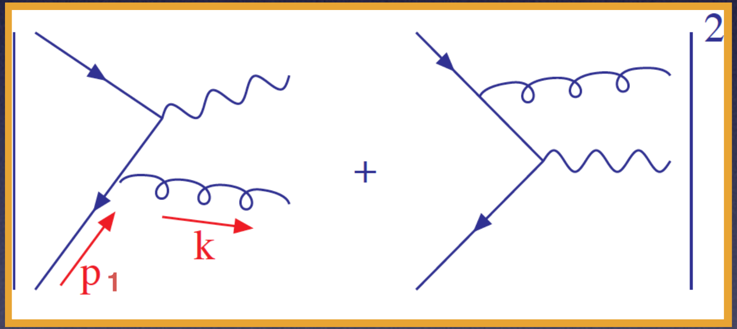

$$\sim \int d^3k \, \frac{1}{(p_1 - k)^2 \, (p_2 - k)^2} \to \infty \;\; \text{for } (k \to 0) \;\; \text{or } (k \parallel p_i)$$

IR soft/collinear divergence

- We will work in dimensional regularization where **d = 4-2ϵ** to regulate the UV and IR singularities in intermediate steps. These singularities will appear as **1/ϵ poles**.
- In general UV poles are removed using UV renormalization. Soft poles cancel in the sum of real and virtual diagrams. Remaining initial-state collinear poles are removed using PDF renormalization (also called mass factorization).

Drell-Yan @ NLO in QCD

- In **d = 4-2ϵ** the LO partonic cross section becomes:

$$\boxed{\hat{\sigma}_{q\bar{q}',LO} = \frac{\pi}{12\,\hat{s}} g_w^2\,(1-\epsilon)\,\delta(1-z)} \qquad z = M_{l\nu}^2/\hat{s}$$

can rewrite it as: $\hat{\sigma}_{q\bar{q}',LO} = \sigma_0\,\delta(1-z)$

- In d-dimensions, the strong coupling constant has a mass dimension, i.e.$[g_s] \sim \mu^{\epsilon}$ when ϵ is not 0. The Feynamn rules should read $g_s \to g_s\,\mu^{\epsilon}$

  Fermion field: $[\psi] \sim \mu^{\frac{d-1}{2}}$ gluon field: $[G] \sim \mu^{\frac{d-2}{2}}$

- In d-dimensions, gluons have d-2 = 2-2ϵ polarizations. This changes the spin averaging over the initial state, which is relevant for the qg and gq channels. The number of quark polarizations is 2.

Drell-Yan @ NLO in QCD

- The virtual corrections for the $q\bar{q}'$ channel:

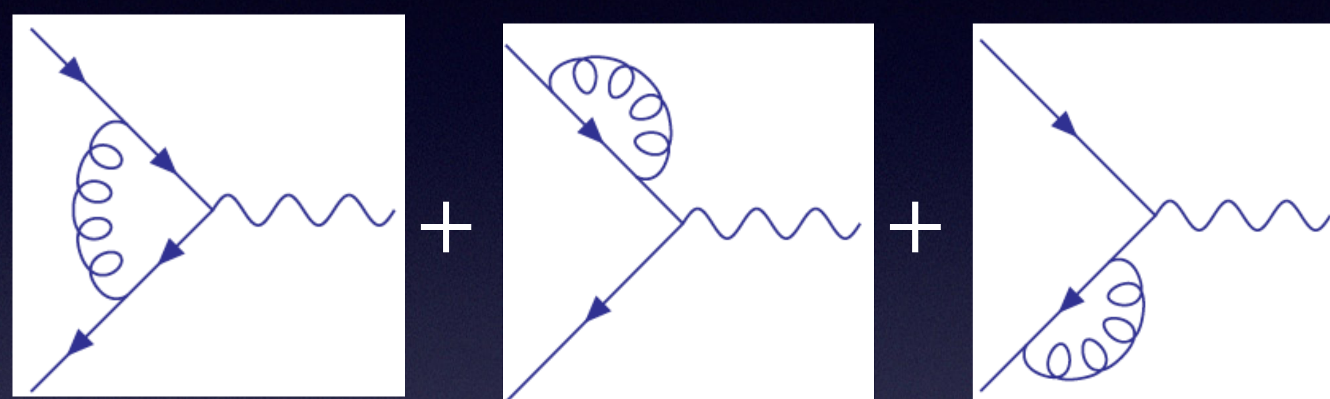

- In dimensional regularization, external self-energy diagrams vanish for massless quarks as the corresponding integral is scaleless:

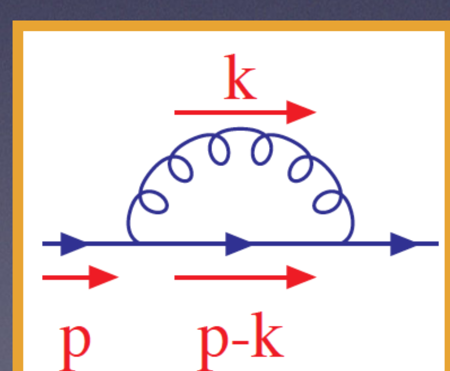

$= 0$ (prove this as an exercise)

- We therefore need to consider the vertex 1-loop diagram only

Drell-Yan @ NLO in QCD

- The virtual vertex corrections for the $q\bar{q}'$ channel taking only $O(g_s^2)$:

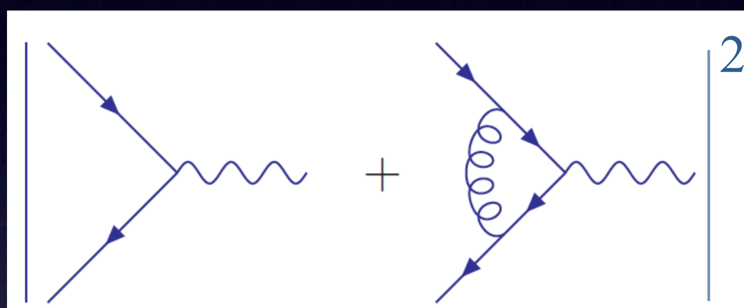

$\rightarrow 2\,Re\,($ { 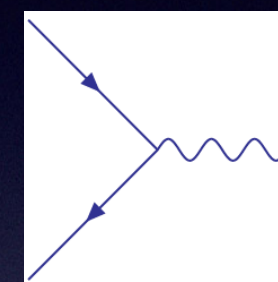 $\}^*$ x 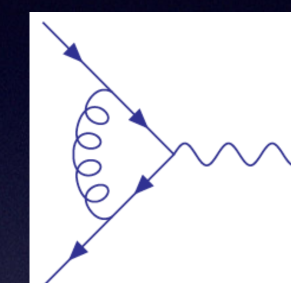)

- Let's work on the $O(g_s^2)$ vertex:

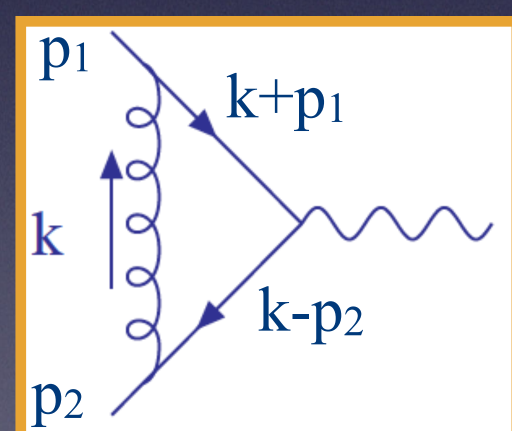

$= V_{q\bar{q}'}$

$$V_{q\bar{q}'} = -\frac{g_w}{2\sqrt{2}} g_s^2 \mu^{2\epsilon} \int \frac{d^d k}{(2\pi)^d} \frac{\bar{v}(p_2)\gamma^\mu(\not{k}- \not{p}_2)\ \not{\epsilon}_w(1-\gamma_5)(\not{k}+ \not{p}_1)\gamma_\mu u(p_1)}{k^2(k+p_1)^2(k-p_2)^2}$$

Drell-Yan @ NLO in QCD

- Combine the denominators using the following Feynman parametrization, then shift the momentum $k \to k - xp_1 + yp_2$

$$\frac{1}{a\,b\,c} = 2\int_0^1 dx\,dy\,dz\,\delta(1-x-y-z)\,\frac{1}{[x\,a + y\,b + c\,z]^3}$$

- The shift leads to the simplified integral:

abbreviated numerator

$$V_{q\bar{q}'} = -\frac{g_w}{2\sqrt{2}}g_s^2\mu^{2\epsilon}\int_0^1 dx\,dy\,dz\,\delta(1-x-y-z)\int\frac{d^dk}{(2\pi)^d}\frac{N}{(k^2 + x\,y\,\hat{s})^3}$$

- Applying the same shift to the numerator, keeping in mind that terms odd in k^μ integrate to zero, and using on-shell conditions leads to the following numerator:

$$N = -2(1-\epsilon)\,\frac{2-d}{d}\,k^2\,\bar{v}(p_2)\;\not{\epsilon}_w(1-\gamma_5)\,u(p_1)$$
$$-2\hat{s}\,\bar{v}(p_2)\;\not{\epsilon}_w(1-\gamma_5)\,u(p_1)\;((1-x)(1-y) - \epsilon xy)$$

Drell-Yan @ NLO in QCD

- Our integral now becomes:

$$V_{q\bar{q}'} = -iM_{LO}\, 2\, g_s^2\, \mu^{2\epsilon}\, \int_0^1 dx\, dy\, dz\, \delta(1-x-y-z)\, \int \frac{d^d k}{(2\pi)^d} \frac{1}{(k^2 + x\, y\, \hat{s})^3}$$
$$\times \left[\frac{4\,(1-\epsilon)^2\, k^2}{d} - 2\hat{s}\,((1-x)(1-y) - \epsilon x y) \right]$$

with $$\boxed{-iM_{LO} = -\frac{g_w}{2\sqrt{2}}\, \bar{v}(p_2)\ \not{\epsilon}_w (1-\gamma_5)\, u(p_1)}$$

- It remains to do the loop integral. We use the following results:

$$\int \frac{d^d k}{(2\pi)^d} \frac{1}{[k^2 - \Delta]^3} = -i\, \frac{\Gamma[1+\epsilon]}{2\,(4\pi)^{d/2}}\, \Delta^{-1-\epsilon}$$

$$\int \frac{d^d k}{(2\pi)^d} \frac{k^2}{[k^2 - \Delta]^3} = i\, \frac{d}{4}\, \frac{\Gamma[1+\epsilon]}{\epsilon}\, \frac{\Delta^{-\epsilon}}{(4\pi)^{d/2}}$$

and get:

UV-divergence

$$V_{q\bar{q}'} = -iM_{LO}\, g_s^2\, \mu^{2\epsilon}\, \frac{\Gamma(1+\epsilon)}{(4\pi)^{d/2}}\, i \int_0^1 dx\, dy\, dz\, (-x\, y\, \hat{s})^{-\epsilon}\, \delta(1-x-y-z) \left\{ \frac{2\,(1-\epsilon)^2}{\epsilon} + \frac{2\hat{s}\,((1-x)(1-y) - \epsilon\, x\, y)}{(-x\, y\, \hat{s})} \right\}$$

Soft+Collinear divergences

Drell-Yan @ NLO in QCD

- Doing the parametric integrals, adding the color structure $[T^aT^a]_{ij}$ (i and j are the quark color indices), and taking the *2 Re(*$V_{q\bar{q}'}M^*_{LO}$*)*:

$$2Re(V_{q\bar{q}'}\, M^*_{LO}) = |M_{LO}|^2\, C_F\, \left(\frac{\alpha_s}{2\pi}\right) \left(\frac{\hat{s}}{4\pi\mu^2}\right)^{-\epsilon} \frac{\Gamma(1-\epsilon)}{\Gamma(1-2\epsilon)} \left(\frac{-2}{\epsilon^2} - \frac{3}{\epsilon} + \frac{2\pi^2}{3} - 8\right)$$

$$\boxed{\sigma^{\text{virtual}}_{NLO,q\bar{q}'} = \sigma_{LO}\, C_F\, \left(\frac{\alpha_s}{2\pi}\right) \left(\frac{\hat{s}}{4\pi\mu^2}\right)^{-\epsilon} \frac{\Gamma(1-\epsilon)}{\Gamma(1-2\epsilon)} \left(\frac{-2}{\epsilon^2} - \frac{3}{\epsilon} + \frac{2\pi^2}{3} - 8\right)}$$

- Need the real radiation contributions as well:

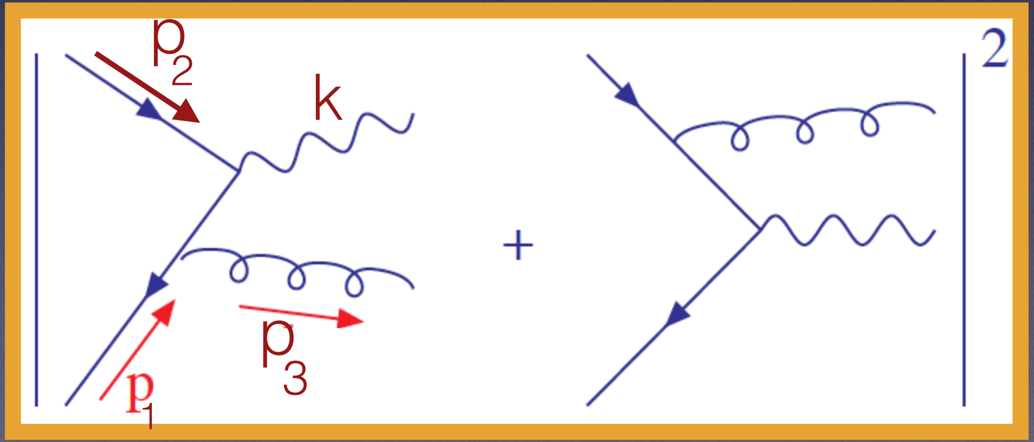

$$\hat{\sigma} = \frac{1}{2\,\hat{s}}\overline{|\mathcal{M}|}^2 \cdot \mathcal{PS}_2$$ and

$$\hat{s} = (p_1 + p_2)^2 = 2\,p_1 \cdot p_2$$
$$\hat{t} = (p_1 - p_3)^2 = -2\,p_1 \cdot p_3$$
$$\hat{u} = (p_2 - p_3)^2 = -2\,p_2 \cdot p_3$$

Drell-Yan @ NLO in QCD

$$\overline{|\mathcal{M}_{q\bar{q}'}|}^2 = -\underbrace{\left(\frac{1}{2}\cdot\frac{1}{2}\right)}_{\text{spin avg.}}\underbrace{\left(\frac{1}{3}\cdot\frac{1}{3}\right)}_{\text{color avg.}}\cdot Tr(T^aT^a)\cdot(g\mu^\epsilon)^2\cdot g_w^2\cdot 2(1-\epsilon)$$

$$\cdot\left((1-\epsilon)\left(-\frac{\hat{u}}{\hat{t}}-\frac{\hat{t}}{\hat{u}}\right)-\frac{2\hat{s}M^2}{\hat{t}\hat{u}}+2\epsilon\right)$$

$$PS_2 = \frac{1}{8\pi}\left(\frac{4\pi}{M^2}\right)^\epsilon\frac{1}{\Gamma(1-\epsilon)}z^\epsilon(1-z)^{1-2\epsilon}\int_0^1 dy(y(1-y))^{-\epsilon}$$

with

$$y = \tfrac{1}{2}\left(1+cos\theta\right)$$

$$\hat{t} = -\hat{s}\left(1-\tfrac{M^2}{\hat{s}}\right)(1-y)$$

$$\hat{u} = -\hat{s}\left(1-\tfrac{M^2}{\hat{s}}\right)y$$

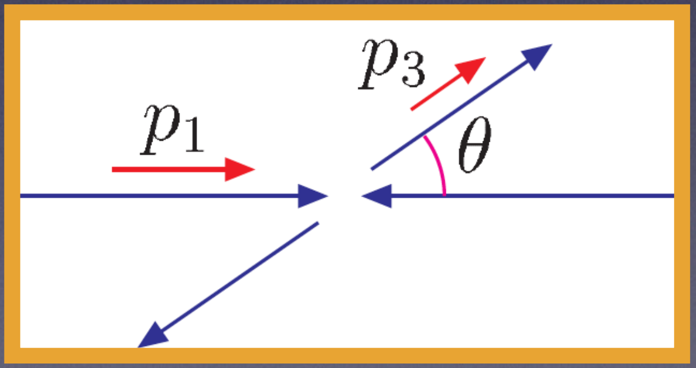

partonic CM frame

and $\int_0^1 dy\, y^\alpha\,(1-y)^\beta = \frac{\Gamma(1+\alpha)\,\Gamma(1+\beta)}{\Gamma(2+\alpha+\beta)}$, $z = M^2/\hat{s}$ and $M{=}M_W$

Drell-Yan @ NLO in QCD

- The result for the real radiation contribution for the $q\bar{q}'$ is:

$$\hat{\sigma}^R_{q\bar{q}',NLO} = \sigma_0\, C_F\, \left(\frac{\alpha_s}{2\pi}\right) \left(\frac{\hat{s}}{4\pi\mu^2}\right)^{-\epsilon} \frac{\Gamma(1-\epsilon)}{\Gamma(1-2\epsilon)} \left\{ \frac{2}{\epsilon^2}\delta(1-z) - \frac{2}{\epsilon}\frac{1+z^2}{(1-z)_+} + 4(1+z^2)\left[\frac{\ln(1-z)}{1-z}\right]_+ \right\}$$

You will need to use the plus-distribution expansion defined through the following formulae:

$$\frac{1}{(1-z)^{1+2\epsilon}} = -\frac{1}{2\epsilon}\delta(1-z) + \frac{1}{(1-z)_+} - 2\epsilon\left[\frac{\ln(1-z)}{(1-z)}\right]_+ + \ldots$$

$$\int_0^1 dz \left[\frac{\ln^n(1-z)}{1-z}\right]_+ f(z) = \int_0^1 dz\, \frac{\ln^n(1-z)}{1-z}\, (f(z) - f(1))$$

- Combining this result with the virtual corrections one shown on a previous slide leads to:

$$\hat{\sigma}_{q\bar{q}',NLO} = \sigma_0\, C_F\, \left(\frac{\alpha_s}{2\pi}\right) \left(\frac{\hat{s}}{4\pi\mu^2}\right)^{-\epsilon} \frac{\Gamma(1-\epsilon)}{\Gamma(1-2\epsilon)} \left\{ \frac{-2}{\epsilon} P_{qq}(z) + \left(\frac{2\pi^2}{3} - 8\right)\delta(1-z) + 4(1+z^2)\left[\frac{\ln(1-z)}{1-z}\right]_+ \right\}$$

where $$P_{qq}(z) = \frac{3}{2}\,\delta(1-z) + \frac{1+z^2}{(1-z)_+}$$

- While the leading pole cancels in the sum of real and virtual corrections for the $q\bar{q}'$ channel, the left over $1/\epsilon$ pole requires performing mass factorization (also called PDF renormalization), in order to cancel it.

Drell-Yan @ NLO in QCD

- Absorb remaining initial-state collinear singularities into PDFs, which amounts to adding the following counterterm:

One for each PDF

$$2 \times \frac{\alpha_s}{2\pi} \left(\frac{4\pi}{e^\gamma}\right)^\epsilon \frac{1}{\epsilon} P_{qq} \otimes \hat{\sigma}_0(z) \quad \text{where} \quad f \otimes g(z) = \int_0^1 dx\, dy\, f(x)\, g(y)\, \delta(z - xy)$$

$$2 \times \frac{\alpha_s}{2\pi} \left(\frac{4\pi}{e^\gamma}\right)^\epsilon \frac{1}{\epsilon} P_{qq} \otimes \hat{\sigma}_0(z) = 2 \times \frac{\alpha_s}{2\pi} \left(\frac{4\pi}{e^\gamma}\right)^\epsilon \frac{C_F}{\epsilon} \sigma_0\, P_{qq}(z)$$

- Arrive at the final result (we have switched to the MSbar scheme):

$$\boxed{\hat{\sigma}_{q\bar{q}',NLO} = \sigma_0\, C_F \left(\frac{\alpha_s}{2\pi}\right) \left\{2 \ln\left(\frac{\hat{s}}{\mu^2}\right) P_{qq}(z) + \left(\frac{2\pi^2}{3} - 8\right)\delta(1-z) + 4(1+z^2) \left[\frac{\ln(1-z)}{1-z}\right]_+ \right\}}$$

Drell-Yan @ NLO in QCD

- The $g\bar{q}$' channel:

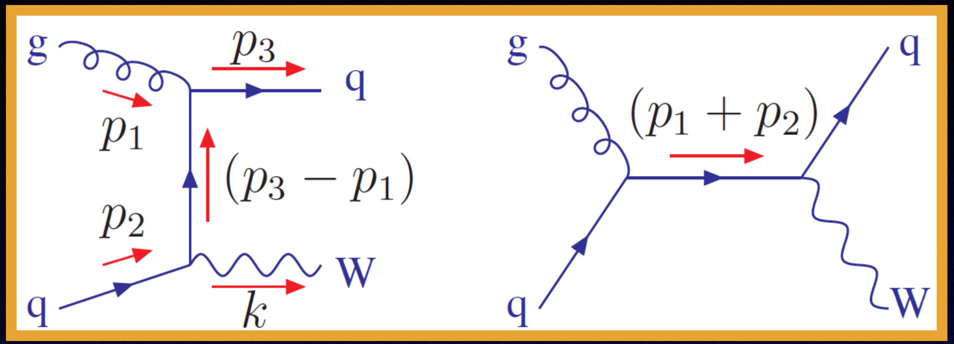

$$\hat{\sigma} = \frac{1}{2\,\hat{s}} \overline{|\mathcal{M}|}^2 \cdot \mathcal{PS}_2 \quad \text{and} \quad \begin{aligned} \hat{s} &= (p_1 + p_2)^2 = 2\,p_1 \cdot p_2 \\ \hat{t} &= (p_1 - p_3)^2 = -2\,p_1 \cdot p_3 \\ \hat{u} &= (p_2 - p_3)^2 = -2\,p_2 \cdot p_3 \end{aligned}$$

$$\overline{|\mathcal{M}|}^2 = \underbrace{\left(\frac{1}{2\,(1-\epsilon)}\frac{1}{2}\right)}_{\text{spin avg.}} \underbrace{\left(\frac{1}{3}\cdot\frac{1}{8}\right)}_{\text{color avg.}} \cdot Tr(t^a t^a) \cdot (g_s \mu^\epsilon)^2 \cdot g_w^2 \cdot 2(1-\epsilon)$$

$$\cdot \left((1-\epsilon)\left(-\frac{\hat{s}}{\hat{t}} - \frac{\hat{t}}{\hat{s}}\right) - \frac{2\hat{u}M^2}{\hat{t}\hat{s}} + 2\epsilon \right)$$

$$PS_2 = \frac{1}{8\pi}\left(\frac{4\pi}{M^2}\right)^\epsilon \frac{1}{\Gamma(1-\epsilon)} z^\epsilon (1-z)^{1-2\epsilon} \int_0^1 dy (y(1-y))^{-\epsilon}$$

Drell-Yan @ NLO in QCD

- The $g\bar{q}$' channel:

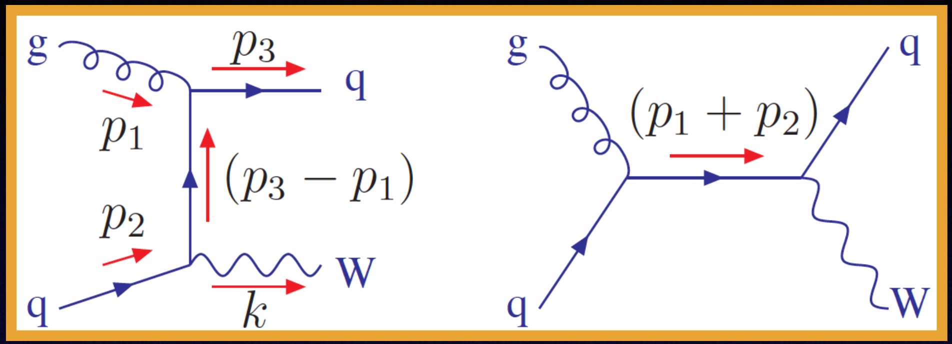

$$\hat{\sigma}_{gq'} = \sigma_0 \frac{\alpha_s}{2\pi} \cdot \left\{ 2 \cdot \underbrace{\left(\frac{1}{2}(z^2 + (1-z)^2) \right)}_{P_{gq}^{(0)}(z)} \cdot \left[\ln\left(\frac{M^2}{\mu^2}\right) + \ln\left(\frac{(1-z)^2}{z}\right) \right] + \frac{3}{4} + \frac{z}{2} - \frac{3}{4} z^2 \right\}$$

- The cross section for the *qg* channel is identical to the $g\bar{q}$' cross section since we are integrating inclusively over the final state.

$$\hat{\sigma}_{qg} = \hat{\sigma}_{g\bar{q}'}$$

Vector Boson Production in Association With Jets

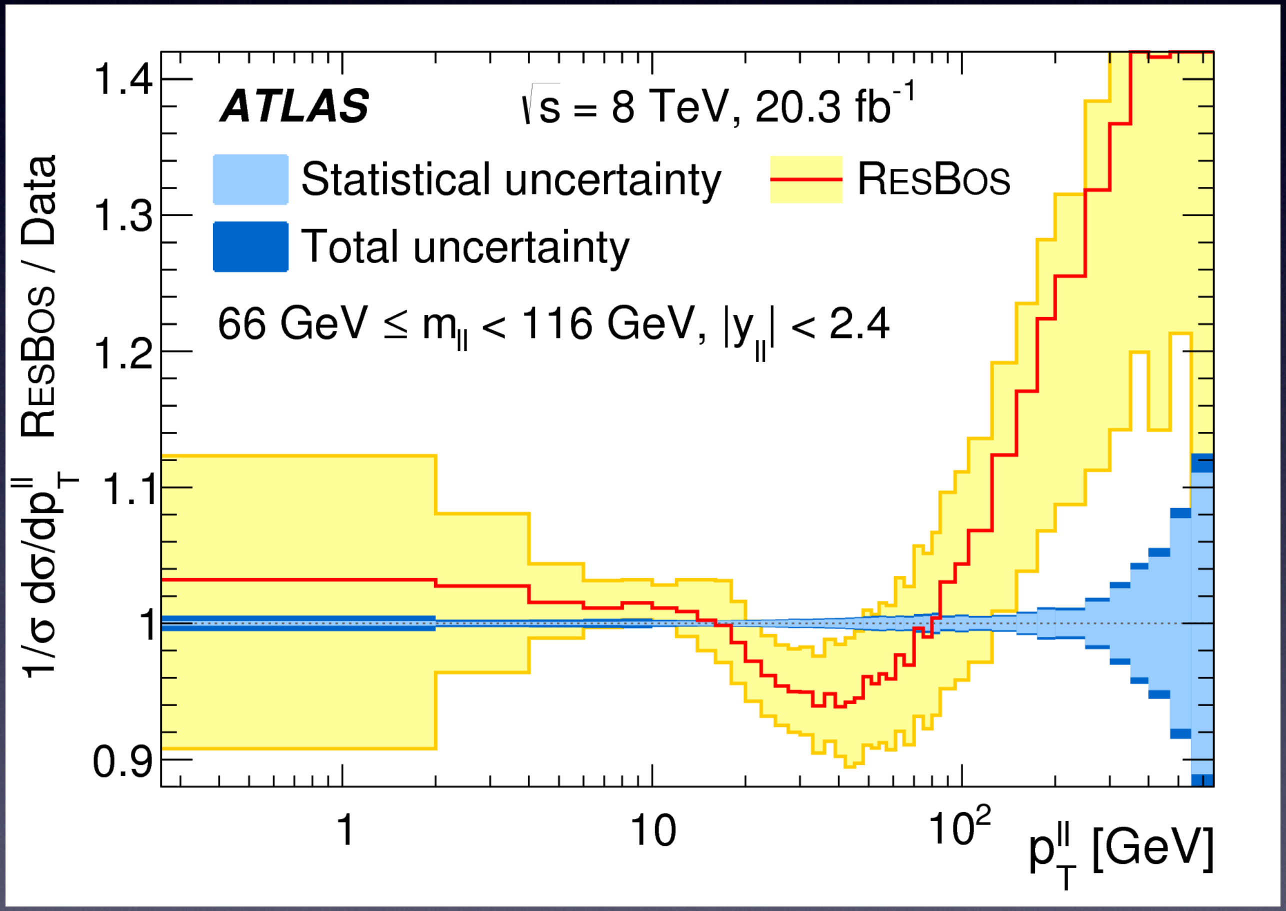

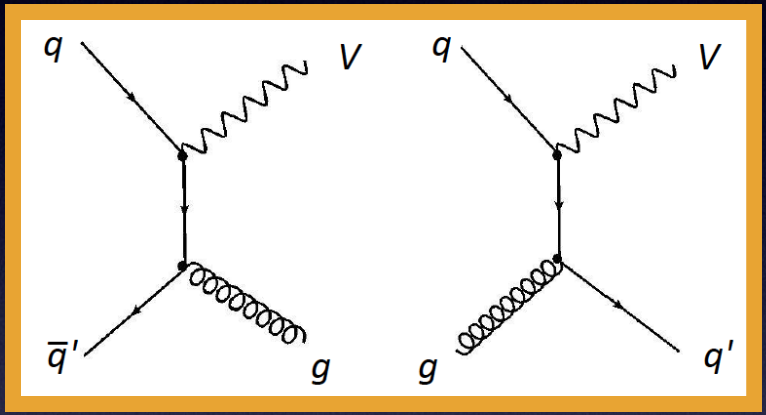

LO

Total experimental uncertainty up to 200 GeV for the P_{TZ} is < 1%

- V+j processes are associated with many signals of BSM physics, such as SUSY and dark matter
- They provide stringent tests of the SM, as they are measured with small errors over a large energy range.
- Important for improving PDFs and detector calibration as well.

Jets

- Jets: collimated, energetic bunch of particles
- They date back to the late 1970s Sterman & Weinberg, Phys. Rev. Lett. 39 1436 (1977)

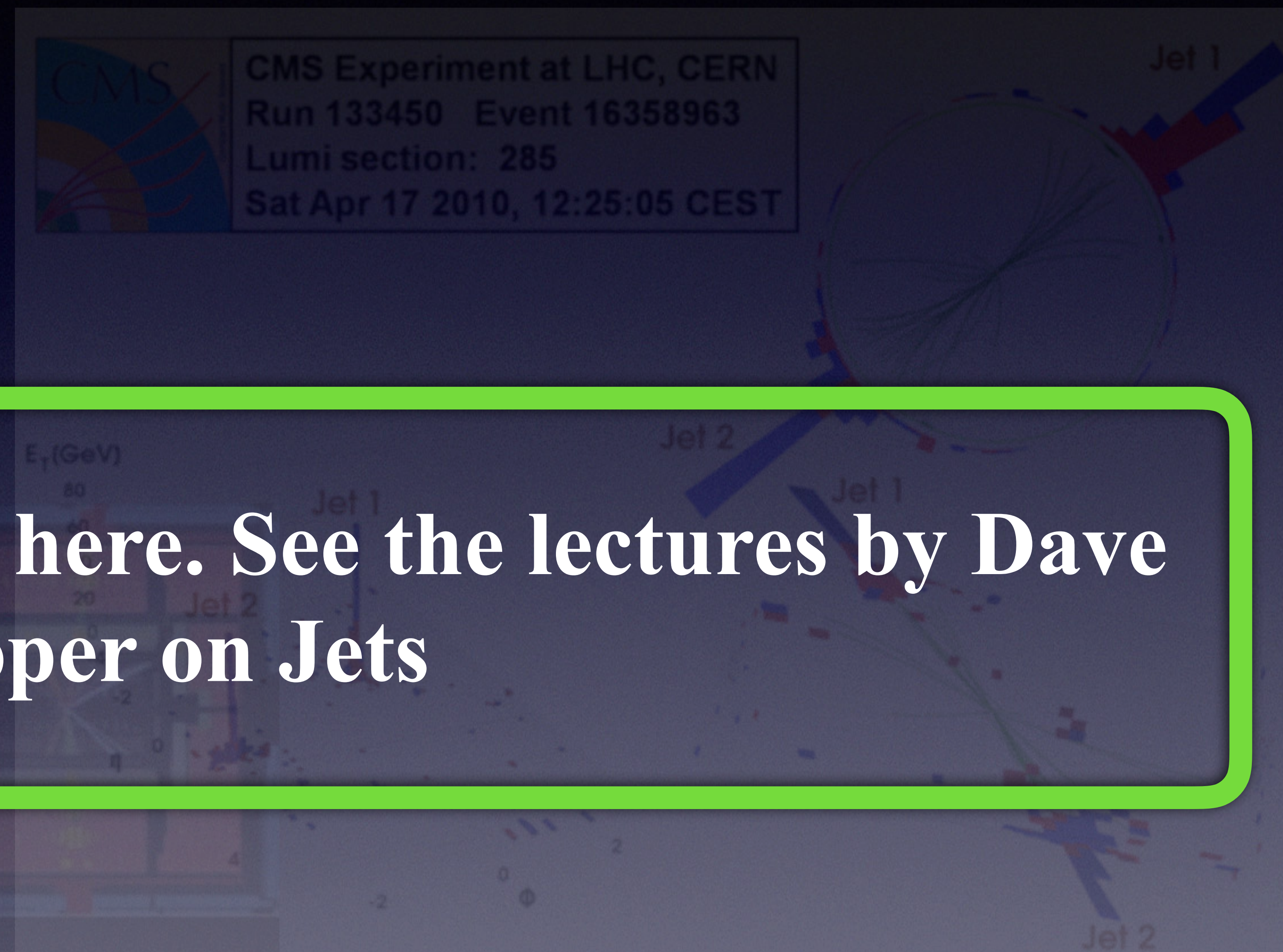

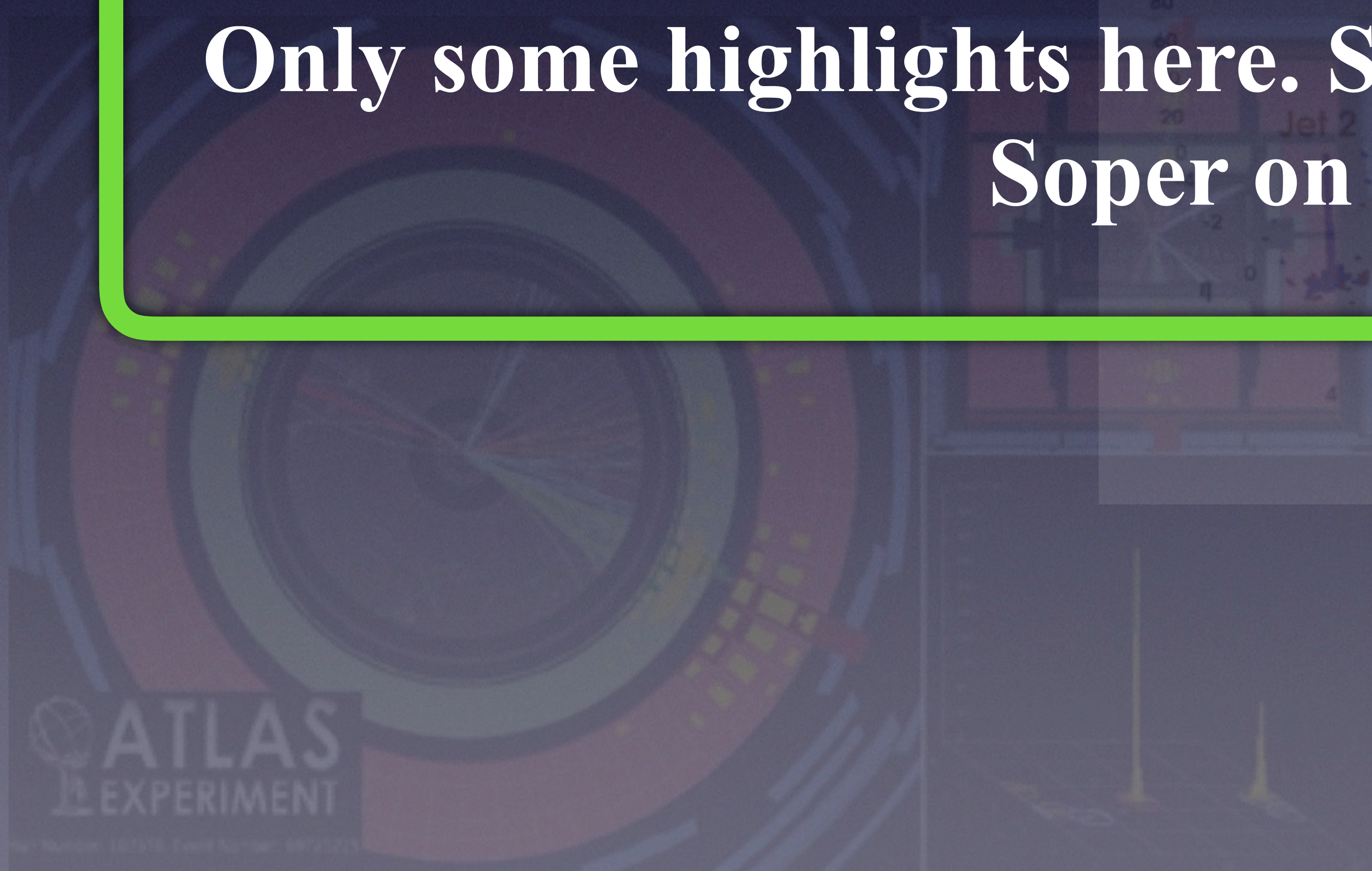

Only some highlights here. See the lectures by Dave Soper on Jets

Jets

- Jets: collimated, energetic bunch of particles

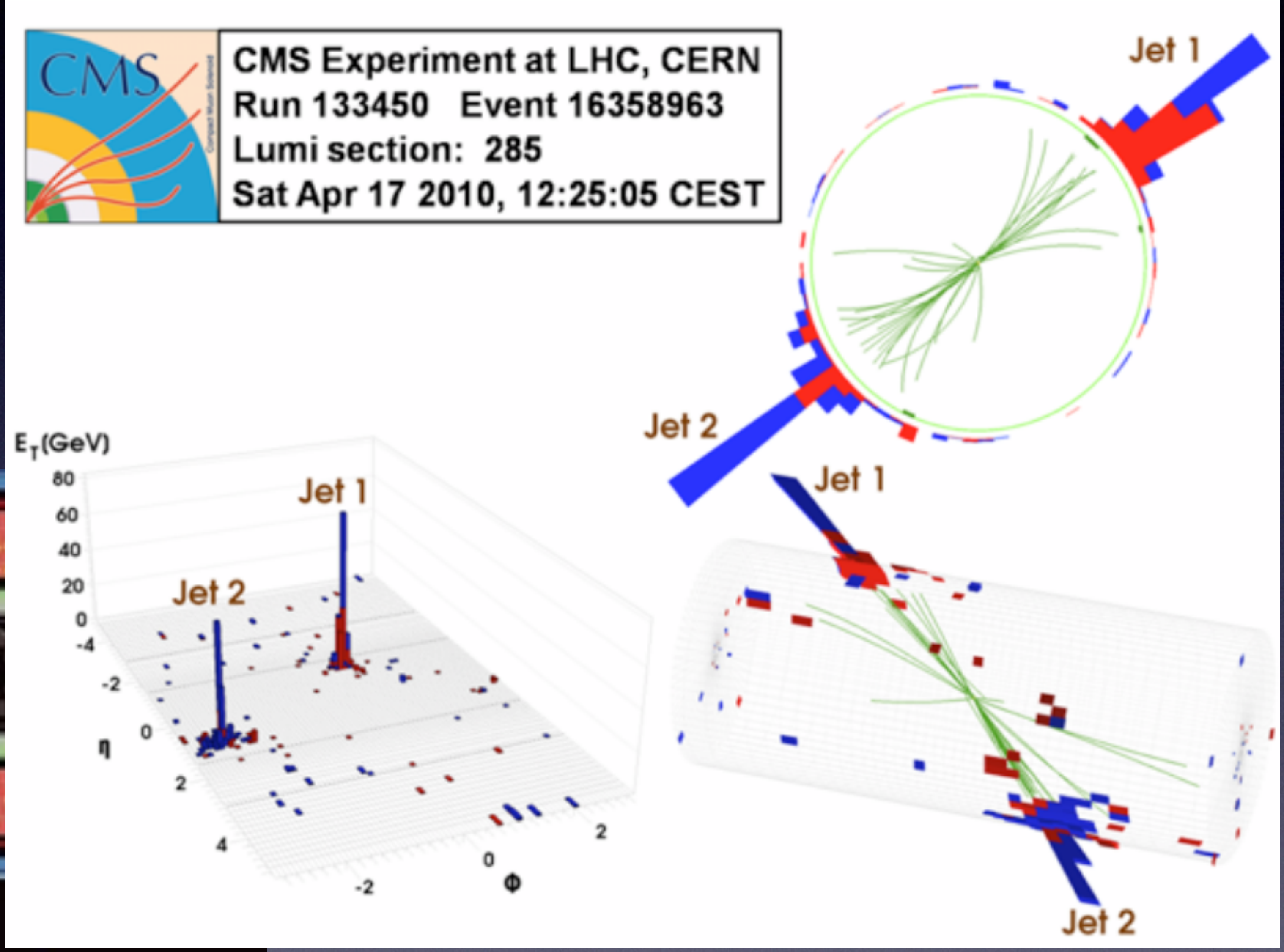

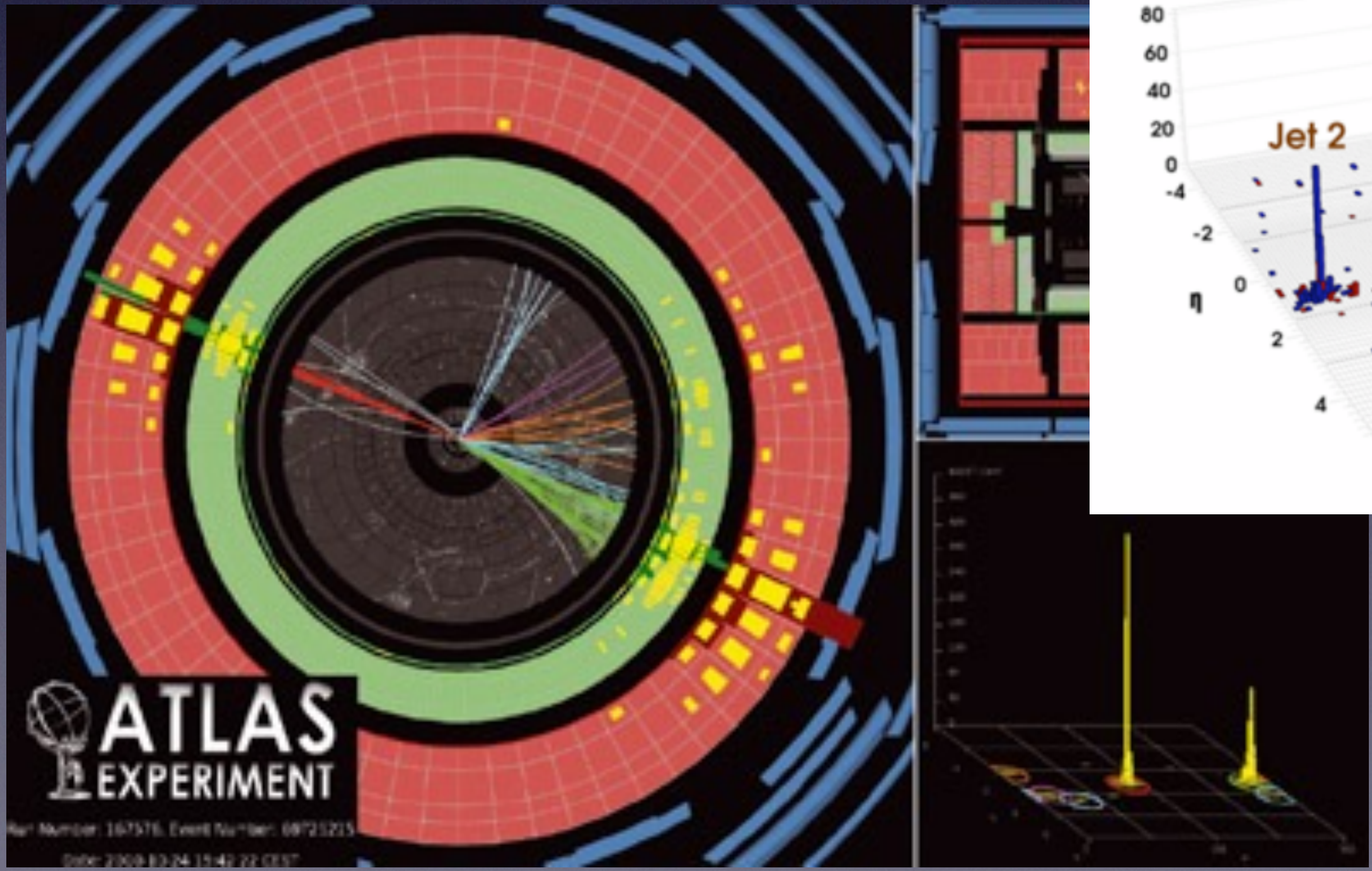

Jets

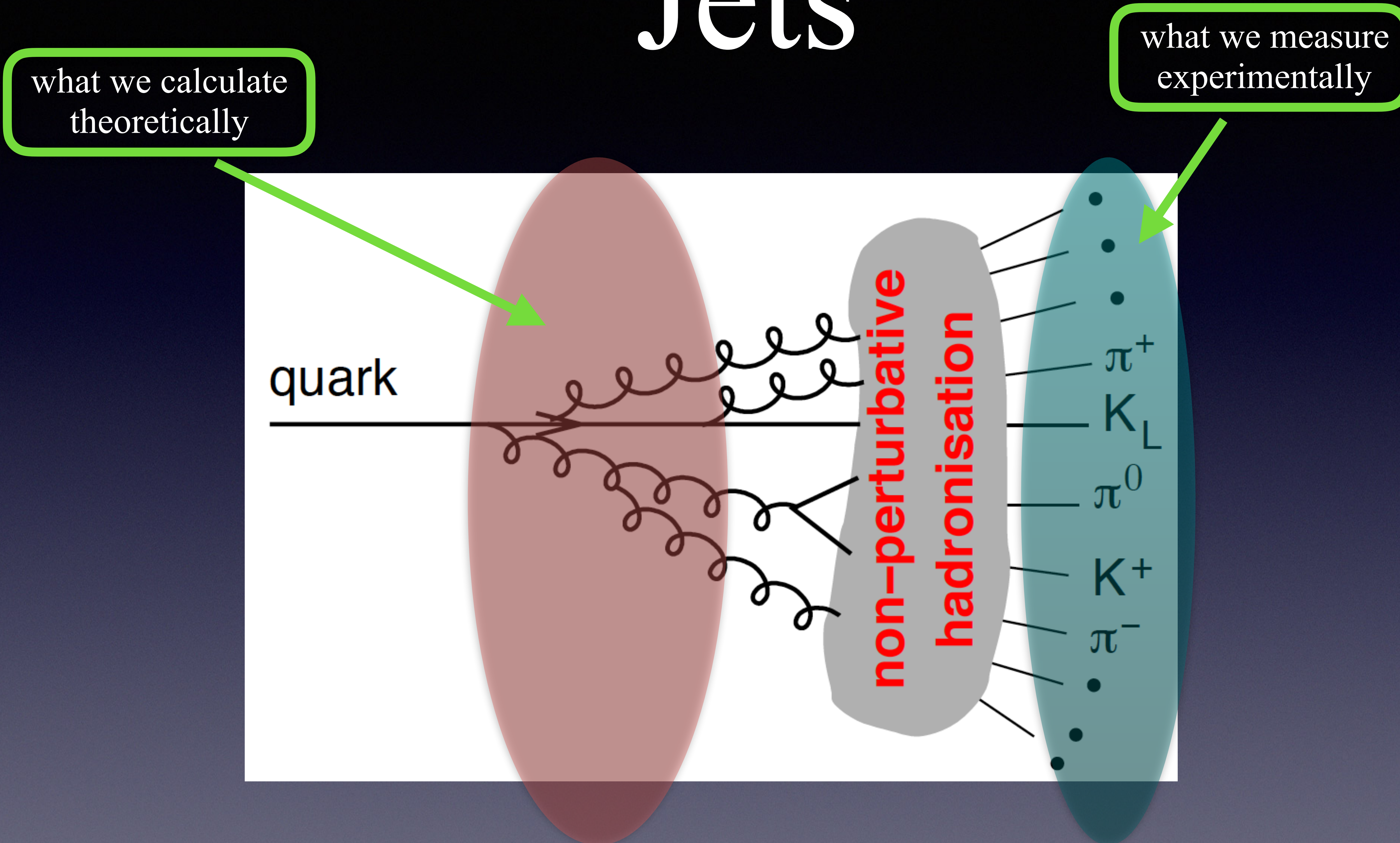

A jet algorithm connects what experimentalists measure with what theorists calculate in a way insensitive to non-perturbative QCD

Jets

- Jet algorithms provide a set of rules for grouping particles into jets. Typically they involve one or more parameters to indicate how close two particles must be before they are combined into a jet (see 0906.1833 by G. Salam for more details).
- A jet algorithm, together with a recombination scheme that indicates what momentum to assign to the combination of two particles, form a jet definition.
- Important properties that should be met by a jet definition are:

1. Simple to implement in an experimental analysis;
2. Simple to implement in the theoretical calculation;
3. Defined at any order of perturbation theory;
4. Yields finite cross sections at any order of perturbation theory;
5. Yields a cross section that is relatively insensitive to hadronisation.

- First jet algorithm dates back to the late 1970s Sterman & Weinberg, Phys. Rev. Lett. 39 1436 (1977)

Jets

- From the theory perspective, a jet algorithm has to be IR safe

- An example of an IR *unsafe* jet algorithm, the IC-PR (iterative cone with progressive removal) jet algorithm (G. Salam, 0906.1833):
  - configuration(c): choose the first seed particle, the one with the hardest momentum in an event. This is the central particle in (c).
  - obtain a stable cone by iterating from this seed, the final result is a single jet in (c)
  - configuration(d): left most particle is the seed (the hardest), since the middle one splits collinearly.
  - iterating from this seed gives a jet that does not contain the rightmost particle
  - right most particle remains, forms a new seed which becomes its own jet.

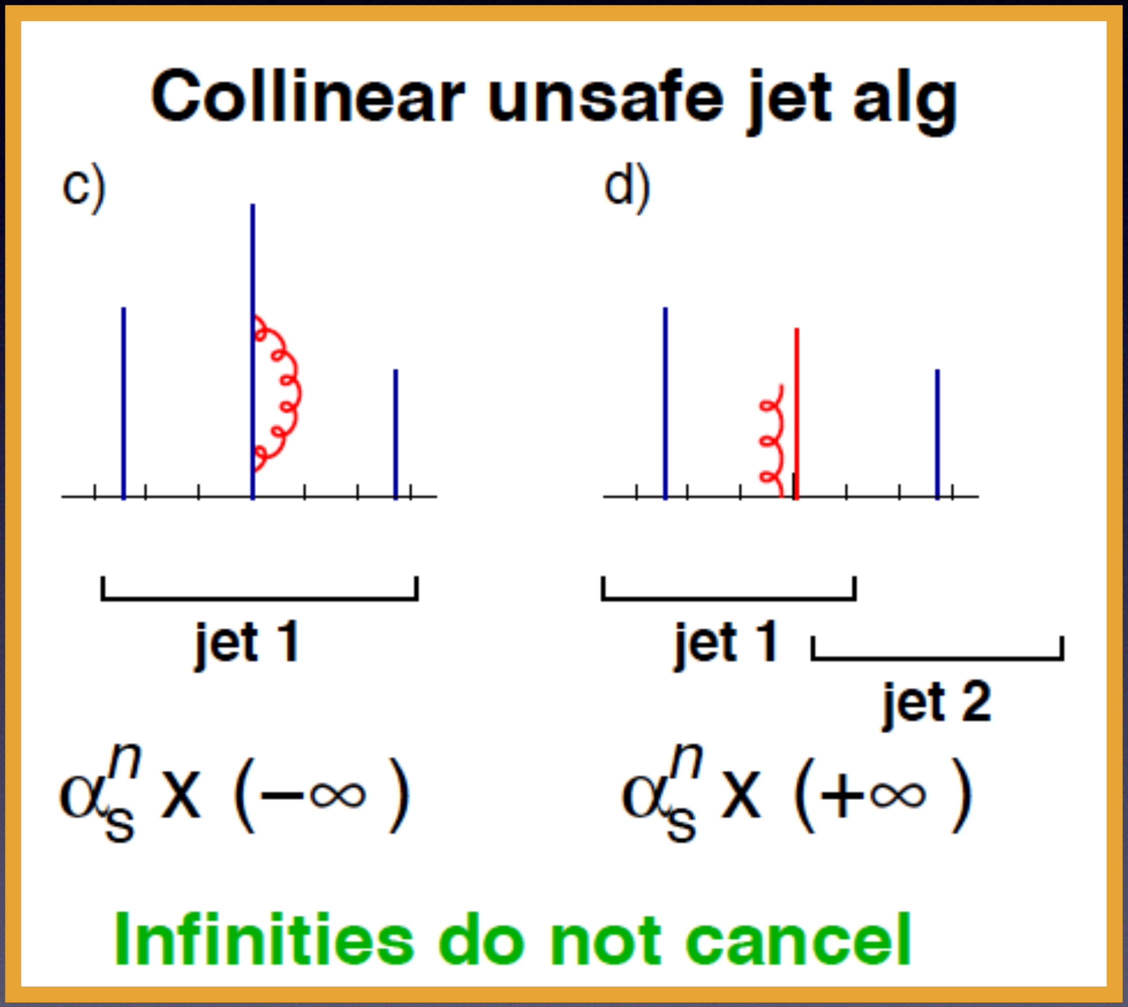

Infinities do not cancel between the sum of the two diagrams as they contribute separately to the 1-jet and 2-jet cross sections after using this jet algorithm!

Jets

- Method of choice at the LHC is anti-kT:

$$d_{ij} = \min(p_{ti}^{2p}, p_{tj}^{2p})\frac{\Delta R_{ij}^2}{R^2}, \qquad \Delta R_{ij}^2 = (y_i - y_j)^2 + (\phi_i - \phi_j)^2,$$

$$d_{iB} = p_{ti}^{2p},$$

p = -1 for anti-KT

y_i: rapidity of particle i
Φi: azimuthal angle of particle i
p_{ti}: transverse momentum
R: jet radius

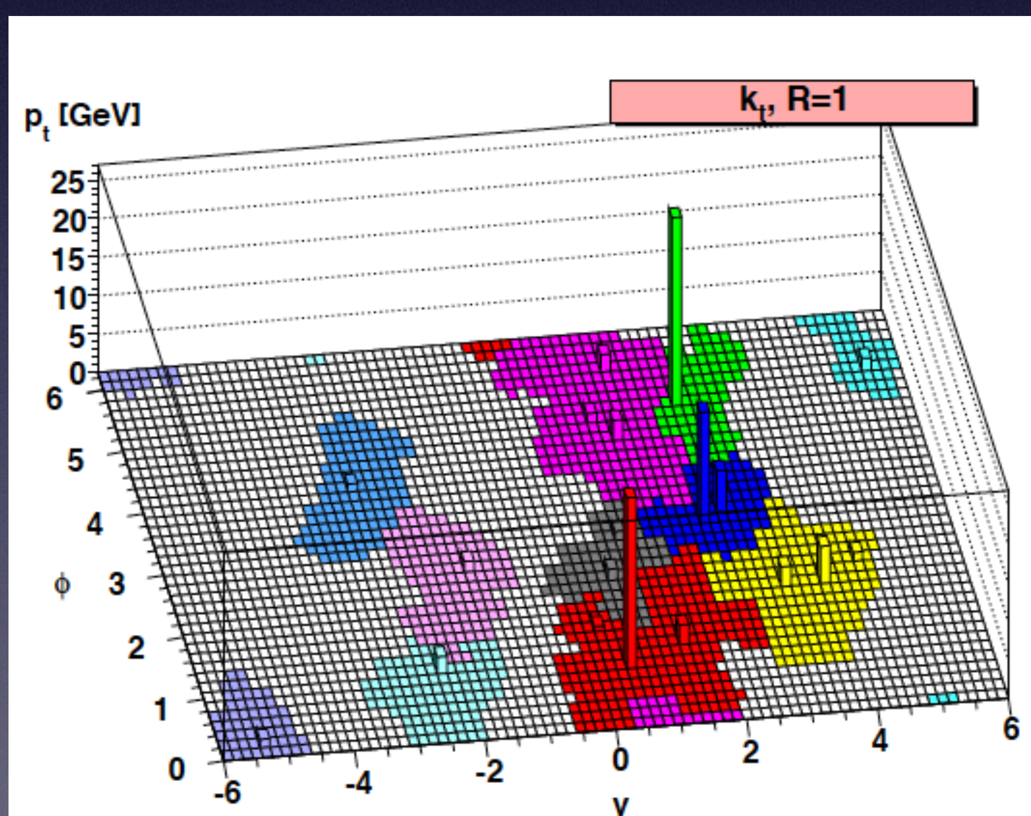

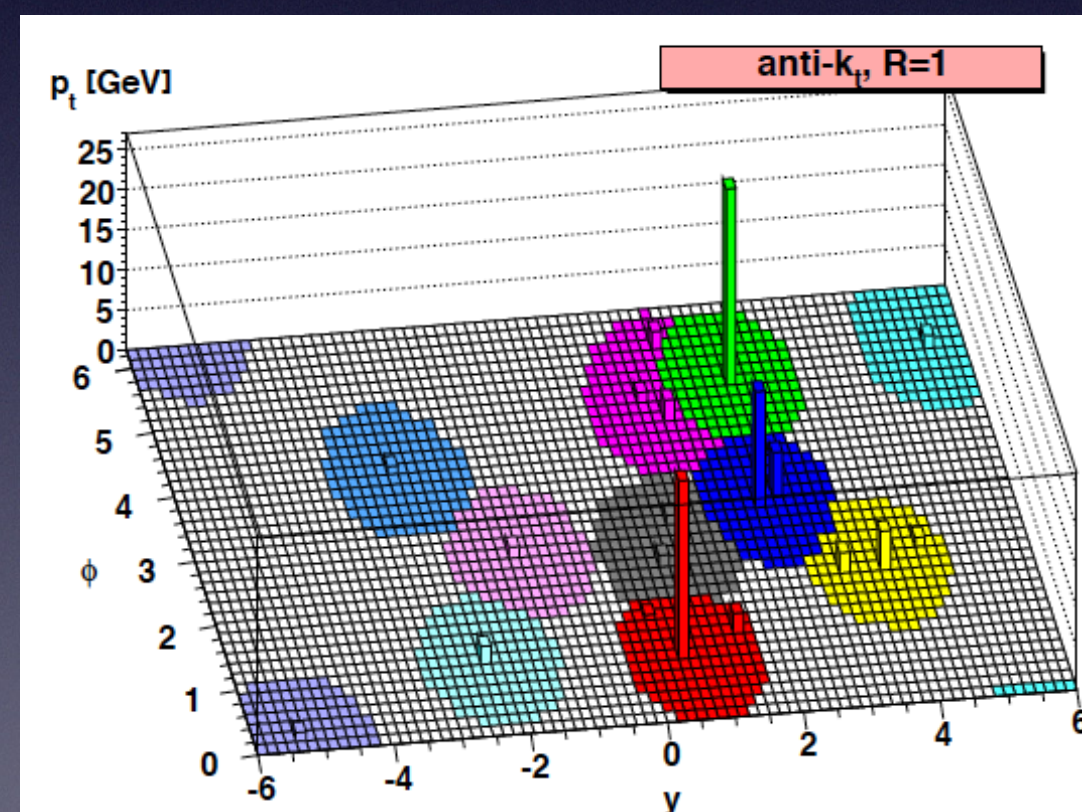

- anti-kT gives nice circular jets unlike other jet algorithms. It is less sensitive to soft emissions.

V+jet Phenomenology

- V+jets backgrounds in MET+jets/monojet searches

irreducible backgrounds:

$pp \to Z(\to \nu\bar{\nu})\text{+jets} \Rightarrow \text{MET + jets}$

$pp \to W(\to l\nu)\text{+jets} \Rightarrow \text{MET + jets}$ (lepton lost)

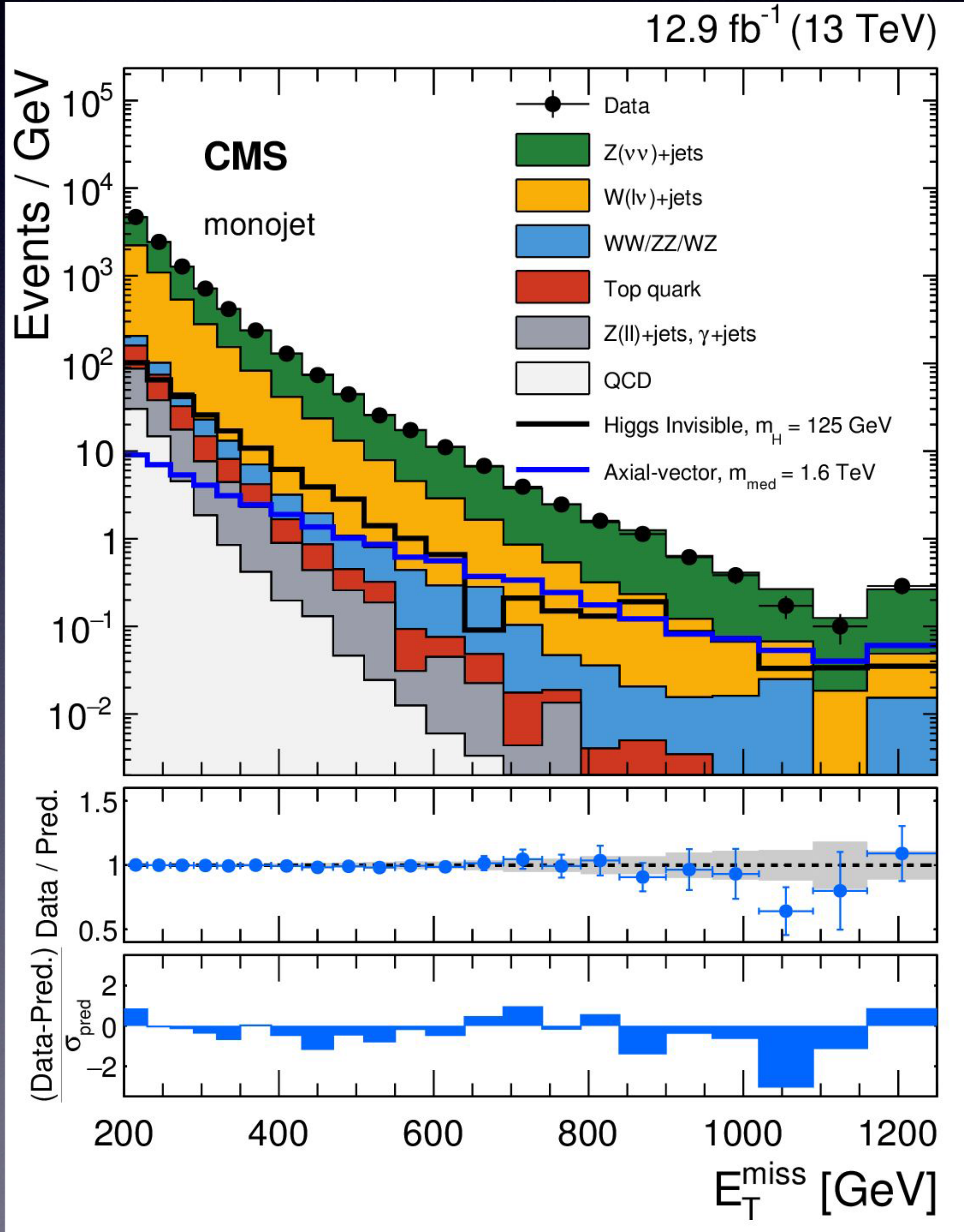

- Major background to SUSY and dark matter searches.
- The determination of backgrounds relies on theory predictions for cross sections

V+jet Phenomenology

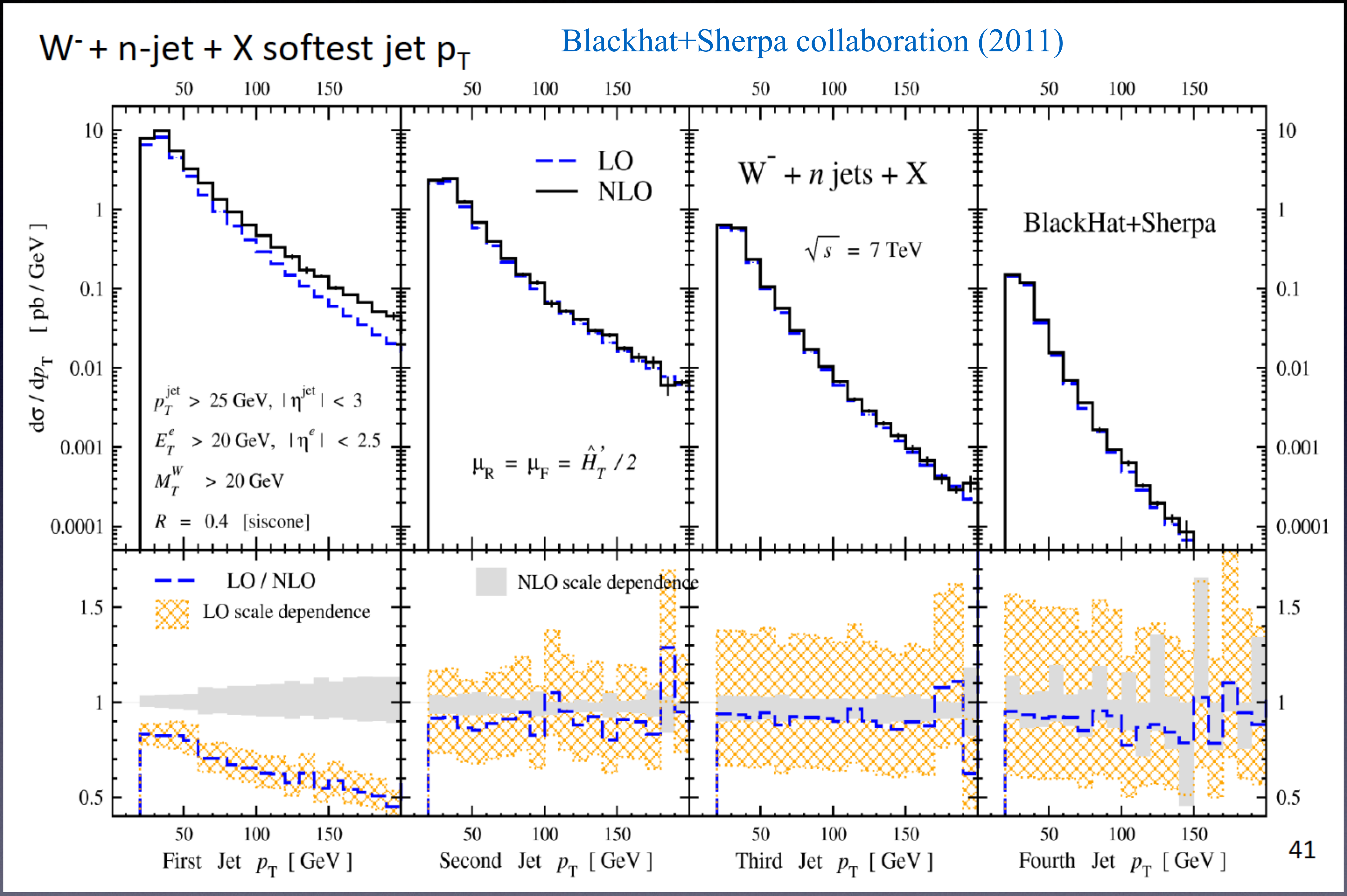

- Better perturbative stability as we go to higher jet multiplicity. The large NLO corrections for V+1jet shows the need for higher order corrections.

V+jet Phenomenology

- NNLO jet distribution corrections small and stable under perturbative QCD. NLO corrections are large and very dependent on kinematics.

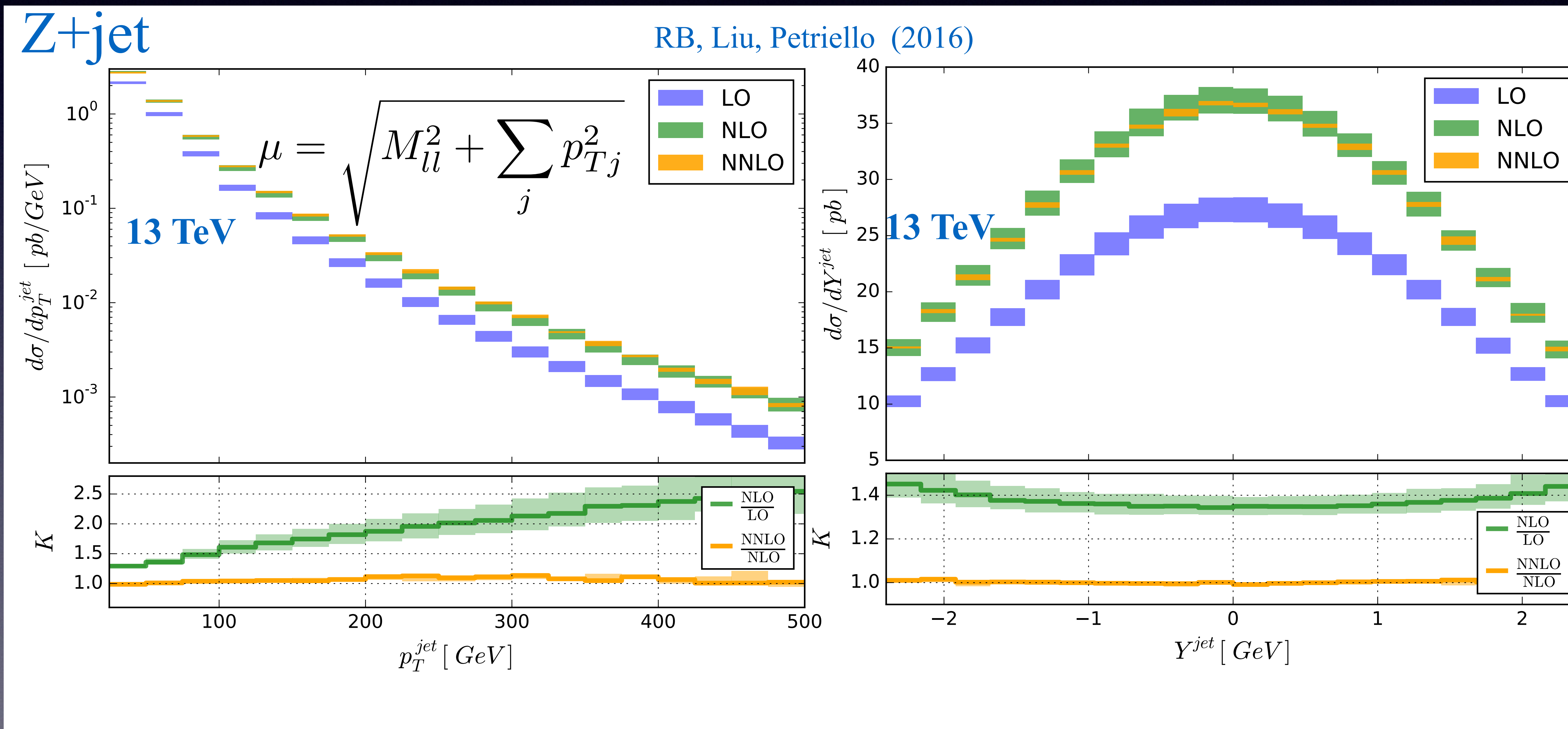

V+jet Phenomenology

- H_T: the scalar sum of the transverse momenta of all reconstructed jets, and is called S_T by ATLAS. Important for BSM searches.

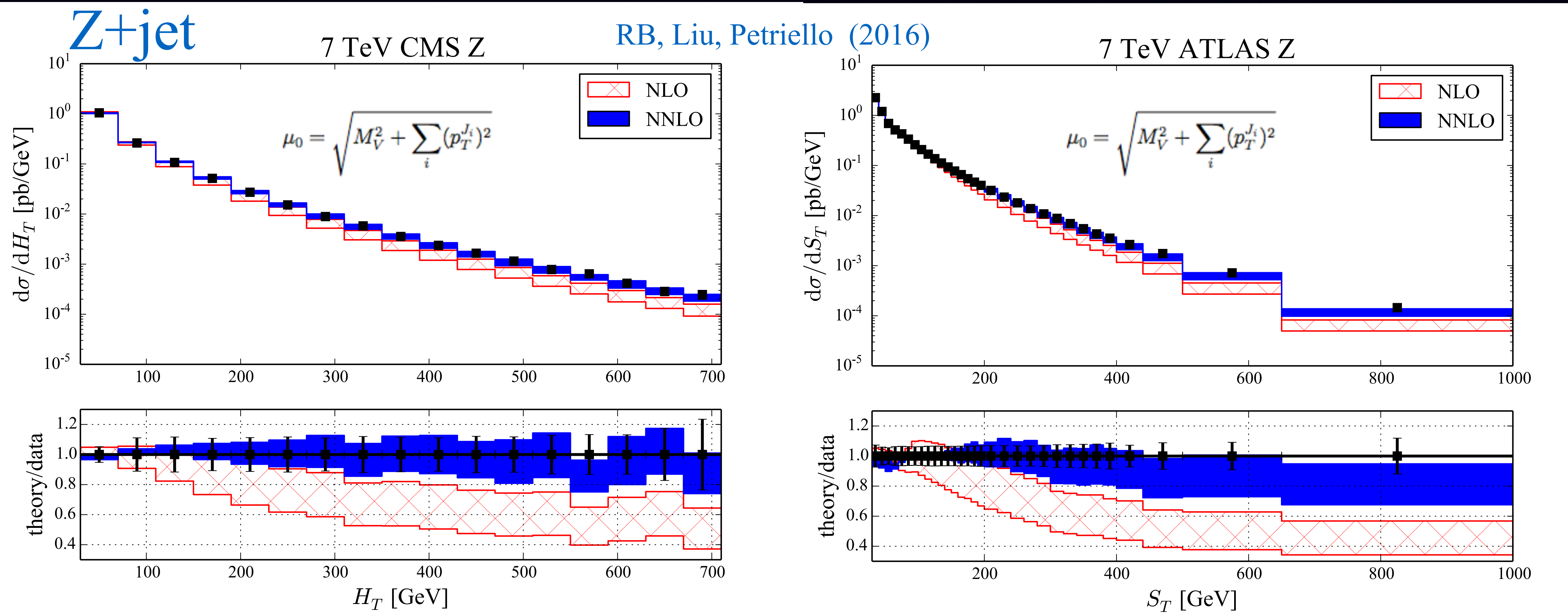

- While NLO QCD results significantly underestimate the cross section at intermediate and high H_T, the ATLAS and CMS data for the entire H_T/S_T range are well described with the NNLO QCD corrections.

Future High Energy Colliders

A future 100 TeV machine?

- There is growing interest in the HEP community to build a future high-energy pp machine with CM energy ~100 TeV
- Initial discussions regarding CERN, Chinese sites. This would possibly be after an e+e- Higgs factory is constructed.

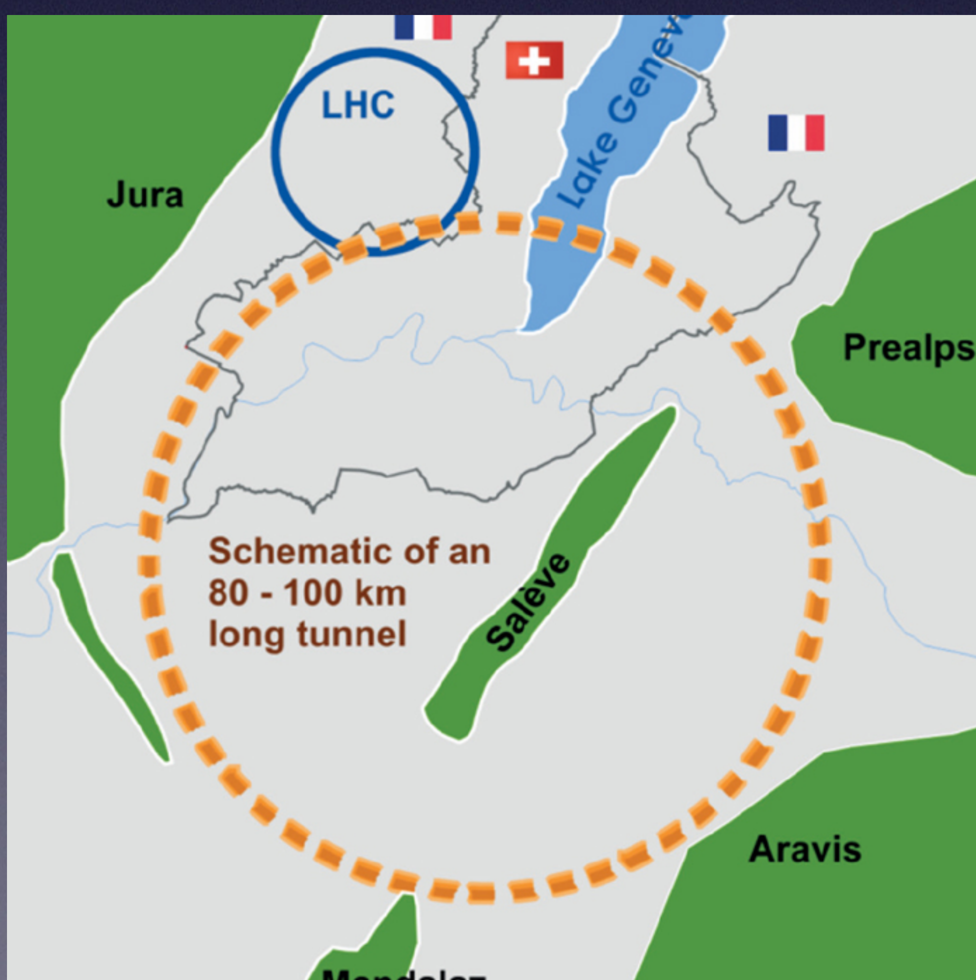

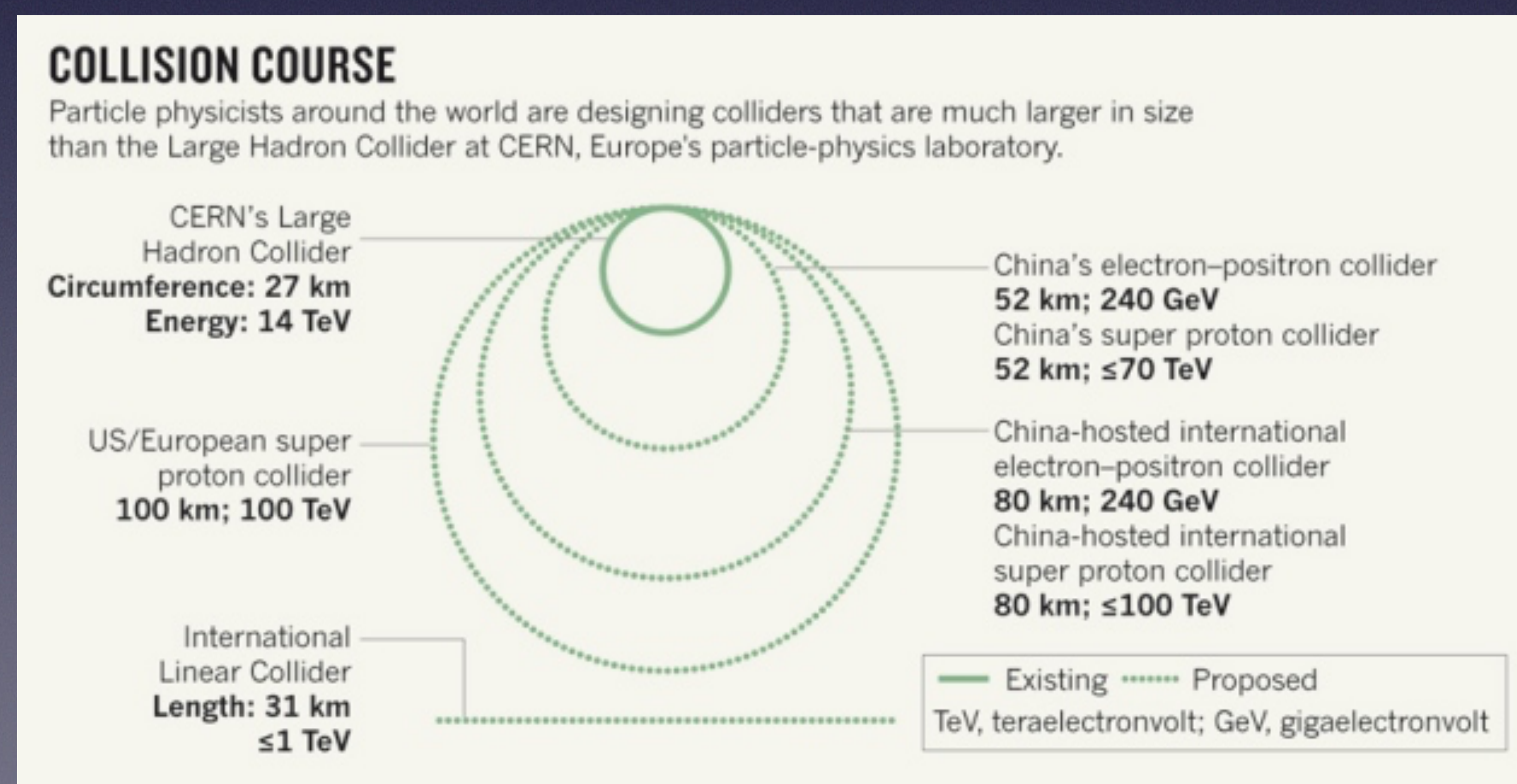

Drell-Yan in the future

- Drell-Yan will continue to play an integral role of the physics program at such future machines.

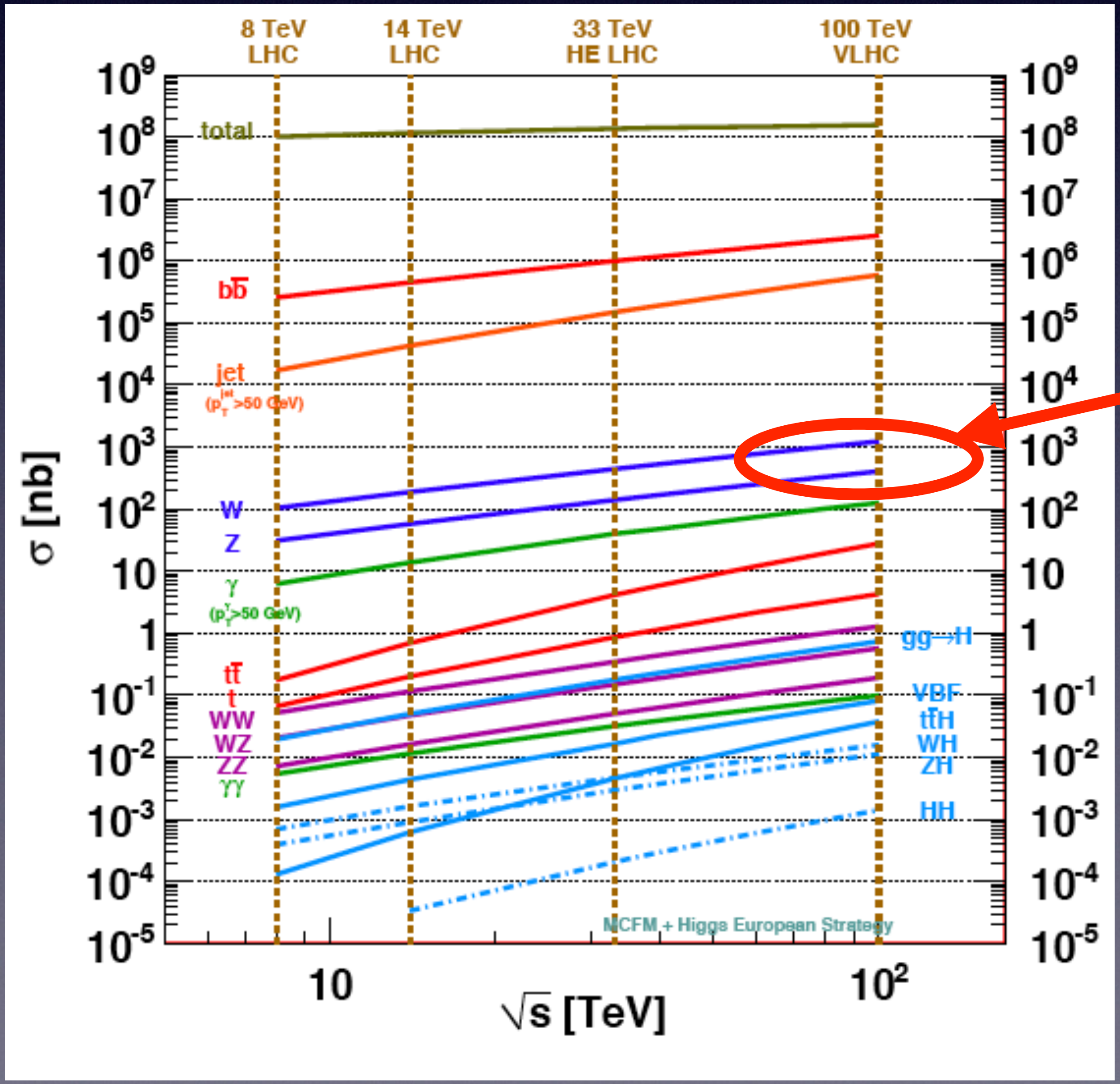

Large production rates for W and Z boson production via Drell-Yan at 100 TeV; will remain an important background to any searches at high energies

Drell-Yan in the future

- Drell-Yan will continue to play an integral role of the physics program at such future machines

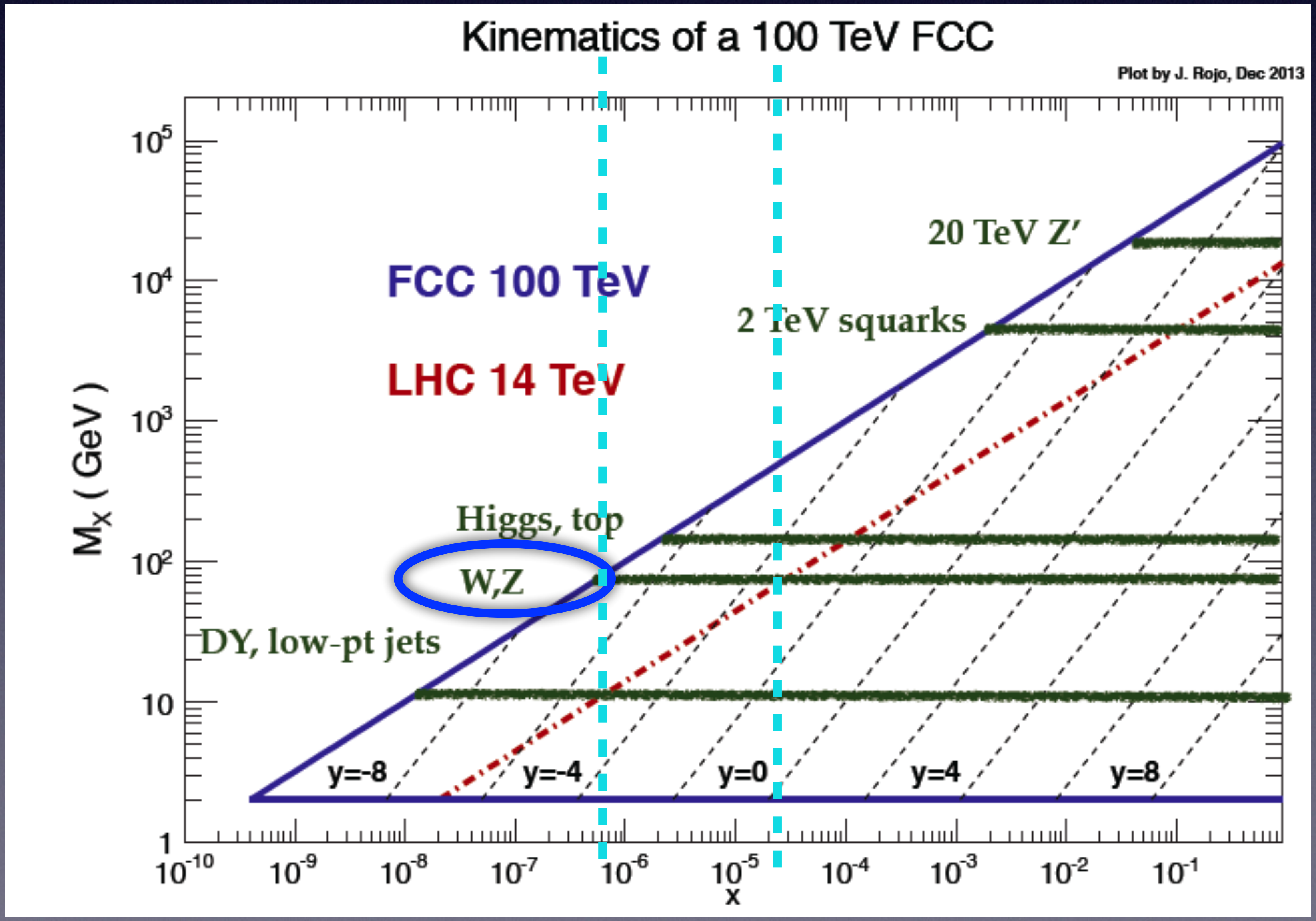

New kinematic regions probed; W/Z production down to Bjorken x~10^{-6}, more than an order of magnitude lower than LHC 14 TeV coverage

New gauge bosons at 100 TeV

- Unmatched reach for new gauge bosons which would indicate new forces of Nature beyond SU(3)xSU(2)xU(1)

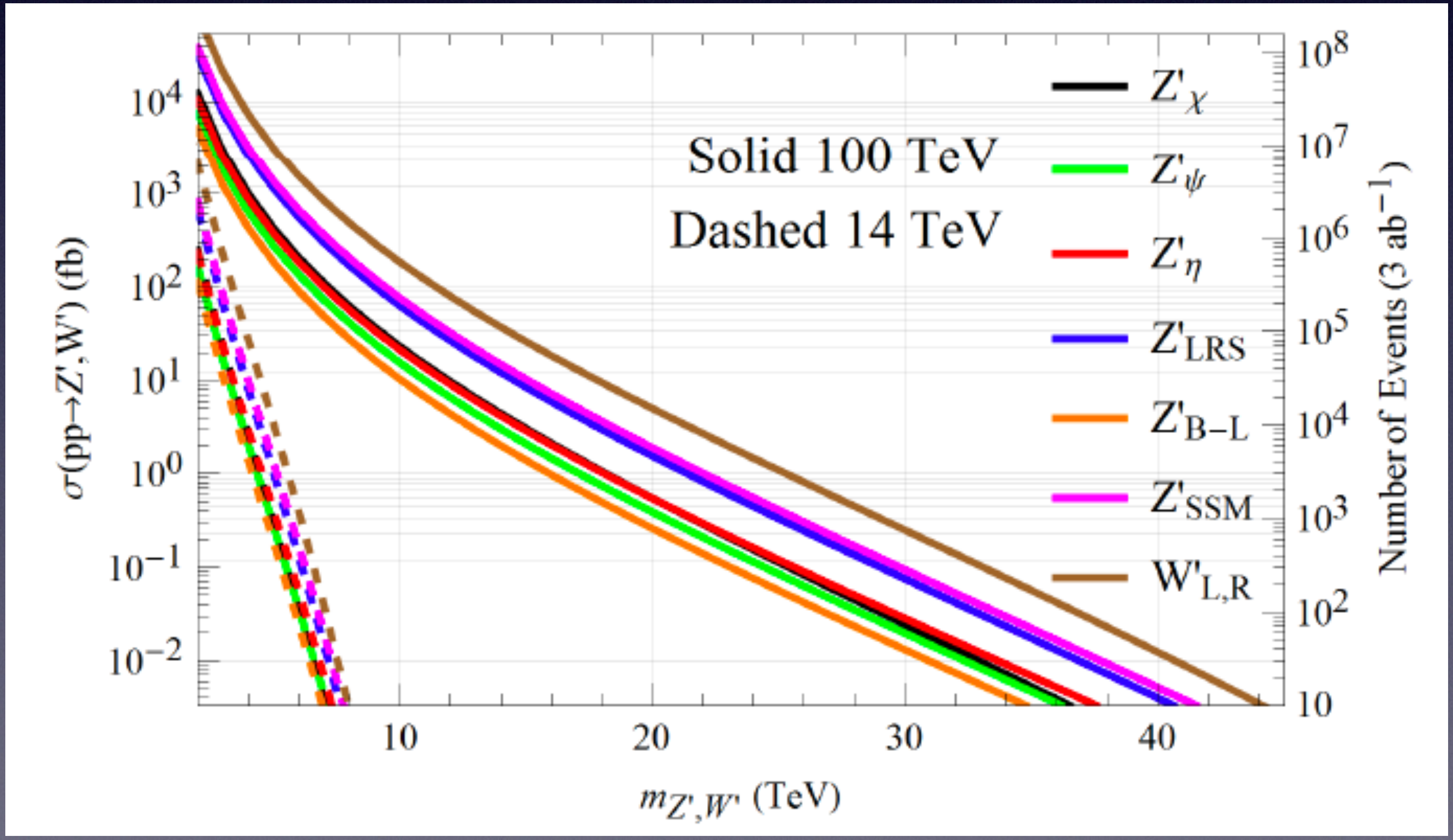

1511.06495

- Ultimate LHC reach in mass is ~7-8 TeV
- A 100 TeV machine extends this out to 35 TeV or beyond, depending on the model

Summary

- Drell-Yan is an important precision tool at hadron colliders
- This is the only process for which we are approaching percent level precision both experimentally and theoretically
- Proven track record for discovery (Z/W-boson, several resonances, etc). Plays an important role in understanding proton structure (PDFs)
- It will continue to play an important role at future hadron colliders